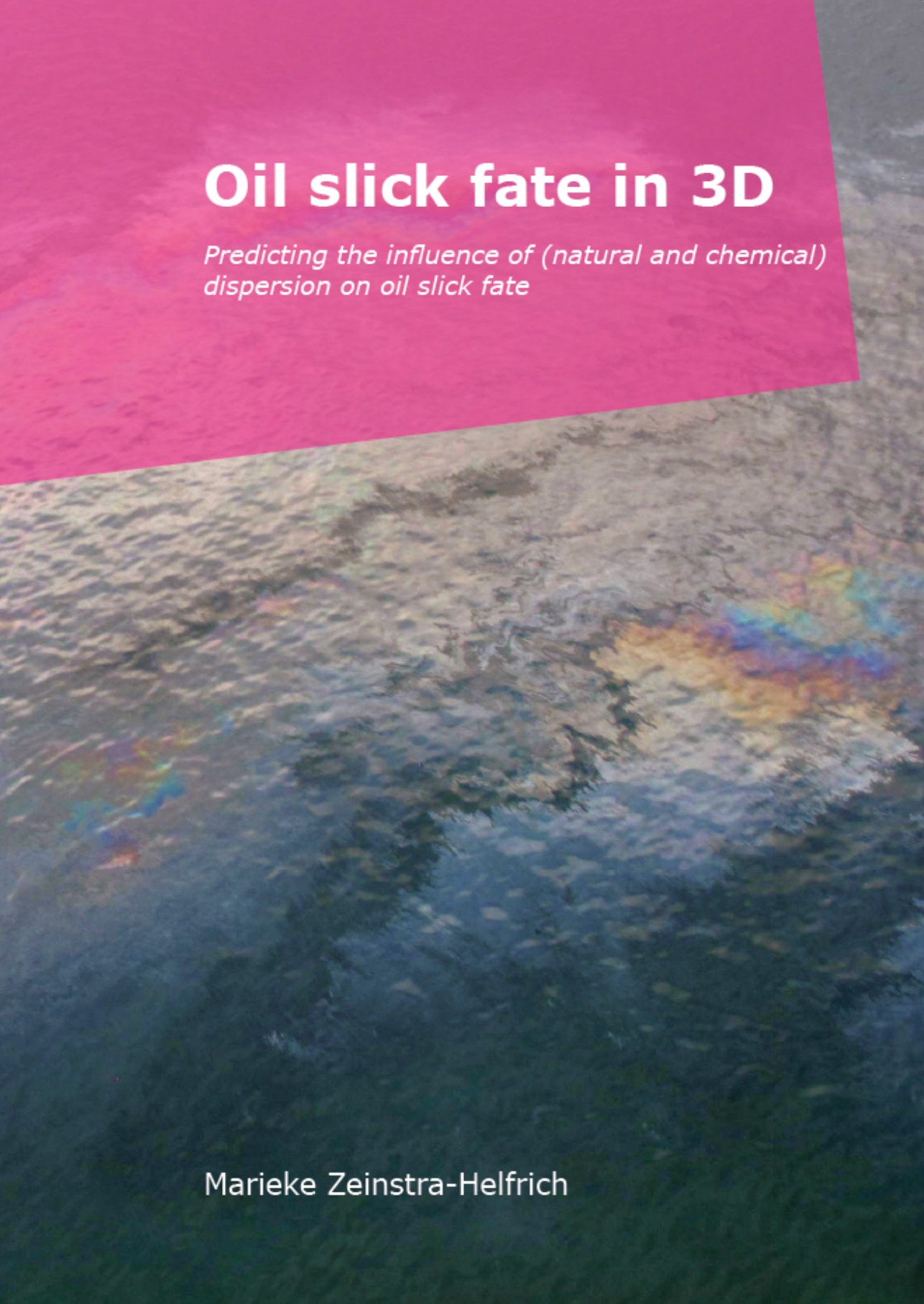

Oil slick fate in 3D

Predicting the influence of (natural and chemical) dispersion on oil slick fate

Marieke Zeinstra-Helfrich

Oil slick fate in 3D

Predicting the influence of (natural and chemical) dispersion on oil slick fate

Marieke Zeinstra-Helfrich

Thesis committee

Promotor
Prof. Dr A.J. Murk
Professor of Marine Animal Ecology
Wageningen University

Co-promotor
Dr W. Koops
Lector (Research Group Chair)
Maritime, Marine, Environment & Safety management
NHL University of Applied Sciences, Leeuwarden

Other members
Prof. Dr H.H.M. Rijnaarts, Wageningen University
Prof. Dr A.J.M. Schoot Uiterkamp, University of Groningen
Dr F. Kleissen, Deltares, Delft
Dr R. Plat, IHC Merwede, Kinderdijk

This research was conducted under the auspices of the Graduate School for Socio-Economic and Natural Sciences of the Environment (SENSE).

Oil slick fate in 3D

Predicting the influence of (natural and chemical) dispersion on oil slick fate

Marieke Zeinstra-Helfrich

Thesis
submitted in fulfilment of the requirements for the degree of doctor
at Wageningen University
by the authority of the Rector Magnificus
Prof. Dr A.P.J. Mol,
in the presence of the
Thesis Committee appointed by the Academic Board
to be defended in public
on Monday 21 November 2016
at 1:30 p.m. in the Aula.

Marieke Zeinstra-Helfrich
Oil slick fate in 3D. Predicting the influence of (natural and chemical) dispersion on oil slick fate
174 pages.

PhD thesis, Wageningen University, Wageningen, NL (2016)
With references, with summaries in Dutch and English

ISBN 978-94-6257-927-9
DOI http://dx.doi.org/10.18174/389993

Table of contents

CHAPTER 1

Introduction

There is no doubt that an oil spill has adverse effects, yet the type and magnitude of damage is very different between spills. The impact of a spill depends on the type and volume of oil spilled, the weather conditions and the marine communities that are exposed (depending on oil fate, spill location, time of year).

The weather and spill conditions also determine the effectiveness of the various available oil spill response options. As oil spill response aims at reducing the impacts of the spill, the decision for the (most) appropriate response technique(s) in a certain situation, is implicitly or explicitly based on Net Environmental Economic Benefit Analysis (NEEBA).

Natural dispersion is a key process in the fate and weathering of oil: Wave action temporarily submerges portions of oil, which remain suspended for a size-dependent time-span before resurfacing. Enhancement of this process by adding dispersants, a response option called chemical dispersion, enables smaller droplets to be formed, which can remain suspended for longer.

The complex processes of natural and chemical dispersion are not yet fully understood, leaving the NET benefit of dispersants on oil fate, uncertain. In a post-hoc assessment of the Deep Water Horizon oil spill, experts could not reach agreement on the amount of oil that was dispersed as a result of the use of dispersants (Federal Interagency Solutions Group, 2010).

The Braer oil spill's unexpected outcome

In January 1993, the crew of the oil tanker MV Braer lost control of their ship during a storm; it ran aground at the south side of the Shetland Islands (Law and Moffat 2011). All oil carried by the tanker: 87000 tons of Gullfaks crude oil as well as 1500 tons of heavy fuel oil, was spilled over the course of about 12 days.

The intense weather conditions and the light crude oil, however, caused much of the oil to be dispersed (Law and Moffat 2011): only 1% of the oil had beached, 14% evaporated, and 85% was dispersed. Following dispersion, part of the oil had sedimented: 36% of the total oil spilled was found to be deposited in sea-floor sediments.

Overall, the impact of the spill was found to be minimal (Kingston, 1999), especially considering the size of the incident and its nearshore location.

1.1 Types of effects of oil spills

The direct adverse effects of an oil spill are found in the (ecological) resources exposed to the pollutant. Exposure does not only occur on the horizontal trajectory of the slick on the water surface, but also by oil components partitioning to the air, water column and the sea floor. Different types of effects can be distinguished in these compartments:

Physical oiling by direct contact with the surface **oil slick** can eliminate the water repellent characteristics of feathers and fur of birds and marine mammals, causing a suite of effects up to death by hypothermia or drowning (Lee et al.,

2015; Tamis et al., 2012). Once such an oil slick reaches a **shoreline**, physical oiling smothers the intertidal benthic organisms as well as exposes those surface dwelling organisms (birds, mammals) again. Vegetation is also affected by physical oiling. Effectiveness of clean-up depends very much on the shoreline type (Owens, 2011). On certain shorelines, clean-up is very difficult and sometimes more harmful than the oil itself. In situations where oil can persist in the shoreline, prolonged (chronic) exposure to the pollutant causes continuing impacts (Tamis et al., 2012).

Much less obvious than the visibly affected birds or coastlines, are the adverse effects of oil-associated compounds in the **water column**. Many laboratory studies prove the toxicity of various oil components to aquatic species, yet the effective impacts 'in the field' are more difficult to assess (Lee et al., 2015; Shigenaka, 2011). As resulting water column concentrations are heterogenic in time and location, evaluation of exposure is difficult. Complicated even further by the fact that (adult) pelagic fish are known to swim away from an oil slick once they detect oil-compounds in the water (Tamis et al., 2012). Impact is considered higher on juvenile fish due to their sensitive life stage, and larvae as they have no means to actively avoid the contamination (Lewis and Daling, 2001). Although quantifying acute and long-term impacts on aquatic organisms proves difficult, field-evidence of serious health effects on aquatic organisms is available, including; morphological deformities in fish larvae from eggs on oiled beaches and the continuing decline in the orca population 16 years after the Exxon Valdez spill (Shigenaka, 2011). In addition, sub lethal exposure of hydrocarbons to fish is known to cause 'tainting' of seafood, creating an off flavour.

The (hydrocarbon) vapours that can form in **the air** above an oil slick, can present a fire or explosion hazard in addition to their toxic nature. These effects, however, are very local to the oil slick itself and therefore, mostly limited to response personnel (IPIECA, 2010; Lee et al., 2015).

Should, by sedimentation, the hydrocarbons reach the **sea floor**; they impose the same toxic effects as they did in the water column. Additionally, as the oil on the sediment is fairly immobile and less prone to biodegradation, their persistence causes prolonged exposure and long term effects on benthic species (Lee et al., 2015).

1.2 Oil spill transport and fate

An undisturbed oil slick **travels** with the underlying water, following the surface current speed and direction. In addition, it is transported by a percentage of the wind speed in the wind direction, generally assumed to be around 3%.

Such unrestricted slick also **spreads** on water to cover a larger area. Radial spreading (a round slick) is described as the result of gravity and interfacial tension, and counteracted by viscosity of the oil (Fingas, 2011a). Additionally, an oil slick tends to elongate in wind direction (Lehr et al., 1984). Smaller scale hydrodynamic features can also slightly concentrate the oil, such as the forming windrows at the convergence zone of Langmuir cells (Lee et al., 2015; Lehr and Simecek-beatty, 2000).

The more volatile components of the oil (light saturates and aromatics) **evaporate** out of the oil slick (Wang et al., 2003). Typically, evaporation rate is higher for thin slicks due to the larger surface area per oil volume, as well as less diffusion required inside the slick to reach the interface (Gros et al., 2014). Additionally, air renewal by wind is thought to enhance evaporation rate. Overall, most evaporation occurs during the first days after the oil is spilled. The loss of these lighter components from the oil slick, affects the properties of the remaining oil, mainly by increasing the viscosity, density and slightly increasing oil-water interfacial tension.

Oil types and properties
Crude oil is a complex mixture consisting of thousands of different components, most of which are various types of hydrocarbons (Merv Fingas 2011; Lee et al. 2015). Each crude oil type has different composition and characteristics, which determine its use and value in the oil industry, as well as behaviour and the effects if spilled.

A way of classifying the hydrocarbon components is by the so called SARA fractions:
Generally, the largest portion of the oil consists of saturates. These saturated hydrocarbons consist only of carbon (C) and hydrogen (H) atoms, connected by single (strong) bonds. Compounds in this fraction are generally considered to be insoluble in water, biodegradable and non-toxic (Lee et al., 2015).
The class of aromatics is comprised of compounds containing at least one benzene ring. The structure of the benzene ring with its alternating double bonds gives the substance specific properties. Aromatic substances are most soluble in water, volatile, and acutely toxic (Lee et al., 2015). Not surprisingly, two major contributors to oil effects are part of this class:
The *BTEX* compounds (Benzene, Toluene, Ethylbenzene and Xylenes) are highly volatile as well as relatively water soluble, therefore easily transported to the other compartments. The BTEX compounds are relatively easily biodegraded. Furthermore, they are considered acutely toxic, as well as carcinogenic (Benzene).
PAH (Polycyclic Aromatic hydrocarbons) consist of at least two benzene rings but exist with any different chemical structures (Fingas, 2011b). Smaller PAH's are more volatile, soluble and

Wave action can break up portions of the oil slick and suspend it as oil droplets in the water column, a process called (natural) **dispersion.** Large suspended lumps resurface back into the slick, whereas small droplets can be kept in suspension by local turbulence (Fingas, 2011a). The more temporary suspension of larger droplets also enables the process called shear spreading, contributing to the elongation of an oil slick in wind direction (Elliott, 1986). Natural dispersion requires a certain amount of wave action to occur, and oil properties must be favourable for breakup into droplets (Delvigne and Sweeney, 1988). Dispersion has no direct effect on the oil properties, yet it does influence the other weathering processes by enhancing the oil-water contact area and removing mass from the surface (Lee et al., 2015). As the Braer case demonstrates, dispersion can have great effects on the fate of the oil spill.

On the oil-water interface **dissolution** of the water-soluble oil components from the oil slick can occur, causing the viscosity and density of the remaining oil slick to increase. As the same (lighter) components are soluble and volatile, dissolution and evaporation are competing processes. In most situations more of the oil mass is lost to the air than to the water column (Lee et al., 2015). The relative importance of dissolution increases when evaporation is less (or not) prominent; as is the case in sub-surface spills or continuous dispersion where oils is more in contact with the water phase than the air. In addition, due to the different temperature dependence of vapour pressure and solubility, lower temperatures are expected to be more favourable for dissolution (Gros et al., 2014). Despite its small contribution to the oil mass balance, dissolution is

biodegradable, as well as less toxic then larger PAH (Lee et al., 2015). Certain PAH are very resistant to biodegradation.
The formal definition of the resins, is based on solubility in certain solvents, however most of these components are unsaturated hydrocarbons and hydrocarbons with other elements (S, N, O) in their structure. Resins are very poorly biodegradable, and are slightly more polar and water soluble than saturates (Lee et al., 2015).
Like resins, the formal definition of asphaltenes lies in (in-)solubility in 2 solvents. Asphaltenes are much like resins, yet include the complex high molecular weight components Biodegradation of these compounds even more difficult than the resins (Lee et al., 2015).

In relation to oil behaviour and spill response, oil is often described by its density (light – heavy): The density provides insight in whether an oil type consists of predominantly light or heavy hydrocarbon fractions, which in turn determine the behaviour (O'Sullivan and Jacques, 2001): The light fractions are considered to be more volatile, more soluble and more toxic than heavy fractions. An oil type with predominantly light fractions is less viscous and less sticky. Heavier oils have increasingly higher viscosities and stickiness and are generally more persistent in the environment.

For refined products these same rules based on oil density generally apply. In addition, refining generally concentrates the more toxic compounds in the lighter products (Lewis and Daling, 2001).

considered an important process due to its implications on aquatic toxicity (Tamis et al., 2012).

Suspended oil droplets (dispersion) can **interact with suspended sediments** or other negatively buoyant particles to form aggregates (Fingas, 2011a). The importance of this process depends on the droplet and sediment concentrations (interaction potential) as well as their affinity to interact with each other (Wang et al., 2011). The resulting aggregates are less buoyant than the original or droplets, which can cause them to be more efficiently (stably) suspended (Li et al., 2007) or sink to the sea-floor (**sedimentation**). The large mass of dispersed oil associated with the Braer spill in combination with the high sediment loads as a result of the nearshore location and the severe weather conditions, indicate high potential for sedimentation, explaining the large deposits of oil in the sediments.

Studies in the Gulf of Mexico after the Deepwater Horizon spill (2010) indicate an increase of sea floor marine snow[1] deposition. These deposits include hydrocarbons as well as materials that must have originated at the water surface (Vonk et al., 2015). A possible explanation is the **MOSSFA** (Marine Oil Snow Sedimentation & Flocculent Accumulation) mechanism; in which the spill enhanced the formation of mucus-rich marine snow with incorporated oil droplets.

Some of the oil components (mainly aromatics) are susceptible to sunlight-enabled **photo oxidation** reactions. Although the reaction products are more water soluble, photo oxidation does not have a big direct impact on the mass balance. This process is relatively slow compared to the other weathering processes and can only affect the exposed top film of the oil. Photo oxidation is, however, suspected to cause a rigid film on the slick surface hindering other weathering processes (evaporation, dispersion) and might increase toxicity of some compounds (Lee et al., 2015; Shigenaka, 2011).

Incorporation of water droplets into the floating oil layer (**emulsification**) causes it to increase in volume and viscosity and eventually give it a red-brown colour. Emulsification is caused partly by the repetitive stretching and compression of the slick on the waves. Water incorporation, as refloating droplets rejoin with the slick, could also contribute to this process. Generally, viscous oil types are more prone to form an emulsion, especially with high resin

[1] Marine snow is defined as sinking biological debris from the upper water column. This mechanism provides nutrients in the deeper parts of the ocean.

and asphaltenes content (Fingas and Fieldhouse, 2004). The increase in viscosity (up to 1000-fold) and effective volume of pollutant (up to 5-fold) make emulsification a negative influence on spill response (Lee et al., 2015).

Certain micro-organisms available in the marine environment are capable of degrading oil components, a process called **biodegradation**. Different oil components have different biodegradability. In addition, biodegradation is optimal in high temperature, aerobic conditions with a lot of (oil-water) surface area accessible to the micro-organisms. Therefore biodegradation is much more efficient in well aerated surface water than buried in the sediment (Lee et al., 2015).

The combined outcome of these transport & weathering processes, determine the mass, composition and properties of the remaining slick over times as well as its exposure to the other compartments.

A surface oil slick is considered to have larger detrimental effects than (less visible) oil in the water column. The physical effects of surface oil are equally serious across the entire slick area (above a threshold oil layer thickness), and the length of oiled shoreline (as a measure for total shoreline impact) is also directly proportional to surface slick size. Water column impacts by the hydrocarbons are dose dependent, in which dose is either the ingested amount or related to concentration and exposure time. The area within acute-impacts are caused will be smaller than the surface slick. Additionally, due to the expected rapid dilution of the hydrocarbons this impact is more short-lived than surface oil is.

1.3 Dispersants as an oil spill response option

Once oil is released into the environment, different response options are available. Mechanical recovery physically removes oil from the marine environment; its NET effect is therefore quite straightforward. Unfortunately, these techniques are not suitable in all conditions (Fig. 1-1), and have relatively low capacity to deal with larger spills.

Chemical dispersion can be an alternative: Dispersants are applied to the oil slick by airplane, helicopter bucket or ship. Surfactants in the dispersant reduce the oil-water-interfacial tension to make the oil more susceptible to breakup in small droplets. As a result, the natural dispersion process is enhanced as more of the oil is broken up into small, stably suspended droplets. These small droplets are more easily transported away from the slick and the enhanced oil-water surface area is said to accelerate biodegradation.

Application of dispersants has several goals (Curd, 2011; EMSA, 2009; IPIECA and IOGP, 2015; Prince, 2015; Wissenschaft, 2016): The main goal of application of chemical dispersion is to reduce the environmental impact caused by the floating slick on the water surface and on the shorelines, as well as the effort and waste associated with subsequent shoreline clean-up. In addition, the enhanced dispersion is considered to increase availability of the oil for biodegradation and reduce harmful vapours in the air, creating a safer workplace for response personnel.
On the downside, enhancing dispersion creates a potential risk of exposing marine organisms to hydrocarbons to a greater extent (EMSA, 2009; IPIECA and IOGP, 2015). Oil is not removed from the environment but displaced to another

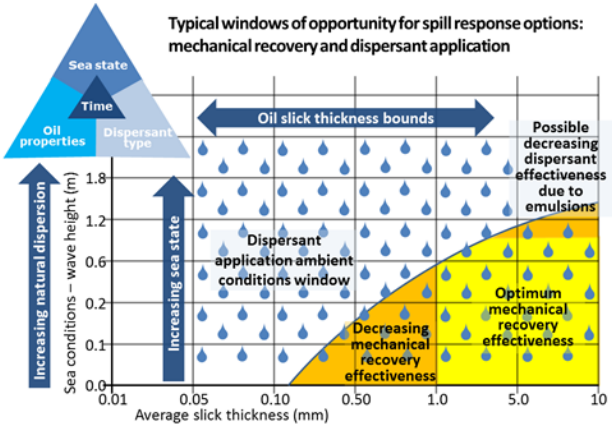

Fig. 1-1. Applicability of oil mechanical and chemical oil spill response as a function of sea conditions and slick thickness (figure source: www.amsa.gov.au *(AMSA, n.d.)).*

compartment; although no harm is expected after the more rapid dilution (and biodegradation). A conclusive answer on the effects after a spill is near-impossible to determine, let alone predict beforehand.

1.3.1 History of dispersant use

During the Torrey Canyon spill (1967), industrial detergents were used to clean the shoreline. In retrospect, the solvents used in these detergents were highly toxic to marine life, and caused more damage than the spilled oil itself (Lewis and Daling, 2001).

This incident did trigger development of detergents specifically for oil spill response (EMSA, 2009):
The first generation of dispersants, available in the 1970's, used hydrocarbon solvents with lower amount of aromatics. These were not very effective; the required dosage was 30-50%.
A more concentrated product was developed to overcome the logistic challenges associated with ship-board spraying of the required dosage of dispersants. Upon use, these concentrated products were diluted 10 times in seawater and applied with the existing equipment (for 30%50% dosing).
From 1985 modern concentrate dispersants were available, with much lower required dosage (3 to 5%). These dispersants can be applied from aircraft (helicopter and fixed-wing), and have shown efficiency with a wider range of oil types. These newer products have been proven relatively low-toxic themselves; potential adverse effects are limited to the enhanced exposure to oil itself.

Test methods
In addition to the development of better dispersants, a vast amount of research has been performed; ranging from field trials, to wave tank tests and various laboratory systems. Although the larger scale tests provide results more representative for real-life application, the level of control (of input and output) decreases (National Research Council of the National Academies, 2005). The different types of tests have their own advantages and disadvantages and provide insight in different aspects of the dispersion process. A selection of test types is described here:

Planned **sea trials**, including spill of opportunity testing, inherently provide the most realistic results. Due to costs and logistical constraints however, these cannot be performed frequently. In addition, many of the test-conditions cannot be controlled. As a consequence, the information provided on oil slick fate is somewhat anecdotal. Field testing has allowed operational testing of dispersant application systems and has been used as a means of validating modelling

studies, furthermore it has provided some important general insights in oil slick behaviour over time (National Research Council of the National Academies, 2005).

Wave tank testing provides a more controlled environment, and includes most of processes associated with dispersion (not all!). Although these tests provide a suite of qualitative information, obtaining quantitative results is difficult as oil concentrations in the test system are heterogenic in time and place. It is uncommon to achieve a 'closed mass balance' in these tests (CRRC, 2006), meaning that they do not provide conclusive answers on the short term fate of all the oil. Wave tank testing has allowed researchers to investigate the influence of wave action on the surface slick and the incorporation of dispersants (applied on top of the slick) into the oil, as well as compare effectiveness of dispersion under many different conditions (National Research Council of the National Academies, 2005; Zeinstra-Helfrich et al., 2015c).

Bench-scale testing allows for more repetitive testing and provides higher reproducibility through better control of conditions, yet the outcomes are less representative for application in the field. The bench scale tests differ in their methods of imparting mixing energy as well as analytical procedures, yet their main mode of action is quantification of the more stably suspended droplets. Some examples:
The **Baffled Flask Test (BFT)** (and its predecessor Swirling Flask Test (SFT)) is a small scale (120 ml seawater + 0.1 ml oil) laboratory tests, standardized for use for dispersant authorization (Sorial, 2006). Oil and dispersant are consecutively added to a flask containing seawater. The contents are mixed on a reciprocal shaker for 10 minutes then left to settle for 10 minutes. A 30 ml bottom sample is subsequently spectrophotometrically analysed for oil(/dispersant) content. The bottom sample analysis quantifies the portion of oil that remains in the water column after 10 minutes, either suspended in very small droplets or dissolved. This is a measure of the susceptibility of the treated oil to break up, and thus the 'chemical effectiveness' of the oil dispersant combination. These tests have proven to be reproducible between laboratories (Venosa et al., 2002). Baffled flask test results could not be successfully related to larger scale test results (Holder et al., 2015), presumably as this test does not encompass all elements of the dispersion process. Striking is the lack of a reference test (without dispersants), authorisation is therefore based on the performance of the dispersant-oil combination rather than the added benefit of the dispersants.
In the Institut Français de Pétrole (**IFP**) test, mixing is provided by a ring oscillating below the water surface. Sampling occurs continuously during and after mixing by a downward flow current, representing the dilution at sea. This

test is considered to represent low wave energies (Leirvik et al., 2012). The Mackay Nadau Steelman (**MNS**) test uses an air flow across the water surface to create surface waves in the circular test basin. After an initial mixing period of 5 minutes, a water sample for subsequent analysis is near the bottom of the tank while the mixing continues. In the Warren Spring Laboratory (**WSL**) test the test funnel (containing seawater, oil and dispersant) is rotated end-over-end for 5 minutes. A bottom sample is taken after one minute of settling.
Despite their limitations, bench scale test have allowed a lot of research in the effect of environmental conditions (temperature, salinity) on dispersant performance.

The test methods described here mainly focus on effectiveness of dispersion and dispersants. Research efforts on ecological effects and biodegradation of dispersants and dispersed oil, are equally impressive(Fingas, 2008; National Research Council of the National Academies, 2005)

1.3.2 Current dispersant use

Currently, there is an abundance of operational guidelines for dispersant use, their overall opinion is that before deciding on dispersant use, three points need to be considered; 1) the potential effectiveness, 2) the net environmental benefit, 3) the logistical feasibility;

1) Effectiveness
   In conditions with low wind speeds, mixing energy is insufficient for successful (effective) chemical dispersion. Chemical dispersion effectiveness in high energy conditions is also limited, as the added value compared to natural dispersion is limited and it becomes operationally difficult to successfully apply dispersants (National Research Council of the National Academies, 2005). Between these two extremes, the effectiveness of chemical dispersion is less tangible and will be dependent on the precise conditions.

Effectiveness of dispersant application to surface oil spills is mostly based on oil properties and wind speed, a few examples: In the Netherlands, chemical dispersion is considered feasible between 3 and 13 m/s winds and with oil viscosities from 0.5 to 5 Pa.s (Rijkswaterstaat, 2011; Rijkswaterstaat Noordzee, 2014). Australia considers 5 to 15 m/s winds suitable for chemical dispersion and ranges effectiveness based on viscosity in Pa.s: likely > 2 > possible > 5 > uncertain > 10 very unlikely (Australian Maritime safety Authority, 2013). The EMSA dispersant guidelines include a combined influence of sea state and oil properties (Fig. 1-2). These guidelines remain broad and not very quantitative, indicating that the assessment of expected effectiveness relies heavily on expert judgement in a spill situation (National Research Council, 2005a).

Available oil spill fate and transport models can only provide limited information on the net effectiveness of dispersants. Natural dispersion is modelled based on the formulations by Delvigne and Sweeney (1988), that are considered too empirical and based on too narrow conditions (National Research Council of the National Academies, 2005; Reed et al., 1999). Chemical dispersion is modelled as a separate process, instead of as an enhancement of natural dispersion. In these models chemical dispersion calculation requires input of the dispersant effectiveness rather than provide output on it.

2) Environmental benefit

In most guidelines about dispersant use, adverse effects in the water-column are assumed not to occur if hydrocarbon concentrations remain sufficiently low. Many dispersants policies include a minimum depth, so that there is enough water for dilution and direct exposure of the (less mobile) benthic system is avoided (see the box on this page).

Combining the absence of water column effects with the avoidance of

Sea State / Oil Viscos.	0-1	2-3	>3
<500 cSt	Possible on limited spill with mixing energy	easy	easy
500-5 000cSt	none	possible	easy
5 000-10 000cSt	none	uncertain	possible
>10 000cSt	none	none	uncertain
>>10 000cSt	none	none	none

Fig. 1-2. Feasibility of chemical dispersant application based on sea state and oil viscosity.(Figure source: FX Merlin & K Lee, taken from (EMSA, 2016)). For comparison; 1000 cSt ≈ 1 Pa.s.

surface effects, provides a positive indication of net environmental benefit (EMSA, 2009).

3) Logistical feasibility
Logistical feasibly of chemical dispersion requires that: 1) The required amounts of dispersant and equipment are available; 2) The slick can be reached and treated within the window of opportunity for effective dispersant use; and 3) the weather conditions allow mobilisation of the equipment as well as successful dispersant application.

National and international policies dictate if and when dispersant application as a spill response is deemed appropriate. The policies differ in their attitude towards dispersants as well as the limits within which dispersants are deemed acceptable (EMSA, 2014). Such policy reflects a nation's overall oil spill response strategy and their local species and habitats.

It is clear that despite the shear amount of research that has been conducted over the years, dispersant use on spilled oil remains a topic of debate and questions (Chapman et al., 2007; CRRC, 2006; EMSA, 2009; Lee et al., 2015). This can partly be attributed to the inherent uncertainty in environmental impact of an accidental spill, but might also be due to the fact that natural and chemical

Some examples of dispersant policy:

In the Netherlands, dispersants are considered if mechanical recovery of the oil proves insufficient in protecting sensitive areas (Rijkswaterstaat Noordzee, 2014). Adverse effects are avoided by dispersion in waters deeper than 20 meters and not near sensitive resources (shellfish beds, aquaculture, nearshore fish spawning areas) (Rijkswaterstaat, 2011). The Dutch rely on external contractors for dispersant application and base dispersant authorization on test results of the other Bonn Agreement countries (EMSA, 2014).

In the United Kingdom, dispersants are considered the preferred oil spill response method for logistic reasons (unlikeliness of an oil spill response vessel reaching the site in time) (EMSA, 2010). Dispersant application is pre-approved for water depths exceeding 20 meters, within the 20m isobath a case-by-case decision is made in consultation of (nature conservation agencies, fisheries, marine environmental scientists and marine fisheries agency inspectors). Specific facilities (ports, oil handling facilities) can be granted pre-approval for a limited amount of dispersants. Dispersant approval protocol includes an (WSL) effectiveness test, as well as a sea-toxicity test and a rocky shore-toxicity test on both the dispersant as dispersed oil (EMSA, 2016). The UK considers a separate class of 'offshore' products, which will not be used on or near sensitive rocky shorelines and therefore do not have to undergo the rocky-shore toxicity test.

In France, three geographical limits are pre-defined, outside which pre-authorization exists for dispersion of 3 different spill sizes (10, 100, 1000 tonnes). The geographical limits are generally based on water depth (>5, >10, >15 m) and distance to the mainland (>0.5, >1, >2.5 nm), but do also include presence of ecologically sensitive areas. France permits use of specific brands of dispersants after they pass an (IFP) effectiveness test, a toxicity test, and a biodegradability test.

dispersion are simultaneous and complementary processes. All types of effects (fate, environmental impact etc.) are due to the combined influence of natural and chemical dispersion, making the NET effects difficult to separate.

1.4 Aim and outline

Given the uncertainties with regard to natural and chemical dispersion, this thesis aims to; increase the understanding of the physical processes of natural and chemical dispersion, in order to create more insight in the fate of the oil with and without dispersants. With this insight we aim to provide a means to predict the performance of chemical dispersion based on the (incident) parameters readily available.

The outline of this thesis follows the chronological approach during the course of the project:

A conceptual model for the (natural & chemical) dispersion process was defined (**chapter 2**). Based on this model, literature is analysed to understand how well each of the steps is understood, and which topics need further research.

In order to investigate the entrainment process and initial breakup into droplets, a plunging jet test system was developed (**chapter 3**). Using the plunging jet system, the effect of oil properties on the entrainment and breakup process was investigated (**chapter 4**) and incorporated into algorithms.

A model for slick elongation and transport was developed (**chapter 5**), and used to investigate the effect of key parameters on the slick surface expression, yielding quantitative indications of the net benefit of dispersants.

In the general discussion of this thesis (**chapter 6**), the results are summarized and discussed. Implications of the findings are given, and topics for further research are defined.

CHAPTER 2

The NET effect of dispersants - A critical review of testing and modelling of surface oil dispersion

M. Zeinstra-Helfrich[a,b], W. Koops[b], A.J. Murk[a]

Zeinstra-Helfrich, M.; Koops, W.; Murk, A. J.(2015): The NET effect of dispersants — a critical review of testing and modelling of surface oil dispersion. Marine Pollution Bulletin. 100. 102-111

---

[a] Wageningen University and Wageningen-IMARES, Sub-department of Environmental Technology
[b] NHL University of Applied Sciences, Dept. Maritime, Marine, Environment & Safety

Abstract

Application of chemical dispersants or mechanical dispersion on surface oil is a trade-off between surface effects (impact of floating oil) and sub-surface effects (impact of suspended oil).Making an informed decision regarding such response, requires insight in the induced change in fate and transport of the oil. We aim to identify how natural, chemical and mechanical dispersion could be quantified in oil spill models. For each step in the dispersion process, we review available experimental data in order to identify overall trends and propose an algorithm or calculation method. Additionally, the conditions for successful mechanical and chemical dispersion are defined.

Two commonly identified key parameters in surface oil dispersion are: oil properties (viscosity and presence of dispersants) andmixing energy (often wind speed). Strikingly, these parameters play a different role in several of the dispersion sub-processes. This may explain difficulties in simply relating overall dispersion effectiveness to the individual parameters.

2.1 Introduction

In order to reduce the adverse impact of an oil spill, different response options are available, including mechanical and chemical dispersion of surface oil. Both these oil spill mitigation options enhance the natural dispersion process thereby modifying the fate of the oil from the water surface into the water column. This means that effective chemical (or mechanical) dispersion results in a trade-off between surface effects and subsurface effects.

In order to carefully weigh the pros and cons of enhancing the natural dispersion process, the **net effects** of such action should be known. The net effects of chemical dispersants or mechanical dispersion are the additional or reduced effects compared to natural dispersion. Among others, such net effects could be:

- Decreased evaporation of volatile organic compounds (VOC) when there is less surface oil (Curd, 2011).
- Enhanced water accommodated fractions (WAF) of oil as a result of enhanced dissolution from oil being mixed into the water column (Ramachandran et al., 2004).
- Less oil reaching coastal areas (Prince, 2015), due to changed fate and thinning of the slick.

The exact extent of these effects depends on how chemical or mechanical dispersion affects oil fate. This **net effectiveness** is the change in fate of the oil due to the response, in terms of slick size, location and the resulting oil concentration in the water column. Net effectiveness of (mechanical or chemical) dispersion depends on several factors, among which environmental conditions and oil type. This will be further discussed in paragraphs 2.3 and 2.4.

To assess the net effectiveness of chemical dispersion, the mass balance and trajectory of the oil slick without dispersants should be compared to the mass balance and slick trajectory for the slick treated with dispersants. In general, this is done by modelling.

Several commercial and academic oil spill fate models are available, some of which calculate both horizontal transport (location of oil) and physical fate or weathering (oil properties & amount), while others only assess the weathering. Some well-known models, available to spill responders are; SIMAP (French-McCay, 2004; French-McCay and Payne, 2001), OSCAR (Aamo et al., 1997; Reed et al., 2004, 1997, 1995; Reed and Rye, 1995), ROC (Dale, 2011; Galt, 2014; Galt and Overstreet, 2009; Genwest Systems, n.d.) and ADIOS2 (Lehr et al., 2002; NOAA/HAZMAT, 2000).

In all these models, algorithms for natural dispersion are based on the work of Delvigne and Sweeney (Delvigne and Sweeney, 1988; Reed et al., 1999). Several authors have pointed out Delvigne and Sweeney's work to be highly empirical and based on a too narrow range of parameters, including the authors themselves (Delvigne and Sweeney, 1988; National Research Council of the National Academies, 2005; Reed et al., 1999).

Some of the oil spill models are claimed to simulate the effect of chemical dispersion; however these models require INPUT of dispersant effectiveness (which is not yet quantified) rather than this being output of the model (National Research Council of the National Academies, 2005).

In summary, current oil spill models still use the calculations of Delvigne and Sweeney for entrainment and natural dispersion of surface oil, although the underlying algorithm leaves room for improvement. Chemical dispersion algorithms in these models are comparatively simple and require a user-specified dispersant efficiency. In these models, natural dispersion and chemical dispersion are simultaneous but separate processes.

We consider chemical dispersion as an amplification of natural dispersion instead of a separate and additional process. This means that one approach or algorithm could be used for all dispersion options, where only the values of the input parameters (e.g. the oil properties) differ depending on the response. This will enhance the transparency and reliability of the model calculations to aid responders in their decision making process.

This study aims at identifying how natural, chemical and mechanical dispersion can be quantified with different parameters in one algorithm. We do so, by identifying the distinct steps in the dispersion process. Following mechanistic understanding of the sub-processes, reported field and laboratory test results are used in an effort to extract missing parameters. Finally, knowledge and information gaps are identified, and future perspectives for extending the current oil dispersion models discussed.

2.2 Approach

The dispersion process was split up into smaller sub-processes (par. 2.3). The processes relevant for effectiveness of mechanical or chemical dispersion are reviewed one by one (par. 2.4). The goal of this analysis was to define; the relevance of the process in determining the net effectiveness of the response and net effects on the environment; which factors are likely to influence this

process, and, how these factors influence the process according to the different publications.

Based on these findings we identify what is still needed to improve modelling of natural, chemical and mechanical dispersion.

2.2.1 Defining a conceptual model

Based on review of a collection of descriptive literature (Cedre, 2005; EMSA, 2009; ITOPF, 2012; Merlin and Peigné, 2007), a conceptual model was defined in which the dispersion of oil at sea was separated into several smaller steps (par. 2.3, Fig. 2-1).

In the conceptual model, we consider the physical and chemical processes that lead up to the (net) effects. In our subsequent analysis we focus on the processes that determine the net effectiveness; the fate of oil with and without chemical or mechanical dispersion.

2.2.2 Collection of experimental dispersion data

An abundance of data is available on dispersion testing, including numerous literature reviews. A particularly comprehensive and accurate review was performed by the Committee on Understanding Oil Spill Dispersants: Efficacy and Effects, as published by the National Research Council of the National Academies(2005). As this review is very complete, either information regarding work prior to 2005 was taken from their reference list, or the conclusions from the NRC report were adopted.

For work published between January 2005 and July 2015; a search was performed via Science direct and Google Scholar with various combinations of keywords: oil spill, crude oil, dispersion, dispersant, chemical dispersion, mechanical dispersion and the names of the different processes as mentioned in chapter 3. Additionally, a web search was performed with these search words, to reveal experimental results in the field of oil spill science that only are available in grey literature. All sources were included that discuss experimental results of (physical and chemical processes of) oil-in-water dispersion in the field of mineral oil spill fate or behaviour.

2.3 Main processes involved in dispersion at sea

The dispersion of oil in seawater is the result of multiple simultaneous processes. These processes can work in conjunction or against each other. In

this chapter we describe the conceptual model that was defined based on sub-processes of dispersion.

Oil gets initially suspended into the water column ([A] in Fig. 2-1) via breaking waves that 'push' local portions of the slick beneath the water surface, so called entrainment. Entrainment of very viscous oils or emulsions results in large lumps that are temporarily submerged. Oils that are less viscous and thus less resistant to deformation are broken up into droplets by the underwater turbulence and/or the shear of the plunging movement of the waves. The droplets formed are mixed or distributed within a water layer of a distinct depth below the sea surface, the so-called mixed layer. Within this mixed layer, a balance exists between droplet break up and coalescence. The droplets in the mixed layer are broken up further by the turbulence and encounter between droplets leads to coalescence and formation of larger droplets. When suspended, the droplets are transported by turbulence, local currents and their tendency to rise.

Most oil types are positively buoyant, and therefore formed droplets will always

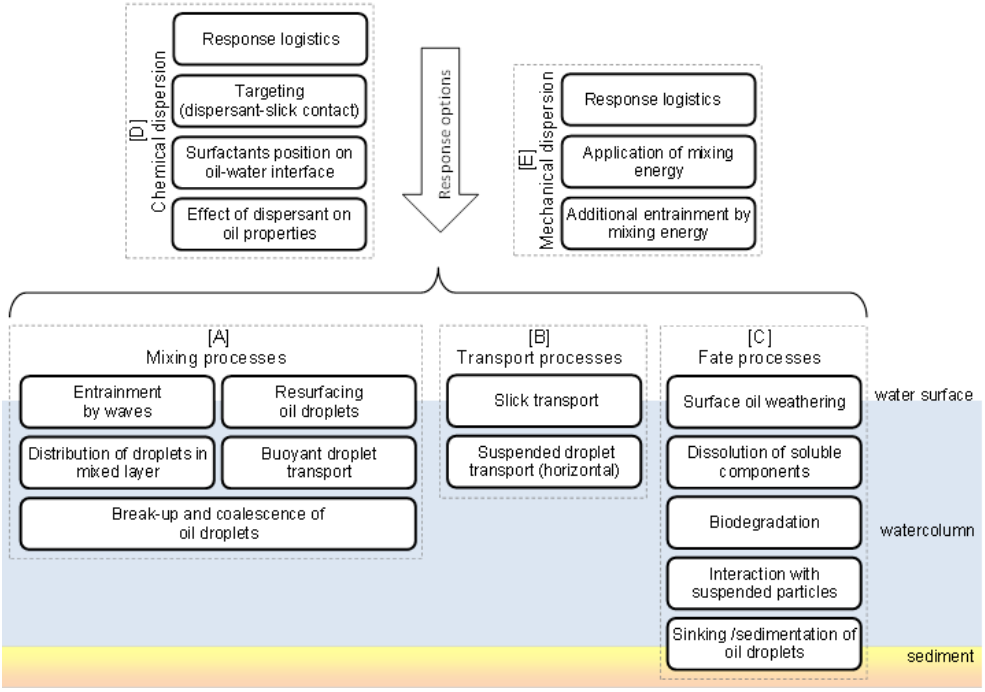

Fig. 2-1. Schematic overview of our conceptual model of the sub-processes involved in oil dispersion at sea. As the (net) effects of dispersion is the scope of this paper, our literature review focuses on the processes A, D & E.

rise in quiescent water. The largest oil droplets will rise back to the surface slick fast, while smaller droplets can remain suspended longer before they resurface. Some droplets are so small that they are semi-stable and local turbulence can keep them suspended.

The (environmental) benefit of dispersion is based on the changed transport of the oil and resulting dilution ([B] in Fig. 2-1). Enhanced vertical transport also causes altered horizontal oil transport. Suspended oil droplets move with the speed and direction of the local currents, but a floating oil slick moves with the currents and by wind drag. This wind drag is the main differential movement between the slick and the suspended oil droplets. How the fate of an oil droplet or lump differs relative to the oil slick, depends on how long it remains in the water column before resurfacing (Fig. 2-2).

Droplets remaining in the water column until the next breaking wave are redistributed along the mixing depth, together with the newly entrained oil. Droplets remaining suspended for a sufficiently long period of time will resurface outside of the slick that is moved by the wind, forming the thinner 'tail' of the slick. This wind shear effect creates a comet-like tail on the oil slick, as has been observed in several field trials at sea (Daling et al., 2003; Lewis et al., 1995; Merlin et al., 2006).

While the oil droplets are suspended in the water column, other processes occur ([C] in Fig. 2-1), like dissolution of more soluble light oil components, interaction between the oil droplets and particulate matter and biodegradation. This will

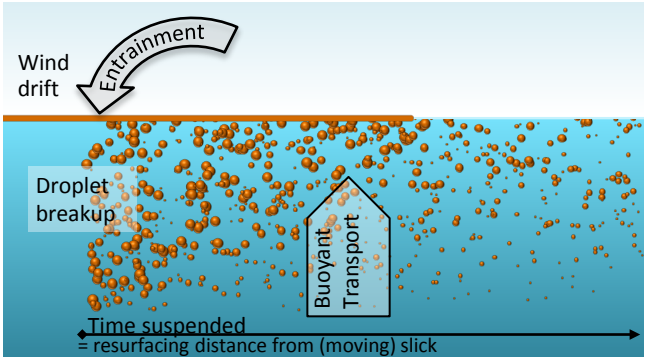

Fig. 2-2. Visualization of the mixing processes. Under a breaking wave oil is entrained, broken into droplets of various sizes and distributed over a certain depth. While the oil droplets are suspended the slick is pushed along by the wind. Droplets resurface upwind from their original location (in the moving slick), of which the distance depends on the time in suspension. As a droplets rise speed is determined by its diameter, the residence time in the water column is determined by its mixing depth and droplet diameter.

change the properties of the oil droplets, which may even sink to the sea floor.

Specific for surface oil is the process of weathering, including water-in-oil emulsification, evaporation of volatile components and photo-oxidation. This too will greatly influence oil properties.

The processes distinguished are relevant for natural dispersion as well as for chemical and mechanical dispersion. To include the consequences of an oil spill response, some additional processes have to be considered: Mechanical dispersion adds energy to that provided by the waves, so enhanced entrainment is expected. How much oil is affected by mechanical dispersion depends on (Fig. 2-1, E): the logistics of the response (how much oil can be treated), and the entrainment efficiency (how much of the treated oil is entrained).

Chemical dispersion changes the oil properties, thus affecting the oil behaviour in the distinguished processes. The effect of chemical dispersion depends on (Fig. 2-1, D): response logistics and targeting (how much oil is treated?), dispersant incorporation on the oil-water interface (what effective dose is reached?) and the effect of the dispersants on the oil properties (how effective is the dispersant on this specific oil type?).

As the scope of present paper is to define the net effectiveness of chemical or mechanical dispersion, we limit our analysis to; Mixing processes [A], Chemical Dispersion [D] and Mechanical Dispersion [E]. The fate processes [C] can greatly influence the net effects of chemical and mechanical dispersion, but as their impact on the short term (sub-surface) oil mass balance is very small their contribution to the overall effectiveness (changed fate) is limited. The (horizontal) transport processes [B] do play an important role in the dispersion process by facilitating the differential transport between slick and entrained droplets. This depends on local environmental conditions at time of the spill and will be the same for natural, mechanical or chemical dispersion in a given situation. As the horizontal fate processes are not affected by the response, they are excluded from our current analysis.

2.4 Results

The majority of the data sources found could be assigned to specific sub-processes, based on either the input variables or the measured output. For instance: sources that include droplet size measurements are applicable for modelling break-up and coalescence, consequences of variation of wave types is usable to describe the entrainment, and so on. We had to ignore (the abundance of) sources that investigate dispersion effectiveness with oil-dispersant

combination as only input variable and dispersion effectiveness as output variable, due to their limited relevance for our particular aim.

2.4.1 General aspects of the dispersion process

Known key parameters with a great influence on the natural dispersion process as well as on the effectiveness of chemical dispersion are oil viscosity and wind speed:

High viscosity of the oil (originally, or by weathering) is known to impede natural dispersion as well as chemical dispersion. Developments in dispersant formulation as well as in application method and strategy have raised the upper 'limit' for chemical dispersability from 2000 cP in the 1980s to up to 20000 cP at present (Committee on Effectiveness of Oil Spill Dispersants et al., 1989; Fiocco et al., 1999; Guyomarch et al., 1999 in National Research Council of the National Academies, 2005). At very low viscosities (<1000 cP) chemical dispersion is deemed unnecessary as natural dispersion will suffice (ARPEL Emergency Response Planning Working Group, 2007; EMSA, 2009; ITOPF, 2012; Lewis, 2007; Rijkswaterstaat, 2011). This is a 'rule of thumb' guideline and also depended on energy conditions (at higher energy, higher viscosities can be dispersed) (SL Ross Environmental Research LTD et al., 2005).

Sufficient mixing energy is necessary for either form of dispersion. For natural dispersion a minimum wind speed 5 m/s is required, as this is the onset of formation of breaking waves (Delvigne and Sweeney, 1988; National Research Council, 2005b). Above that, a higher wind speed ensures a higher dispersion rate by both the increase in frequency of breaking waves as well as increase in energy exerted by those waves (indirectly, via wave height) (Delvigne and Sweeney, 1988). The limit of 5 m/s is backed up by sea trials, where no dispersion was observed at wind speeds 8 to 9 knots (4.1 – 4.6 m/s) and considerable dispersion at 14 knots (7.2 m/s) (Trudel et al., 2005).

2.4.2 Mixing processes (oil in water)[A]

The natural dispersion of oil is currently modelled based on the work of Delvigne and Sweeney(Delvigne and Sweeney, 1988). In their formulae the entrainment rate of oil droplets (Q_r) is calculated for each (user defined) droplet size interval Δd around do per unit surface area, $Q_r(d_o)$ (in $kg/m^2.s$). Input parameters are: oil constant C* based on oil properties, dissipated breaking wave energy D_{ba} (in J/m^2), a fraction of sea surface hit by breaking waves per unit time F_{bw} (in /s), and the fraction of sea surface covered by oil S_{cov}. Based on empirical findings, Delvigne and Sweeney's algorithm is: $Q_r(d_o) = C^* \cdot D_{ba}^{0.57} \cdot S_{cov} \cdot F_{bw} \cdot d_o^{0.7} \cdot \Delta d$.

This relationship indicates entrainment as well as net droplet breakup (& coalescence). Subsequently, the resurfacing of the droplets can be calculated based on their submergence depth (droplet mixing depth z_i = 1.5 · breaking wave height, H_{bw}) and rise speed.

Dispersants change the interfacial tension between oil and seawater resulting in creation of smaller droplets. As the Delvigne & Sweeney algorithm does not allow input of the interfacial tension or dispersant to oil ratio (DOR), it is not suitable for calculation of the effect of chemical dispersion. Our suggestion is to calculate entrainment, droplet formation and vertical droplet transport as a function of energy input and oil properties, the latter being subject to dispersant induced changes.

Entrainment

The initial entrainment of oil is an important step in the dispersion process, as it determines the amount of oil available for other processes such as dissolution of more hydrophilic compounds. Without entrainment, no dispersion can occur.

We propose to determine entrainment flux as a balance between vertical energy input and oil layer resistance. To calculate the (vertical) entrainment energy, input is needed based on breaking wave height, impact surface, and a term for oil layer resistance governed by layer thickness, oil viscosity and possibly oil-water interfacial tension.

The important contribution of breaking of waves to dispersion efficiency (DE) has been demonstrated in several wave tank studies by Li and colleagues (Lee et al., 2009; Li et al., 2010, 2009a, 2009c, 2008). Plunging breaking waves increased dispersion DE with 25% compared to regular (non-breaking) waves. Spilling breaking waves are more efficient than regular waves and less efficient than plunging breaking waves. Regular waves merely move the oil on the water surface, rather than dispersing it (Venosa et al., 2008).

Under non-breaking waves in a medium scale wave tank, only lower viscosity oil could be chemically dispersed (SL Ross Environmental Research LTD et al., 2006a). The same group of researchers found negligible natural and chemical dispersion under such regular waves in a realistic full scale wave tank. However, chemically treated oil already dispersed after other (unintentional) vertical energy inputs such as measuring systems transecting the water surface and a rain shower.

Although a negative effect of viscosity on oil dispersion is anticipated, its specific effect on entrainment is not quantified. The effect of oil layer thickness on entrainment has only recently been reported (Zeinstra-Helfrich et al., 2015a).

One study investigated oil layer resistance to entrainment: Artificially weathered oil layers, with increasing viscosity and layer thickness, required higher plunging jet energy (from a greater height) in order to become submerged (Johansen et al., 2015; Reed et al., 2009). Very viscous oil types could not be submerged by the plunging jet at all. In these experiments no dispersants were applied.

More specific information on the effect of oil layer properties and energy input on the entrainment of oil is needed to be able to improve the entrainment prediction.

Breakup & coalescence

The net droplet breakup and coalescence rate, determines the droplet size distribution of the dispersed oil. The droplet size of the dispersed droplets greatly influences their (buoyant) transport, as well as subsequent processes such as dissolution of less hydrophobic compounds and biodegradation.

More information on the mechanism of droplet formation is available from interfacial and colloid sciences, performed for example in the context of food sciences research. The currently available theories on droplet formation apply to steady-state situations in closed systems, which will not be the case at sea. The main principles, however, will still apply at sea and can be included to explain the test results.

The breakup and coalescence of droplets is a balance between external hydrodynamic forces deforming the droplet and the internal forces within the droplet counteracting. The first is determined by the mixing energy, the latter depends on oil characteristics (with or without dispersants).

In general, dispersants lower the interfacial tension between the phases which enables breakup into smaller droplets. A higher oil viscosity results in larger droplets. A greater volume fraction of oil will lead to a higher coalescence chance of the droplets with larger average droplet size as result. Greater mixing energy leads to smaller droplets. Additionally, the characteristics of the continuous phase, such as viscosity and density will slightly affect droplet size. In the case of seawater this is deemed irrelevant as the viscosity of seawater is fairly constant and also density will not be too different under average oceanic conditions. Deep sea brine and colder water, though, will have greater density.

Wave tank and laboratory results of size of oil droplets formed are consistent with these theories:

The effect of dispersants on the size of oil droplets formed in wave tanks is very clear (Fig 2-3). The median diameters of naturally dispersed oil are above 80μm

(o) whereas for chemically dispersed oils most median diameters are below 80μm (•), with some exemptions for oils with a viscosity of more than 2000 cP.

Similar differences in average droplet size are observed under plunging breaking waves at the Bedford Institute of Oceanography wave tank (Fig. 2-4, lower panel): without dispersants, all mean droplet sizes are above 80μm while with dispersants, the mean droplet diameter for medium to low viscosity oils is below 100μm. The same exemption for higher viscosity oil was found with IFO 180 (2471 cP), where application of dispersant reduced the droplet size from approximately 200 to 150 μm. In the SINTEF wave flume, a low viscosity oil (MC252, viscosity not measured) had a volume median droplet size after 5 h of 75 μm without dispersants, and 17 μm with dispersants (Brakstad et al., 2014).

It is clear that for low and medium viscosity oil dispersants drastically decrease the droplet size formed under plunging breaking waves. For high viscosity oils the effect of dispersants is less prominent both in large (Fig. 2-3, Fig. 2-4)) and small scale tests (Mukherjee et al., 2012).

Furthermore, in different laboratory experiments the droplet sizes are found to decrease with increasing DOR (Brandvik et al., 2013; Johansen et al., 2013;

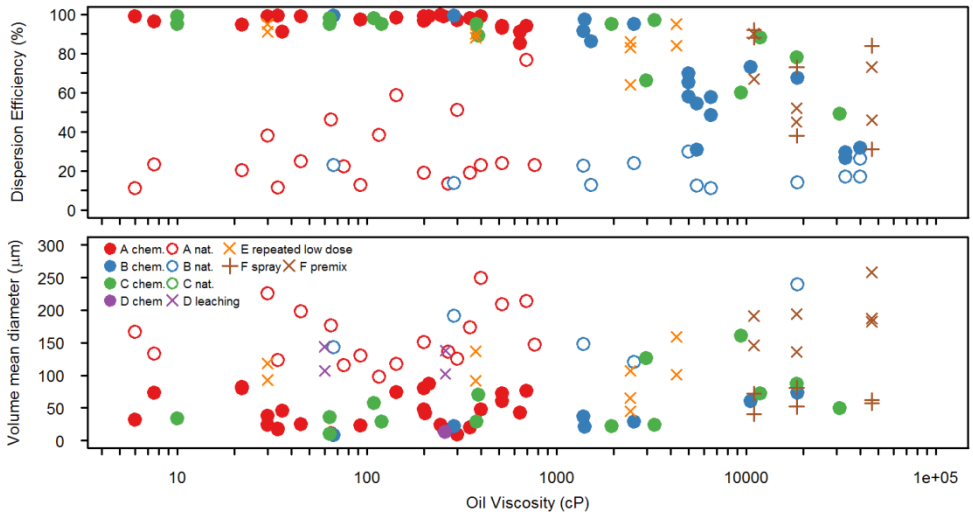

Fig. 2-3. Droplet size (Volume Median Diameter) and Dispersion efficiency (DE) of naturally (open symbols) and chemically (closed symbols) dispersed oil under plunging breaking wave conditions in wave tank tests, vs viscosity. Data sources A (Belore et al., 2009), B (SL Ross Environmental Research LTD and MAR Incorporated, 2011)*, C (Trudel et al., 2010). (x's represent alternative application strategies; D (Lewis et al., 2010), E (SL Ross Environmental Research and MAR Incorporated, 2010), F* (SL Ross Environmental Research and MAR Incorporated, 2009) *as described in chapter 2.4.3).*

Mukherjee et al., 2012; Mukherjee and Wrenn, 2011) until the optimal DOR of around 1:20 is reached. With higher DOR the droplet sizes of dispersed oil remain the same or even increase (Khelifa et al., 2007; Khelifa and So, 2009).

In general, the droplet size increases with viscosity (Fig. 2-4). For a set of lab-experiments with the same DOR and energy, the 'Sauter mean diameters' (d_{32})[b] consistently ranked in order of both viscosity as well as interfacial tension (example in Table 2-1Table 2-1). A consistent relationship between viscosity and droplet size cannot be identified (Canevari et al., 2001; Fingas et al., 1991). The effect of viscosity seems less pronounced in large scale tank or field tests than in laboratory tests, especially at lower mixing energies (Mukherjee and Wrenn, 2011).

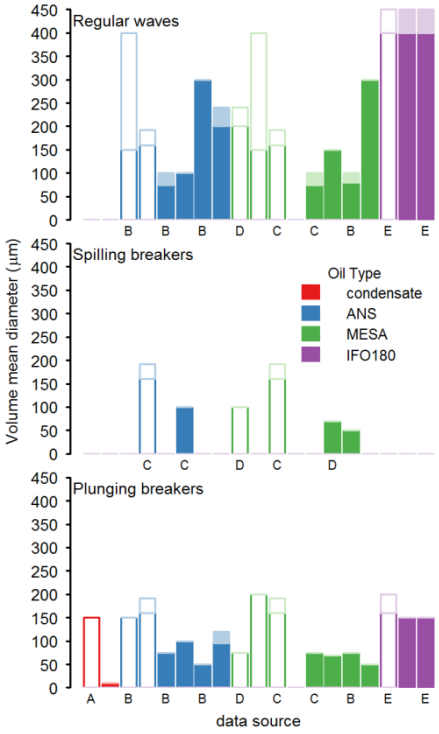

Fig. 2-4. Droplet sizes (Volume Mean Diameter) depending on wave conditions studied in wave tanks, with (filled) and without (open) dispersants. The figure is constructed based on data from: A (Li et al., 2007), B (Li et al., 2009a) C (Lee et al., 2009), D (Li et al., 2008) E (Li et al., 2010), single (dark) bars are single values, lighter upper bars indicate a range). Oil types (colours) are ranked in order of increasing viscosity (left to right).

[b] The Sauter mean diameter of a droplet size distribution is the diameter of a droplet with a volume-surface area ratio equal to the mean of the entire distribution.

Table 2-1. Droplet sizes formed in Baffled Flask tests with DOR 1:100 and 0.16 W/kg mixing energy, with physical properties as indicated in the table (Mukherjee et al., 2012).

Crude oil name:	Arabian Light	Mars	Lloyd
Viscosity (Pa.s)	0.0162	0.163	8.580
Interfacial tension (mN/m)	0.21	1.35	14.73
Sauter mean Diameter, D_{32} (μm)	7.5	11	22.5

Wave tank experiments show the expected effect of energy on the dispersed droplet size (Fig. 2-3). Plunging breakers (being the most energetic wave type) generate smaller droplets than the other wave types do. This can be explained by the (much) higher energy dissipation rate (ε) in plunging breaking waves (1 m^2/s^3) compared to spilling (0.1 m^2/s^3) or non-breaking waves (0.005 m^2/s^3).

In laboratory tests, higher mixing energy creates smaller droplets (Mukherjee and Wrenn, 2009, 2011). Researchers have managed to scale droplets size with energy dissipation rate (ε) by using dimensionless numbers associated with flow around bubbles and bubble formation (Reynolds & Weber) (Mukherjee et al., 2012). This droplet size model could also be fit to the droplet sizes determined in Delvignes wave tank experiments(Delvigne and Sweeney, 1988; Mukherjee et al., 2012). The observed scaling factors for droplet size ($\varepsilon^{-1/4}$ and $\varepsilon^{-2/5}$), indicate that a 10 fold increase in energy dissipation rate (the difference between spilling breakers and plunging breakers), would make droplets a factor 1.78 to 2.51 smaller.

Although droplet sizes generally decrease with increasing mixing energy, there is interaction with the oil properties (Mukherjee, 2008; Mukherjee and Wrenn, 2009). At higher mixing energy, the influence of viscosity on droplet size, is less pronounced (Mukherjee et al., 2012; Mukherjee and Wrenn, 2011).

Interestingly, multimodal droplet size distributions (mostly tri- and bi-modal) appear in both wave tank (Lee et al., 2009; Li et al., 2009b, 2007; Wang et al., 2011) as well as bench-top experiments (Li et al., 2011a; Mukherjee, 2008; Mukherjee et al., 2012; Mukherjee and Wrenn, 2009, 2011; Wrenn et al., 2009). An explanation given for this multimodality is so called tip streaming, where the relative water flow around a moving oil droplet pushes the surfactant surrounding the oil to the back of the droplet (Gopalan and Katz, 2010; Katz, 2009). The resulting locally elevated dispersant concentrations cause micro threads extending from the oil droplets that then can breakup into much smaller droplets.

The location of the modes of these multimodal distributions, differ between test setups (lab modes ~ 3.5, 10.5 and 30 μm, wave tank modes ~ 27, 81 and 142 μm), but appear constant within the setups. Overall observations of the size distribution behaviour (in this case, distribution among groups instead of mean

droplet size) do indicate similar relationships as described earlier in this paragraph:

the probability of droplets forming in the smallest size category, increased from just above 0% to near 100% with application of dispersant (Corexit 9500) (Li et al., 2011b). This average probability is also higher for breaking waves (67%) than regular waves (40%) (Li et al., 2011b).

In another laboratory study, increasing DOR from 1:100 to 1:25, enhanced the average percentage of the smallest size droplets from 8% to 25% (Mukherjee and Wrenn, 2011). Here, oil type also had clear effects: With the highest mixing energy and DOR, the percentage of droplets in the smallest size category was 60-70% for the low & medium viscous oil (0.182 and 1.563 cP) and dropped to below 10% for the highest viscosity oil (64.10 cP). At the lowest mixing energy, the fractions were almost 30% for the low viscosity oil and below 5% for the medium and high viscosity oil. Increasing the mixing speed also favours smaller droplets: the average presence of droplets in the smallest size class increased from 6% (125 RPM), to 14% (150 RPM) and 30% (200 RPM).

The droplet sizes discussed here are measured as result of (the balance between) break-up and coalescence of oil droplets. Hardly, these processes are studied specifically. Dispersant application enhances breakup, but does not seem to counteract coalescence (Sterling et al., 2004).

The (mean) droplet size is an indication of the relative portion of (entrained) oil in each size group (with suspension time t), but does not indicate the quantity of oil suspended. As can be seen in the top panel of Fig. 2-4, dispersion efficiency (% of oil) does not correlate with droplet size of the dispersed oil. This has been shown in bench-scale experiments as well as in wave tanks (Byford et al., 1984; Daling et al., 1990; Fingas et al., 1995; Lunel, 1995) in (National Research Council of the National Academies, 2005).

The droplet size results are consistent with general relationships in colloid science theory. There is still a need for algorithms to predict droplet sizes formed under the mixing conditions at sea, based on the environmental conditions and oil properties at hand.

Vertical transport of droplets

Almost all oil is lighter than water, after being pushed down in the entrainment process it will therefore resurface due to buoyancy. The vertical transport of the suspended oil droplets, determines their residence time in the water column and therefore their differential horizontal movement from the oil slick.

We suggest to estimate the vertical movement of oil droplets by modelling or assuming an initial intrusion depth during entrainment, and modelling subsequent droplet transport to the surface with Stokes law and local hydrodynamic conditions such as Langmuir circulation, turbulence, currents and of course subsequent breaking wave events.

In wave tank experiments, the oil intrusion depth increases with wave energy from 9 cm for non-breaking waves, to 17 cm for spilling breakers and 100 cm for plunging breakers (Li et al., 2008). The same group of scientist also reported energy dissipation rates of plunging breakers to extend to greater depths than those of regular waves (Lee et al., 2009). It is unclear whether this deeper intrusion is merely due to higher energy dissipation rate of the breaking waves, or whether the more complicated wave mechanics in plunging breakers plays a role.

In the models discussed, a mixed layer with uniform oil concentrations is assumed. Dye trials visualizing the mixed layer revealed that oil concentrations were not uniform within this layer (French McCay et al., 2007; Payne et al., 2009), this was attributed to Langmuir circulation. Transport of the dye (thus that of suspended or dissolved substances) could not be modelled with advection alone, therefore diffusion coefficients were determined. Net vertical diffusion coefficients were one to two orders of magnitude smaller than horizontal diffusion coefficients, indicating that vertical transport by passive diffusion is not relevant compared to the buoyant rising velocity of oil in water.

Modelling of the buoyant transport of oil droplets under quiescent conditions, can be done following Stokes' law, for example when describing the oil in water settling step in dispersion testing (Robbins et al., 1995; Sterling et al., 2004). Under turbulent conditions, the net droplet rising velocity generally also follows stokes law (Katz, 2009). Exception is in the case of very high turbulence where droplets rise faster than their rise rate in quiescent conditions (Katz, 2009).

Finally, when the dispersed oil resurfaces, it can re-coalesce with the slick, or form a new slick depending on where it resurfaces. Additionally, oil resurfacing underneath a slick is a mechanism that can result in the formation of water-in-oil emulsion, due to encapsulation of water between the oil droplets. This will impede further dispersion as viscosity of water in oil emulsion is higher than that of the pure oil.

No model yet exists describing resurfacing of oil. It also is unknown whether the properties of un-emulsified, resurfaced oil differ from those of oil that remained on the water surface. Wave tank experiments suggest that resurfacing oil does

not spread evenly but forms small patches or streamers (DeCola and Fingas, 2006; Fingas and DeCola, 2006), however this might be an effect of the confinement of the wave tank (Nedwed and Coolbaugh, 2008).

Summarizing main mixing processes

The stimulating effect of breaking waves on oil dispersion is threefold: 1) Breaking waves entrain more oil than regular waves due to the plunging breakers vertical motion. 2) Intrusion depth of oil droplets increases 10 fold with plunging breakers compared to regular waves. 3) The higher energy dissipation rate causes breakup into much smaller droplets, resulting in longer water column residence times.

Oil viscosity is the main oil characteristic that determines entrainment and residence time of oil in water. A viscous oil layer is expected to impede entrainment and viscous oil is expected to form larger suspended oil droplets that will resurface relatively quickly. Although viscous oils in general have higher densities and thus slightly lower rise velocity, this cannot be compensated by the relatively higher rise velocity due to the larger size of the dispersed oil droplets.

The effect of dispersants is evident in the break-up and coalescence of oil droplets, where the presence of dispersants allows for smaller droplets to be formed. This will slow down the rising velocity of the dispersed oil. The specific influence of dispersants on the other processes is not yet clear, partly because dispersants have such a prominent effect on the droplet break-up that the other processes are indistinguishable.

2.4.3 Chemical dispersion [D]

Objective of this paper is to provide an approach that allows chemical dispersion to be modelled with the same algorithms as natural dispersion. For correct inclusion of response options in oil fate modelling, some additional parameters have to be modelled or determined. One of them is an estimate of the slick portions treated and the dispersant dosage (DOR) based on available logistics and an estimated targeting efficiency value. Additionally, specific experimental investigation is needed to provide information on physical mixing of dispersants within the oil slick of specific qualities and partitioning of dispersants from the oil slick into the water body. Finally, the oil properties should be expressed based on their physical properties, including changes therein following to the achieved dosage of dispersants. Each of these steps is discussed below.

Logistics & targeting

The portion oil that is chemically dispersed is proportional to the portion of the oil slick that is successfully treated. The logistics-based calculation of the slick area treated with dispersants, can be rather straightforward and based on; travel speed, travel distance, application rate and application dosage (Aamo et al., 1997; Dale, 2011; Genwest Systems, n.d.; National Research Council, 2005a; Reed et al., 1997) or simply user defined (NOAA/HAZMAT, 2000).

Precise targeting of the slick, however, proves to be difficult. Several factors determine how much of the dispersant sprayed, actually hits the oil slick. Targeting can be very difficult in conditions of low visibility and high winds (Daling et al., 2002; Merlin et al., 2006). Experience-based correction factors could be defined for modelling.

Dispersant migration & leaching

The fraction of dispersant that successfully becomes incorporated into the oil depends on two processes: migration of the dispersant into the oil layer, and loss of dispersants from the oil layer to the water column (leaching).

For dispersant migration into the oil, no suggestion for an algorithm could be made yet. Migration of dispersants into the oil layer depends on the application technique, and is inhibited by high oil viscosity (Canevari, 1984) and weathering of the oil slick surface (Berger and Mackay, 1994).

Test results on dispersant incorporation are inconclusive. It is generally assumed that premixing dispersants into the oil before testing causes an overestimated effectiveness. In Wave tank testing, however, the oil droplet sizes for oil premixed with dispersants (brown x in Fig. 2-4) are much larger than for oil sprayed with dispersants (brown + in Fig. 2-4) (SL Ross Environmental Research and MAR Incorporated, 2010).

In wave tank experiments, SL Ross and MAR incorporated proved that a repeated smaller dose of dispersants can have the same (or even higher) dispersion efficiency as one larger dose (SL Ross Environmental Research and MAR Incorporated, 2009). Oil droplet sizes resulting from this treatment are generally more in the range of naturally dispersed oils, but dispersion efficiency is similar to that of chemically dispersed oils (orange x in Fig. 2-4).

The leaching of dispersants from the slick to the water column is expected to be a combination of partitioning between the oil and water phases and diffusion within the phases. At higher temperatures, surfactants leach more to the water than at lower temperatures (Nedwed et al., 2006; Resby et al., 2007) (Fig. 2-5). The difference in leaching rates between oil types could not be related to either of the oil properties they distinguished (density, viscosity, wax content) (Nedwed et al., 2006; Resby et al., 2007). Dispersion efficiency could not be correlated with the relative concentration or the total amount of the different surfactants in the oil.

A recent study into the loss of surfactants from a low viscosity oil, revealed that the change in interfacial tension over time is greatly influenced by the design of the dispersant, more specifically; the relative proportions of the different surfactants in the dispersant (Riehm and McCormick, 2014). Some surfactants greatly reduce the initial interfacial tension (DOSS), but are rapidly lost to the seawater. Other dispersants adsorb more slowly to the interface but can keep interfacial tensions low for longer periods of time (Span-80, Tween-80). Different combinations of these surfactants can provide different initial interfacial tension and different magnitude and direction of change over time.

Two separate series of wave tank experiments demonstrated that dispersion efficiency decreases faster with increasing underwater currents and with thinner slicks (Lewis et al., 2010; SL Ross Environmental Research LTD et al., 2007, 2006b). This is to be expected as currents will provide a constantly high concentration gradient and thus higher partitioning. Through thinner slicks, diffusion of the dispersant to the interface is faster, so partitioning to the water can start sooner.

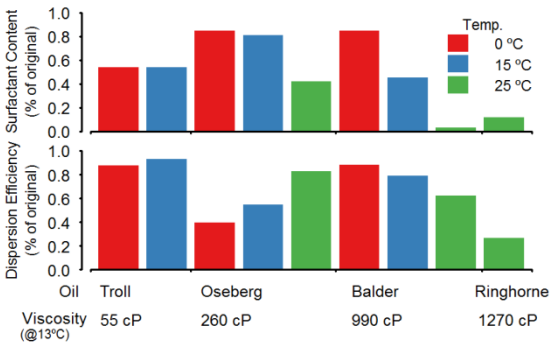

Fig. 2-5. Remaining Surfactant Content (SC) in oil and oil Dispersion Efficiency (DE) after 2 weeks of leaching at different water temperatures (colours). Results given as a percentage of the original value, for 4 different oil types (x-axis) (Data taken from (Resby et al., 2007)).

When applying dispersants under calm water conditions, the loss of surfactants during the period prior to mixing will result in larger dispersed oil droplets (Lewis et al., 2010) (Fig. 2-4, purple x's and •(control)). The dispersed oil droplet size (13 µm for freshly treated oil) increased to 102 µm after 50 h of leaching and 138 µm after 100 h. Similarly, for the lower viscosity oil, the droplet sizes after 100 h of 'leaching' before mixing, were in the range known for naturally dispersed oils.

There is a need for establishment of the mass transfer coefficients for dispersant migration into the oil layer, and for partitioning (leaching) of dispersants from the oil layer into the water (in which internal diffusion also plays a role). This would help understanding how dispersant incorporation into the oil layer could be optimized depending on oil spill characteristics.

Dispersant effect on oil properties

It is well agreed that that effectiveness differs per oil dispersant combination (National Research Council, 2005b) and that reducing the oil-water-interfacial tension is the working principle of dispersants (EMSA, 2009; ITOPF, 2012; Merlin and Peigné, 2007).

Typical interfacial tensions for untreated oils range from 18 to 32 mN/m, and can change due to weathering of oil through evaporation(Hollebone, 2011; Katz, 2009; Khelifa and So, 2009). Interfacial tensions for oil with dispersants have been found to lie between 15 and 0.0002 mN/m (Fig. 2-6).

The optimum Dispersant to Oil Ratio (DOR) of 1:20, is attributed to the critical micelle concentration (CMC). A further decrease of maximum droplet size is less evident above this DOR (Khelifa and So, 2009). This optimum has been confirmed with droplet size measurements (paragraph 4.2.2) as well as dispersion efficiency determination (Clark et al., 2005).

The experimental and analytical procedures greatly influence the outcome of interfacial tension measurements. Different interfacial tensions have been reported from different experiments with similar oil types (blue in A and B, red in A and C in Fig. 2-5). Also, timing (adsorption & leaching of dispersants) and oil volume/surface ratio greatly influence the measured interfacial tension outcomes (Riehm and McCormick, 2014). This might be the reason why it has not been possible to relate the change in dispersion efficiency (Riehm and McCormick, 2014) or droplet size (Khelifa and So, 2009; Mukherjee et al., 2012) to the measured change in interfacial tension (due to dispersants).

In a series of baffled flask tests, oil composition (fractions of saturates, aromatics, resins and asphaltenes) could successfully 'predict' chemical

dispersion efficiency and chemical volume mean diameter (VMD) (Mukherjee et al., 2011), indicating that dispersant/oil interactions indeed is related to oil type.

As the change of oil properties is the working principle of chemical dispersion, it is evident that understanding the effect of different variables (oil type, weathering, dispersants, and seawater salinity) on this parameter is crucial. The most relevant parameter and how to measure it is yet to be determined, as available data from interfacial tension measurements are not yet conclusive.

2.4.4 Mechanical dispersion [E]

No publications were found on the operational implications of mechanical dispersion either in models or in research. In some instances it was reported that local mechanical mixing was employed in trial situations lacking sufficient natural mixing energy (Singsaas and Lewis, 2011; Sørstrøm et al., 2010). Unfortunately, no quantitative data were provided. Furthermore, two patents were found for mechanical dispersion methods, both aimed at very specific cases; sub-sea mechanical dispersion (Rogers and Beynet, 2013) and mechanical dispersion oil in an ice field (Nedwed, 2012).

Judging from the lack of available information, mechanical dispersion is not a very commonly used response option. Some logical assumptions can be made on the implications of this type of response. How fast a responding unit can be on site and with which rate it can treat the slick, will determine the area treated

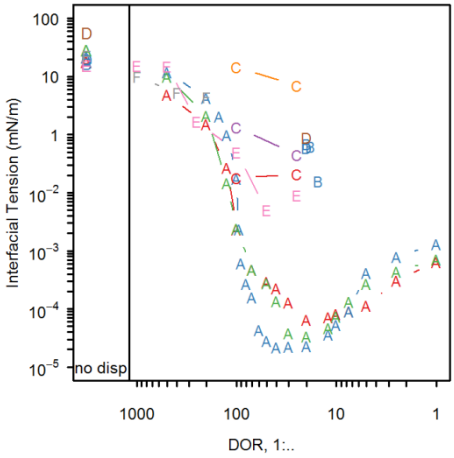

Fig. 2-6. Oil-seawater interfacial tension (in miliNewton per metre) in for different dispersant-oil-ratios (DOR) with corexit 9500. Symbols indicate sources from which the data were obtained (A (Khelifa and So, 2009), B (Katz, 2009) (with corexit 9527), C (Mukherjee et al., 2012), D (SL Ross Environmental Research LTD et al., 2006b)*, E (Brandvik et al., 2013), F (Abdelrahim, 2012)), (corresponding) colours indicate oil types.*

per day. The method of agitation will determine an amount of (vertical) energy added which will cause entrainment and will add some additional turbulence for breakup and coalescence.

Compared to chemical dispersion, the effects of mechanical dispersion are much more straightforward. As mechanical dispersion does not alter the oil properties and thus behaviour, its effect can simply be incorporated in the processes directly affected by the mechanical dispersion: entrainment of oil and increase of local turbulence.

2.5 Conclusions

Current modelling of dispersion in oil spill fate and transport models is based on the empirical Delvigne and Sweeney algorithm. This algorithm, however, does not allow quantification of the effects of chemical nor mechanical dispersion as response option. The aim of this study was to present an approach to improve dispersion modelling by incorporation of three dispersion options (natural, mechanical and chemical). The distinguished sub-processes of dispersion were systematically analysed and literature searches performed to find the available information on the influence of individual parameters to be included in improved models.

The key parameters for dispersion modelling are oil properties (viscosity and interfacial tension), wind speed and (wave) energy. These key parameters have different effects in the dispersion sub-processes, so the net dispersion effectiveness cannot simply be related to these key parameters:

High oil viscosity has a threefold negative influence on dispersion: it can resist entrainment, counteracts breakup into small droplets, and can prevent dispersants from reaching their 'site of action' on the oil water interface. On the other hand, as high viscosity usually correlates with high oil density, high viscosity oil will rise back to the surface a little slower.

Higher wind speeds enhance dispersion by increasing energy and quantity of (breaking) waves. This increases entrainment, facilitates breakup into smaller droplets and mixes the droplets deeper into the water column. Additionally, a high wind speed results in larger differential speed between slick and suspended droplets. On the other hand, targeting of chemical dispersants becomes more difficult in windy situations. The net effectiveness of chemical dispersion in high wind cases, can be questioned as natural dispersion is expected to be very prominent in that case.

Our analysis of the dispersion sub-processes reveals the following topics as being very important for future investigation: entrainment rate as a function of energy and oil layer properties, an algorithm for droplet size based on oil properties and energy levels, mass transfer coefficients for surfactants into the oil layer as well as loss from the oil layer to the water column, quantification of the effects of dispersants on physical oil qualities.

This information is crucial for modelling the NET effectiveness of dispersants, which will be of great benefit when making a rational decision about dispersant use.

CHAPTER 3

Quantification of the effect of oil layer thickness on entrainment of surface oil

M. Zeinstra-Helfrich[a], K.Dijkstra[b], W. Koops[a], A.J. Murk[c]

Zeinstra-Helfrich, M.; Koops, W.; Dijkstra, K.; Murk, A. J. (2015): Quantification of the effect of oil layer thickness on entrainment of surface oil. Marine Pollution Bulletin. 96: 401-409

---

[a] NHL University of Applied Sciences, Dept. Maritime, Marine, Environment & Safety
[b] NHL University of Applied Sciences, Dept. of Computer Vision
[c] Wageningen University and Wageningen-IMARES, Sub-department of Environmental Technology

Abstract

This study quantifies the effect of oil layer thickness on entrainment and dispersion of oil into seawater, using a plunging jet with a camera system. In contrast to what is generally assumed, we revealed that for the low viscosity ‘‘surrogate MC252 oil’’ we used, entrainment rate is directly proportional to layer thickness.

Furthermore, the volume of stably suspended small oil droplets increases with energy input (plunge height) and is mostly proportional to layer thickness. Oil pre-treated with dispersants (dispersant-oil ratio ranges from 1:50 to 1:300) is greatly entrained in such large amounts of small droplets that quantification was impossible with the camera system. Very low interfacial tension causes entrainment by even minor secondary surface disturbances. Our results indicate that the effect of oil layer thickness should be included in oil entrainment and dispersion modelling.

3.1 Introduction

In the event of an oil spill, chemical dispersion remains a popular oil spill response option to limit smothering of coasts, swamps and animals. For instance, during the Deepwater horizon spill 7.000 m^3 of dispersants have been applied, both via surface spraying and injection into the well head. The deep-sea injection of dispersants was new and effectiveness and effects still are under study. Application of dispersants to surface slicks is used as response option since 1967 (EMSA, 2009; Law, 2011), but even for this application still no reliable dispersion effectiveness modelling is available. This, however, is very important to be able to predict water column oil concentrations for both chemically treated and untreated oil and better weigh the (environmental and economic) costs and benefits of dispersant application. Little data currently is available to improve models for natural surface oil dispersion (naturally occurring process without addition of dispersants) as well as chemical surface oil dispersion (enhanced by dispersants). The detailed data needed to describe the mechanism of dispersion are difficult to produce. Dispersion of surface oil is the complex process of floating oil breaking up into small relatively stable droplets suspended in the water column. Available small scale tests, such as the swirling flask test and the baffled flask test (National Research Council of the National Academies, 2005), can be performed relatively easy and parameters can be well controlled. Although their results show good repeatability, the tests do not represent the dispersion process occurring at sea. Large scale tests such as wave tank testing better mimic the mechanical conditions at sea, but in these tests it is very hard to control input parameters and obtain reliable quantitative information on sub processes of dispersion needed for a good model.

Especially the first step in the surface oil dispersion process, entrainment, in which is the oil slick submerses in a transition from floating oil to suspended oil, is not yet fully modelled. One of the parameters not well understood is the effect of oil layer thickness on dispersion rate. According to Delvigne and Sweeney (Delvigne and Sweeney, 1988), whose work is used in most of the currently available oil fate and trajectory models (Reed et al., 1999), the dispersion rate of droplets in each size class is unaffected by oil layer thickness. Therefore in their model the number of small, relatively stable suspended oil droplets, is considered to be independent of the thickness of the floating slick.

The opposite is assumed in the model by Mackay (as cited in Reed et al., 1999), where oil entrainment rate is calculated by multiplying the sea surface area agitated (depended on sea state) with the oil layer thickness. In this model, the fraction of the thus entrained oil that will remain permanently dispersed depends on oil properties and layer thickness, independent of sea state.

In this paper, we present a laboratory method for quantification of entrainment of floating oil, and apply this to different layer thicknesses of a low-viscous oil type with varied energy input.

3.2 Approach

A test method was developed, based on a plunging jet system mimicking the impact of a breaking wave front onto an oil layer. With a set of high speed cameras the underwater entrainment process was recorded. With image analysis the oil entrainment was qualified and quantified from the test pictures.

In a series of experiments with different plunge heights and layer thicknesses, specific parameters were obtained that are needed for oil dispersion modelling.

3.3 Plunging jet apparatus in other studies

A plunging jet apparatus can be used to mimic the vertical energy brought onto an oil layer by a breaking wave. This has previously been used to investigate the droplet sizes formed during natural dispersion of weathered oil under influence of the mechanical energy breaking waves (Reed et al., 2009). In their study it was shown that in their medium size wave tank (± 2.5 m^3, 5x1x0.5 m), the droplet sizes formed under an (instantaneous) plunging jet of 10 cm height are the same as those of a breaking wave of the same height.

Delvigne (1994) used an adapted plunge in a smaller tank (4 l) to obtain oil-specific constants (dispersion rate coefficient) for his entrainment algorithm. The dispersion rate coefficient (obtained by counting the number of droplets smaller than 200 µm) found in the plunging jet, were in agreement with those found in earlier wave tank tests.

Breaking waves are expected to not only entrain oil, but also air. Similitude between air and oil entrainment is expected as in both situations an immiscible, positively buoyant volume is temporary submersed by the vertical movement a of breaking wave. Indeed, a (continuous) plunging jet is also considered a suitable experimental technique for investigation of air entrainment into water due to plunging breaking waves (Chanson and Cummings, 1994; Chanson and Jaw-Fang, 1997; Roy et al., 2013). The investigations of air entrainment are typically performed using a continuous plunging jet. Energy input and flow conditions in such jets can be well defined due to absence of spatial and temporal variation. Different mechanisms have been described for air entrainment by plunging jets and breaking waves, among which;

a) The boundary layer of air along a liquid jet interface creates a semi stable air sheath (annulus) beneath the water surface where air is entrained due to collapse of this sheet by jet surface irregularities (Davoust et al., 2002; Gómez Ledesma, 2004; McKeogh and Ervine, 1981; Roy et al., 2013).
b) A semi turbulent jet with a rippled surface creates a smaller indentation (/cusp) in the water surface around the jet. From this, a radial water flow downwards, created by a radial vortex flow around the impact point, transports the bubbles down (McKeogh and Ervine, 1981; Roy et al., 2013).
c) A turbulent jet impinging the water surface creates a rough surface of the receiving pool where ambient air is entrained continuously (McKeogh and Ervine, 1981; Roy et al., 2013).
d) Entrapment: air sandwiched between the (initial) impacting jet and the receiving pool. This also applies to other/secondary impacts associated with breaking waves (Davoust et al., 2002; Deane and Stokes, 2002; Kiger and Duncan, 2012; Roy et al., 2013).
e) Enclosure of a cylinder of air along the width of the breaking wave, underneath the overturning wave crest (Deane and Stokes, 2002; Kiger and Duncan, 2012).

Important differences between air and oil entrainment are the viscosity of the oil and the limited 'availability' of the oil compared to the ubiquitous air phase. Considering these limitations, it is suspected that 2 of the mechanisms: entrapment at impact and interfacial shear dragging the water surface (and oil) down, are most important in the case of oil entrainment under breaking waves.

The above literature regarding oil dispersion investigation employ a single 'instantaneous' jet, where a (predefined) quantity of water is dropped from a (predefined) height onto the oil layer. Although the settings are easy to control, definition of the energy input on the tank is less straightforward as the impact varies with space and time (paragraph 3.4.4). Such instantaneous jet however, does reflect the intermittent nature of breaking waves, and can generate both the entrapment and interfacial shear entrainment mechanism.

In this paper, we present a method for quantification of oil entrainment as function of oil layer thickness, applied to "Surrogate MC252 oil" with and without dispersants.

3.4 Materials & methods

3.4.1 Plunging jet test

Our plunging jet system (Fig. 3-1A), consists of a rectangular holding tank (1) (30 x 10 x 35 cm), containing just over 9 l of artificial seawater to yield a liquid height of 30 cm. An overflow (5), connected to the bottom of the tank, ensures the water level is equal at the start of each test. The oil layer height depends on the total amount of oil pipetted onto the water layer. From the plunge container (2), 100 ml of artificial seawater is poured upon the water (or oil) surface of the holding tank. The plunge force is adapted by adjusting the height of the plunge container.

The required quantity of oil is added in multiplications of 3 ml, by inverse pipetting using a 5 ml pipette and tip, as this allows drop-wise addition distributed over the entire tank's water surface. For every 0.1 mm of oil height, 3 ml of oil is added. The oil layer is left to 'settle' for 10 minutes prior to the plunge test.

To perform the plunge test, the plunge container is tilted upwards until the upper bracket (3) and 100 ml of artificial seawater is added. Upon release, the container tilts back to its horizontal position onto the lower bracket (4), pouring its contents onto the holding tank.

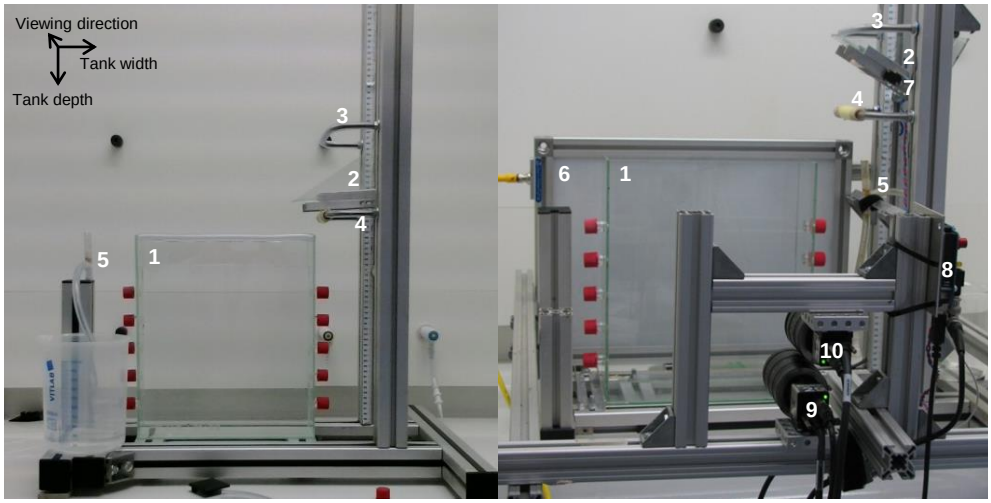

Fig. 3-1. Plunging jet system (left) with image acquisition arrangements (right) and; 1. Holding tank, 2. Plunge container (tilted down in A, tilted up in B), 3. Upper bracket, 4. Lower bracket, 5. Overflow, 6.Background light, 7. Trigger, 8. Microprocessor, 9. Main camera and 10. Close-up camera.

Table 3-1. Camera Specifications. The close-up image is 18% of the main image at 4 times larger resolution.

		Main image	**Close-up image**
Camera Type		IDS UI-3240-CP-NIR-GL	IDS UI-3370-CP-M-GL
Resolution (w*h)	pixels	1280 x 1024	2048 x 2048
Field of view:	- horizontal	Entire tank width: 30 cm	Width: 12,9 cm, starting 11,5 cm from upper left of main view.
	- vertical	From water level down to water depth ± 25 cm	From water level down to water depth ± 12,9 cm
Scaling factor (SF)	px/cm	40.4	158.7
	µm/px	247	63.02
	ml/px^3	1.51×10^{-5}	2.50×10^{-7}
Lens type		Fujinon TV lens HF50SA-1	Fujinon TV lens HF12.5SA-1
Diafragma setting		11	11
Exposure (shutter $speed^{-1}$)	msec	1.669	1.059
Interface		A PC laptop running VisionLab	A PC laptop running VisionLab

After a test, the oil is removed from the water surface with an oil-only absorbent sheet. Wiping with this material also cleans the glass of the tank sides. Once visually clean, the cleaning procedure is repeated with a 'fresh' oil-absorbent sheet.

After a maximum of 10 tests using the same oil type or after 1 test including dispersants, the tank is fully drained, cleaned with water and detergent and rinsed with an abundance of demineralized water before further use. This cleaning approach is important to avoid build-up of dissolved hydrocarbons to the extent that it will affect the test results. The water surface is additionally swept with an absorbent cloth prior to oil addition, in order to avoid water surface contamination that could influence the oil layer spreading.

3.4.2 Image acquisition

Two industrial grade IDS cameras are fixed to the plunging jet system. One camera is set to record a main view of the tank (9) and the second camera (10) is set to get close-ups of the smaller oil droplets (Table 2-1). The illumination(6) is a LED backlight (Smart Vision Light, SOBS-450x300, Stemmer Imaging) placed behind the holding tank to optimise oil droplet visibility and contrast in the images (Fig. 3-1B).

The shutter speed is optimised for both cameras (Table 2-1) to reduce the motion blur of the droplets. The depth of field is optimised via diaphragm and focus. The perspective distortion is minimised by choosing a lens with a relatively high focal length.

Based on scaling factors determined in front and behind the tank, it is revealed that perspective distortion causes a difference of 13% in scaling factor,

measured across 10.8 cm (the entire tank width in de viewing direction including the glass walls). The maximum plunge width in the viewing direction is only 2 cm (Fig 3-3), this could cause a deviation of 2.4 % in measured droplet size (comparing front with back of the tank). As the droplets can expected to be distributed symmetrically (in viewing depth) around the centre of the tank, the effect of perspective distortion is cancelled out.

Both cameras are externally triggered by a microcontroller (8), therefore the recorded images are concurrent between cameras. The image acquisition process is started when the plunge container hits the lower bracket, pushing a small lever (7). When the microcontroller triggers, both cameras are set to simultaneously record 10 seconds of images at a rate of 20 frames per second. After 30 and 60 seconds another 5 frames are recorded at 20 frames per second. After completion of this process, the images are stored for further analysis.

To retrieve data from the test pictures, image analysis is performed. This is done with the same software used for image acquisition (VisionLab). The image analysis of the droplets recorded is performed in three steps: droplet segmentation, classification and volume quantification. By combining the data from the close-up and corresponding main view results, the total volume of oil entrained is calculated. Data points that do not comply with pre-defined assumptions are removed from the data sets. The procedures are explained in more detail in the annex of this chapter: S3.2 Image Analysis Process, performed on Plunging Jet Test Pictures.

3.4.3 Experimental design

The experimental design consists of a full factorial investigation with one oil type, investigating 3 plunge heights and 5 oil layer thicknesses. Each of these experiments is performed in duplicate.

Additionally, 4 dispersant concentrations are investigated with 1 oil layer thickness and 1 plunge height.

The experiments were performed with artificial seawater, prepared from demineralized water with artificial sea salt mix (Coralsea Salt, AquaHolland Dordrecht). Before use the seawater was aerated for at least 20 hours and the seawater conductivity was adjusted to between 41 and 42 mS/cm at 25°C, by either adding demineralized water or sea salt. After sufficient mixing, the water was filtered (pore size 0,053 mm).

The oil used in these tests was surrogate MC252 oil, obtained through the GoMRI program (Pelz et al., 2011). Viscosity, measured with a double gap viscometer at a shear rate of 10 sec^{-1}, was 14,1 mPa.s. Dispersant used was Corexit EC9500A, kindly provided by NALCO (Nalco, 2011). In our experiments, dispersants were pre-mixed with the oil prior to addition to the water surface.

Statistical procedures
Analysis of Variance (ANOVA), type III, was performed to assess significance of effects. Type III ANOVA was chosen as it is not sensitive to unequal 'sample sizes' which might occur when removing unreliable data points.

3.4.4 Plunge characterization

Our quantitative analysis of oil droplet sizes and volumes requires the system to be relatively stable, which is within relatively short time after plunge impact (~2.5 seconds). In order to understand the mechanisms behind the oil being moved from floating to suspended, it is necessary to understand the driving force, in this case the plunge impact, which occurs on a much shorter time scale (< 1 second).

Characterisation of the plunge was performed in two ways: By qualitatively assessing the plunge impact in the test tank in different conditions, and by quantitatively determining surface area impacted.

The jet of water released from the plunge container into an empty tank is visualised in Fig 3-2A. During water jet impact 5 different stages are distinguished (Fig. 3-2, see column titles). As the plunge container empties, the jet loses power and moves towards the origin (= the plunge container, which is outside camera view, on the right side). When the jet plunges onto the sea water surface (Fig. 3-2B), the initial impact creates an air pocket that is stable for about 2 frames, thus 0.1 seconds. As the jet starts to move, the air pocket collapses. In the first approximately 0.15 seconds the moving (sweeping) planar jet is constant and stable(II). As time progresses, the jet becomes increasingly irregular, from an unstable planar jet(III) to a rough jet(IV) and finally the last droplets(V) falling into the tank.

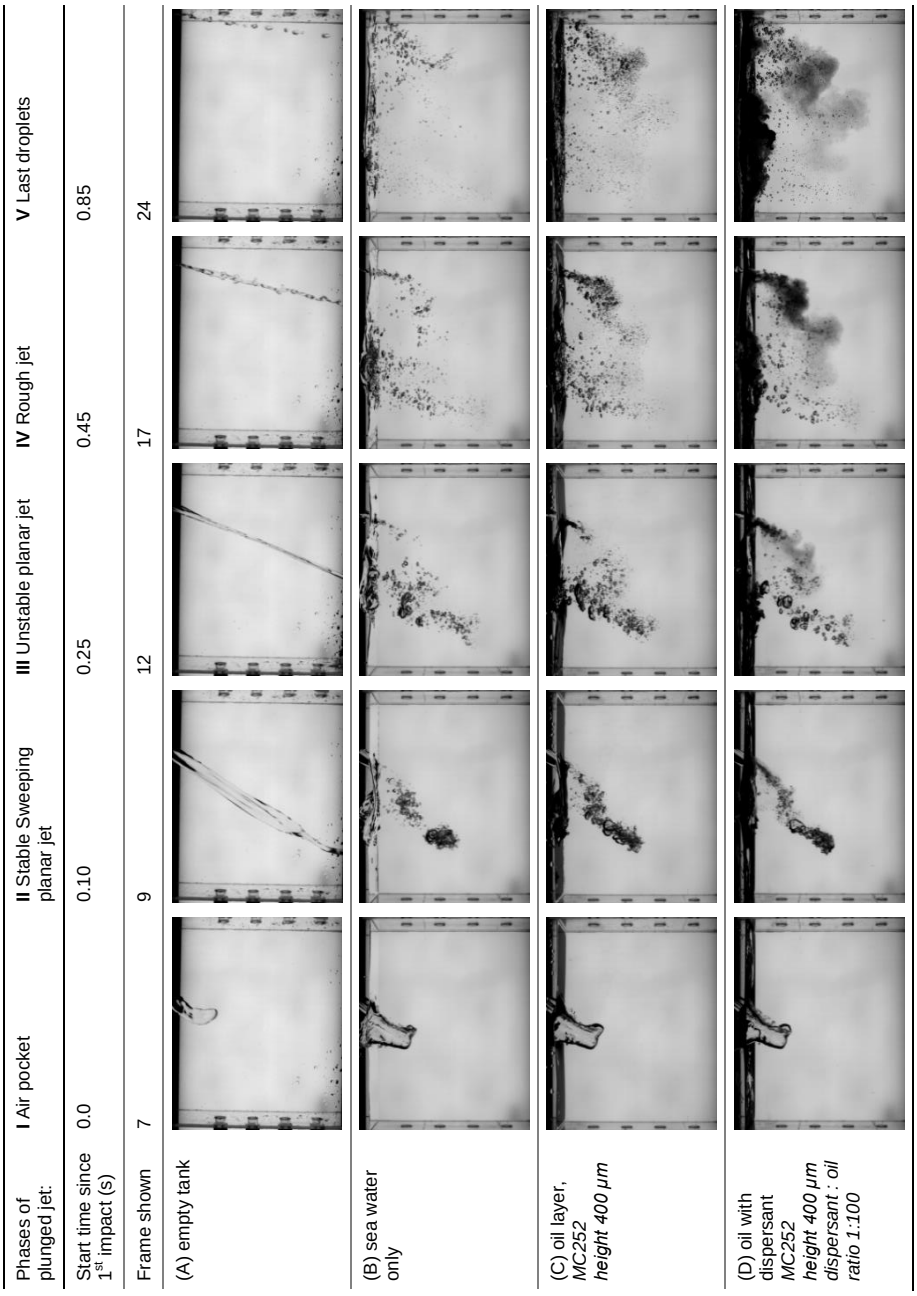

Fig. 3-2. Visualisation of the evlolution of a standard jet of water plunged (A) into the empty holding tank; (B) onto the artificial seawater; (C) onto an oil layer and (D) onto an oil layer with dispersants. The phases of jet plunging are named based on the shape of the jet in series B.

During the 5 stages of plunging distinguished, oil and air can be entrained in the sea water (Fig. 3-2B and C), and the amount entrained changes greatly over the different stages. The collapsing air cavity entrains a lot of air in a big bubble that resurfaces quickly. In this stage only a relatively small amount of oil (Fig. 3-2C) compared to the amount of air (Fig. 3-2B) is entrained. In the stable jet phase, a consistent stream of air bubbles and fine oil droplets are entrained. As the jet becomes unstable and rough and finally with the last droplets, more intermitted entrainment of oil and air occurs in larger bubbles/droplets. When oil is pre-treated with dispersants, the entrained oil immediately breaks up into a very fine mist of droplets. Additionally, a secondary entrainment occurs at the point where the air cavity resurfaces and disturbs the water surface (Fig. 3-2D, phase V, upper left of the picture).

In addition to identification of the plunge phases, the plunge impact area is quantified in more detail during the entire plunge process. For this particular test, the camera's line of sight is rotated 90°, so the view is from left side of the tank (see Fig. 3-1), directly opposite to the plunge container outflow. This camera was set to record at a frame rate of 20 sec^{-1}.

Instead of the holding tank, a reference device was used for determining the size and location of the jet impact. This device consisted of a rectangular frame made of Lego bricks, with reference marks all around the border, and three parallel strings in the location the jet was expected to hit. This frame was placed in such a way that the top indicated the water level in the oil entrainment tests.

The plunge procedure was performed as normal, with the same volume of water. Seawater used was the same as in the oil entrainment tests, with addition of

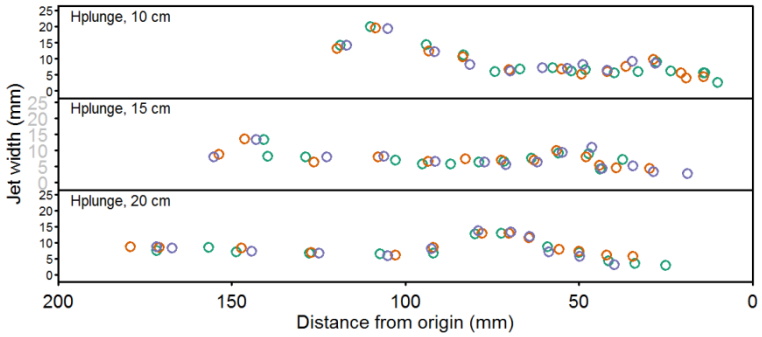

Fig. 3-3. Evolution of jet width and impact location over time, for the three different plunge heights (Hplunge = vertical distance between plunge container outflow and water surface). The different colours represent triplicate measurements. Impact location (x axis) represents horizontal distance of the falling water at the moment of hitting the water/oil surface, measured from the reference point under the outflow location. Total impacted area of water surface is the total area below the curve.

some droplets of green (food) dye.

On the images taken during the plunge, the strings cut through the jet, allowing the intersection between the water and strings to be pinpointed as an X and Y position in number of pixels. The position of this intersection point in the reference frame, and thus distance in the holding tank, was determined by interpolating it within a set of virtual lines between corresponding pegs on both sides of the frame and their known distances.

The width of the jet was obtained by 'measuring' the width in pixels and multiplying this by a scaling factor for this specific distance from the camera, obtained with the (known) distance between both sides of the frame.

Intention was to quantify the plunge impact for the entire plunge process; from initial until the final impact. However, as the last part of the plunge consists of an irregular stream of drops, that part could not be quantified. Quantification of the earlier phases of the jet (Fig. 3-3) show that the evolution of distance and width of the plunge impact is follows a very consistent pattern between the different replications. A jet from a higher plunge height reaches a further distance in the tank and provides a narrower jet at the point of impact.

The overall impacted water surface area, determined in triplicate for each of the plunge heights, was 1113.7 mm^2 on average, not significantly influenced by plunge height (P=0.20; S3.1-ANOVA tables).

3.5 Results

3.5.1 Results without dispersants

Creating a homogeneous thin oil layer required some dexterity and some slight inequality in the oil layer thickness is inevitable. It is registered, though, in the first frames of the test pictures (before the plunge impact). Manipulating the oil layer once it was on the water surface did not improve its equal distribution. The deviations, however, are relatively small compared to the surface of the jet impact and therefore considered not relevant. The planned vs. the determined (with image analysis) oil layer thickness shows a good correlation (Fig. 3-4).

Table 3-2. Number of data points remaining per time-step, after rejection of too crowded (class 5) and too tiny droplets (size detection limit) data points. For natural dispersion, 15 experiments were performed in duplicate. Each experiment yields 3 data points for each time-step, so 90 data points are produced per time-step. For chemical dispersion 5 tests were performed, also with 3 data points per time-step, yielding in total 15 data points per time-step.

T =	Frame numbers	Natural dispersion # points rejected for reason: Class 5	Size detection limit	usable	Chemical dispersion # points rejected for reason: Class 5	Size detection limit	usable
2.5 sec	054, 056, 058	39	0	**51**	9	15	**0**
5 sec	104, 106, 108	3	2	**85**	9	15	**0**
7.5 sec	154, 156, 158	1	8	**81**	9	15	**0**
10 sec	190, 192, 194	3	17	**73**	9	15	**0**
30 sec	202, 204, 206	1	89	**1**	9	15	**0**
60 sec	214, 216, 218	0	90	**0**	9	15	**0**

In total 50 experiments (25 duplicates) were performed for natural dispersion and 10 experiments for chemical dispersion. Based on the reliability criteria given in section 5 of S3(page, indicating that the 'leg' of the droplet size distribution below the detection limit is small enough (px4) and that the relative contribution of 'undefined' droplet shapes (class 5) is not too large, the images obtained 5 seconds after jet impact yield the most usable data-points for natural dispersion (Table 3-2). For chemical dispersion this was not possible because droplet sizes were too small.

The volume of oil entrained in the water column 5 seconds after the plunge jet impact, significantly depends on the oil layer thickness (P=<2.2E-16) and the plunge height (P=9.95E-3) and their interaction (P= 1.93E-4) (Fig. 3-5 , S3.1-ANOVA tables). The increase in volume of oil entrained with oil layer thickness is linear. Using the results based on the measured instead of nominal oil layer thickness, the interaction becomes less prominent. A linear model with the same

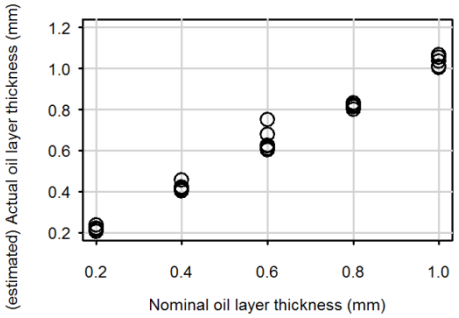

Fig. 3-4. Nominal oil layer thickness vs actual oil layer thickness. Estimated from the pictures prior to impact, by assessment of percentage of water surface free of oil. As the points are transparent, multiple overlapping points are represented by a darker colour.

slope (1.19 ml/mm layer thickness) can be fit for all three plunge heights (Multple R^2; 0.914) (Fig. 3-5).

The droplet size distributions obtained from triplicate analysis the close-up image of two independent replicates are very similar (Fig. 3-6). The density distribution (inset in Fig. 3-6) is slightly asymmetric with a tail to the right of the central mode. This indicates that the data could fit a lognormal distribution function, as suggested by Reed (2009; Johansen et al., 2015). Indeed, a (left-truncated) lognormal distribution fitted the droplet size distribution very well (example in Fig. 3-7). The resulting mean droplet size and standard deviation are significantly influenced by plunge height as well as layer thickness (Table 3-3, S3.1 - ANOVA tables).

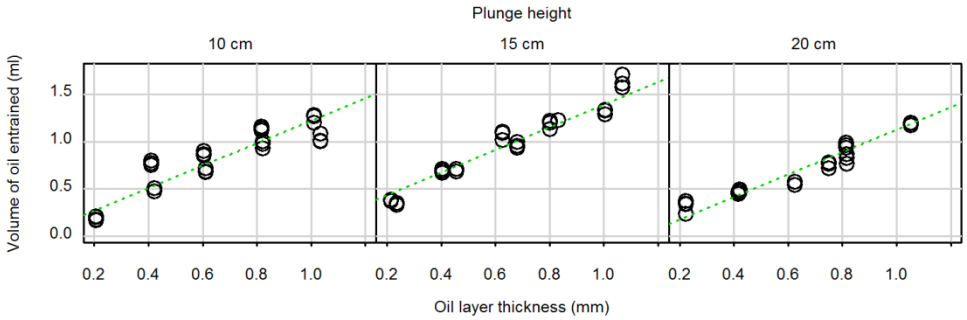

Fig. 3-5. Volume of oil entrained for 3 plunge heights at T = 5 seconds after jet impact (natural dispersion). The regression lines all have the same slope (1.189), but the intercept value depends on plunge height (0.032, 0.119 and -0.062 ml).

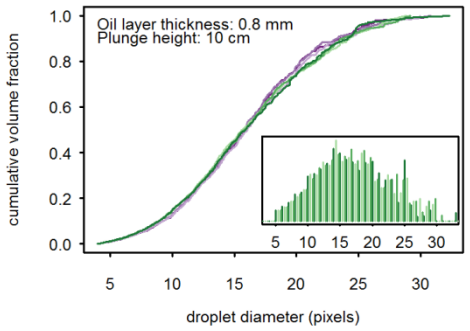

Fig. 3-6. Example of the cumulative droplet volume distribution for one experimental setting. Different lines are individual frames analysed in two (green vs. purple) replicate experiments. The inset is the density distribution for 3 of the tests.

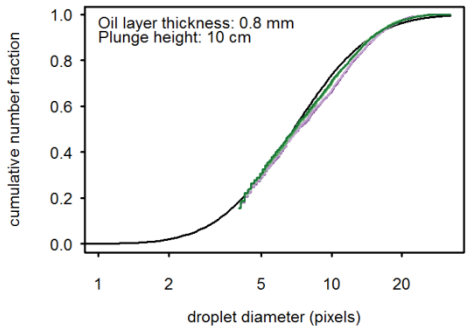

Fig. 3-7. Number based droplet size distribution for one experimental setting. The fitted model (black) compared to the results from separate measurements; green vs purple are the separate replications, the three shades represent the separate frames/pictures analysed per experiment.

Table 3-3. droplet size distribution parameters, averaged for the different experimental conditions.

Plunge height (cm)	Oil layer thickness (mm)	Log (number) mean diameter[1] (px)	Log Stdev[a] (px)	Number mean diameter (µm)	Volume mean diameter[b] (µm)	(volume) fraction of droplets D<500µm[c] -
10	0.2	1.71	0.56	351	896	0.15
10	0.4	1.85	0.56	403	1028	0.10
10	0.6	1.89	0.59	417	1184	0.07
10	0.8	1.93	0.60	435	1283	0.06
10	1	2.01	0.57	474	1279	0.05
15	0.2	1.70	0.55	346	860	0.16
15	0.4	1.83	0.55	394	970	0.11
15	0.6	1.92	0.55	431	1073	0.08
15	0.8	1.96	0.57	449	1210	0.06
15	1	1.94	0.59	440	1250	0.06
20	0.2	1.64	0.49	325	667	0.28
20	0.4	1.60	0.54	314	747	0.23
20	0.6	1.70	0.54	348	831	0.17
20	0.8	1.72	0.55	353	869	0.16
20	1	1.73	0.55	356	882	0.15

[a] Average taken from the fitted distribution per picture (up to 6)
[b] Calculated from logmean and logsd listed here, using Hatch-Choate equations
[c] Calculated from the volume mean diameter and the standard deviation, using the lognormal distribution function

The volume mean droplet diameter decreases with plunge height (Table 3-3). The volume mean droplet diameter slightly increases with layer thickness, which means that the relative fraction of droplets in small size classes slightly decreases (Table 3-3).

Results with chemical dispersion

The plunging jet tests with dispersant added yields a droplet size distribution that extends below the droplet detection limit for the photographical system (Table 3-2). Therefore this detection method is not suitable for quantitative analysis of entrainment of chemically dispersed oil. However, some clear qualitative observations could be made from the pictures 5 seconds after plunge impact (Fig. 3-8). In experiments with Dispersant to Oil Ratios (DOR) > 1:200, vast amounts of miniscule oil droplets form a 'cloud' of oil in the tank which was still visible at 5 seconds, and can last for minutes. This effect was less pronounced with DOR of 1:200 and less than that, but oil droplets still were much smaller than those for oil without dispersants.

As mentioned in the plunge characterisation, we observed a secondary entrainment event for chemically treated oil. (Fig. 3-2D, phase V, upper left of

the picture). In terms of timing and location in the tank, this event can be associated with the resurfacing of the 'air-pocket' created in phase I.

3.6 Discussion

In the present study we aim to quantify the effect of oil layer thickness on entrainment of oil in water, using a plunging jet system combined with camera equipment for close-up and overall pictures. The results show a clear effect of oil layer height, plunge height and dispersant application, and the effects depend on combinations of parameters. Below, we will first discuss the methodology and image analyses and calculations. Subsequently, the observations of the entrainment over time will be discussed, the entrainment of chemically treated oil, and the effect of oil layer thickness on entrainment. Finally we will discuss the implication of this work for modelling natural and chemical dispersion.

3.6.1 Experimental design

The plunging jet approach represents a single impact event allowing visualising of oil entrainment, without interference of air bubbles which would be the case with continuous jets. It also is more similar to the intermittent nature of a breaking wave. Although our jet is not homogeneous in time or space, it proved to be highly reproducible for all test conditions (Fig. 3-3).

The image analysis process and droplet volume calculations used could generate some minor errors, however on the total large number of droplets (lowest droplet count in the 5 second shot was 2711) these minor deviations only have

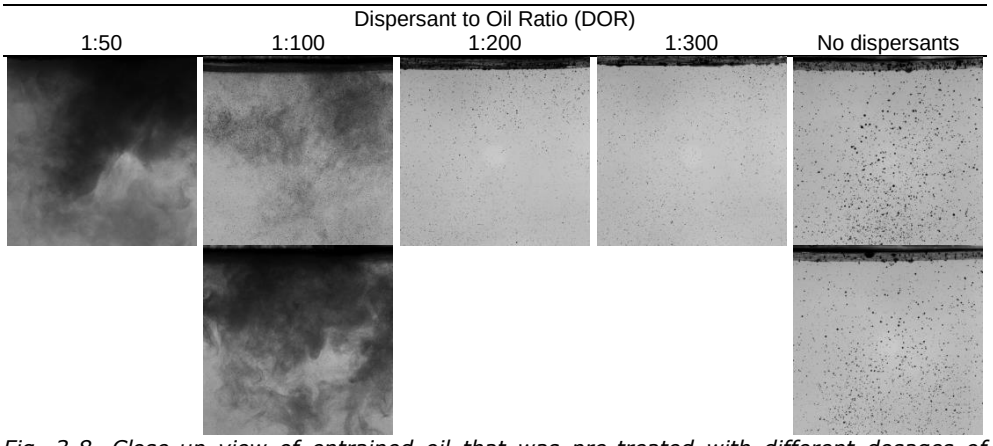

Fig. 3-8. Close-up view of entrained oil that was pre-treated with different dosages of dispersants. Picture time: 5 seconds after jet impact, plunge heights = 15 cm, oil layer thickness = 200 µm. Tests with DOR1:100 were performed in duplicate.

marginal influence.

To be able to exactly control the dispersant concentration in the oil during the test, the dispersants were pre-mixed into the oil. Although surface application of dispersants would be more representative of field conditions, covering the ability of the oil to incorporate the dispersant, this specific parameter is outside the scope of this work and would require more repetitions to yield the consistent results we obtained now.

3.6.2 Oil entrainment

In our plunging jet system, we could distinguish distinct phases in jet flow resulting in different oil entrainment 'regimes' (Fig. 3-2). In the unstable phase of the jet, a relatively large portion of oil is entrained in large droplets. This is most likely due to the so called 'entrapment' process, where oil is sandwiched between the face of a falling drop and the holding tank water, and subsequently travels down with it. The more stable phase of the jet induces more the 'interfacial shear' process comparable to what has been described for air entrainment. The interfacial shear creates an indentation in the water surface around the jet inside the receiving pool, which collapses intermittently. Two mechanisms are possible for interfacial shear to cause oil entrainment; (1) an annulus ('pocket') of air is created, oil flows into this annulus. (2) The jet interface drags down oil instead of air.

In our set-up, the water surface area affected did not differ between plunge heights. A difference in impact speed (as a result of gravitational acceleration) and impact angle (as a result of different distance) is assumed but not determined in these experiments.

Natural dispersion (& entrainment)

The amount of oil initially entrained, increases with oil layer thickness; for all three plunge heights, the increase of entrainment is linear with layer thickness over the entire range of thicknesses tested (0.2 – 1 mm). This linearity is consistent with the 'entrapment' process (Davoust et al., 2002) and with the theory of Mackay (as cited in Reed et al., 1999), stating that all oil affected by a (vertical) source of impact is initially entrained.

Total volume of oil entrained was only slightly affected by plunge height. Prior assumption was that different plunge heights would result in different impacted-area, and thus affect entrainment. The impact-area, however, did not to differ between plunge heights.

The smaller the droplets formed, the longer the oil can be expected to remain in the water column.

The mean droplet size decreases with plunge height (Table 3-3). This is in accordance with colloid science theory (Walstra, 2005) stating that in otherwise similar conditions, a higher energy input, breaks up the oil into smaller droplets.

Furthermore, our results show that the mean diameter increases with layer thickness, thereby reducing the fraction of oil in small droplets (Table 3-3).However, as the total volume of oil entrained increases linearly with layer thickness, the volume of oil in small droplets does increase with layer thickness (as illustrated by Fig. 3-9). Although this is most pronounced at the highest plunge height, this trend is also present at the lower plunge heights.

As the volume of oil in the smaller droplet classes increases with oil layer thickness, after settling of the larger oil droplets the entrained volume of oil is greater. This is in contrast with Delvigne's assumption that the effect of layer thickness is irrelevant for overall entrainment as it will be overcome by rising of the droplets (Delvigne and Sweeney, 1988).

The plunging jet test system was used to investigate mass flux of oil as a function of layer thickness. The droplet breakup only was initiated by a single impact event to further elucidate the entrainment mechanism. Although the energy input was low compared to field situations, we clearly demonstrated that the oil layer thickness influences the total oil mass flux as well as the volume of smaller droplets formed. This effect of layer thickness on oil dispersion is expected to be even stronger under field conditions; where the constant turbulence will favour small droplet formation even more. In addition, greater dilution of oil droplets in the water column will promote breakup over re-

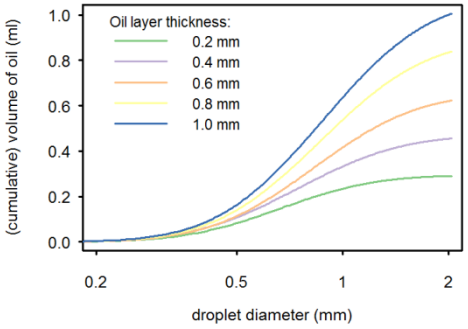

Fig. 3-9. The (cumulative) volume entrained per droplet size, calculated from the volume entrained (Fig. 5) and the distribution parameters (Table 3), for the different oil layer thicknesses at plunge height 20 cm. The absolute increase of volume in small droplets seems slight, but the relative increase of between layer thicknesses IS substantial.

coalescence.

Chemical dispersion
When chemical dispersants were applied, the oil was dispersed in large clouds of tiny droplets forming a cloud that obscured visibility in the tank. The oil droplets were too small to be able to quantify their sizes and entrained volume with our test setup. We could, however, observe that for chemically dispersed oil, a secondary entrainment event occurs when the air bubble created by the plunge (in the air-pocket phase) breaks through the water surface. This clearly shows that chemically treated oil can be entrained by even minor surface turbulence due to the strongly reduced oil/water interfacial tension.

3.6.3 Implications for oil fate modelling

The present study reveals the relevance of oil layer thickness as a parameter in modelling of the entrainment of oil by breaking waves: The amount of oil entrained by a plunging jet impact is directly proportional to layer thickness with the same impacted surface area. This entrained oil is broken into droplets of which a portion is small enough to remain suspended for longer periods of time. The initial amount of oil entrained and the energy input determines the volume of small oil droplets, which are considered to be most relevant for sustained oil entrainment. These results make future inclusion of the effect of oil layer height in oil dispersion modelling highly recommended.

The next step in understanding and quantification of oil entrainment is investigating the relationship between oil properties such as viscosity, oil layer thickness on entrainment and dispersion. Further it will be a challenge to include the effect of dispersant application on this vertical oil fate modelling.

3.7 Conclusions

The applied plunging jet apparatus with coupled camera equipment allows quantitative investigation of the effect of oil layer thickness and mixing energy (plunge height) on entrainment of oil.

For the oil type tested, the amount of oil entrained is directly proportional to the oil layer thickness and the volume fraction of smaller droplets increases with the plunging energy applied. With the current setup entrainment of dispersant-treated oil could only be qualitatively studied.

The effect of oil layer thickness should be included in future oil entrainment and dispersion modelling.

S3. Annex to chapter 3 (supplementary information)

Data are publicly available through the Gulf of Mexico Research Initiative Information & Data Cooperative (GRIIDC) at https://data.gulfresearchinitiative.org (doi: http://dx.doi.org/10.7266/N7RF5S04).

S3.1 - ANOVA tables

for the analysis performed on presented data

Output of a 1-way ANOVA on Area of water surface impacted by the jet

	Df	Sum Sq	Mean Sq	F value	Pr(>F)
Plunge Height	2	38462	19231.1	2.1062	0.2028
Residuals	6	54784	9130.6		

Output ANOVA (type III) on Volume of oil entrained @ T= 5 sec after jet impact (natural dispersion)

	Sum Sq	Df	F value	Pr(>F)
(Intercept)	0.2350	1	27.03	1.90E-06
Hoil (Oil Layer Thickness)	3.3939	4	97.57	< 2.2E-16
Hplunge (Plunge height)	0.0857	2	4.93	9.95E-03
Hoil:Hplunge (interaction)	0.3129	8	4.50	1.93E-04
Residuals	0.6087	70		

Output ANOVA (type III) on the fitted logarithmic number-based mean droplet size @ T= 5 sec after jet impact (natural dispersion)

	Sum Sq	Df	F value	Pr(>F)
(Intercept)	37.071	1	8342.580	< 2.2E-16
Hoil (Oil Layer Thickness)	0.490	4	27.581	2.80E-14
Hplunge (Plunge Height)	0.670	2	75.395	< 2.2E-16
Residuals	0.347	78		

Output ANOVA (type III) on the standard deviation of the fitted logarithmic number-based droplet size @ T= 5 sec after jet impact (natural dispersion)

	Sum Sq	Df	F value	Pr(>F)
(Intercept)	1.875	1	8029.9	< 2.2E-16
Hoil (Oil Layer Thickness)	0.008	4	8.8	8.38E-06
Hplunge (Plunge Height)	0.015	2	32.3	1.16E-10
Hoil:Hplunge (interaction)	0.011	8	5.7	1.30E-05
Residuals	0.016	70		

S3.2 Image Analysis Process, performed on Plunging Jet Test Pictures

To retrieve quantitative oil entrainment data from the plunging jet test pictures, image analysis is performed. This is done with the same software used for image acquisition (VisionLab). The image analysis of the droplets recorded is performed in three steps: droplet segmentation (1), classification (2) and volume quantification (3).

By combining the data from the close-up with the corresponding main view results, the total volume of oil entrained is calculated (4). Data points that do not comply with pre-defined assumptions are removed from the data sets (5).

Table S3-1. *Typical tests, chosen for validation purposes. Frames 56, 106, 156 & 190 of each experiment are analysed.*

Case	Oil.Type	Oil Layer thickness (µm)	Hplunge (cm)	Test Date	Test #
1	1	400	15	2013 11 18	16
2	1	1000	15	2013 11 18	10
3	1	600	10	2013 12 11	H10h600
4	1	600	20	2013 12 05	20_600

A subset of four 'typical' experiments was chosen for validation and illustration purposes (Table S3-1). These experiments span the entire range of settings used and give very different end results. Of these experiments images taken at four time intervals (2.5, 5, 7.5 & 10 sec after plunge impact) were used, giving a set of in total 16 'results'.

Droplet segmentation

We follow the general strategy in image analysis to first create a binary image

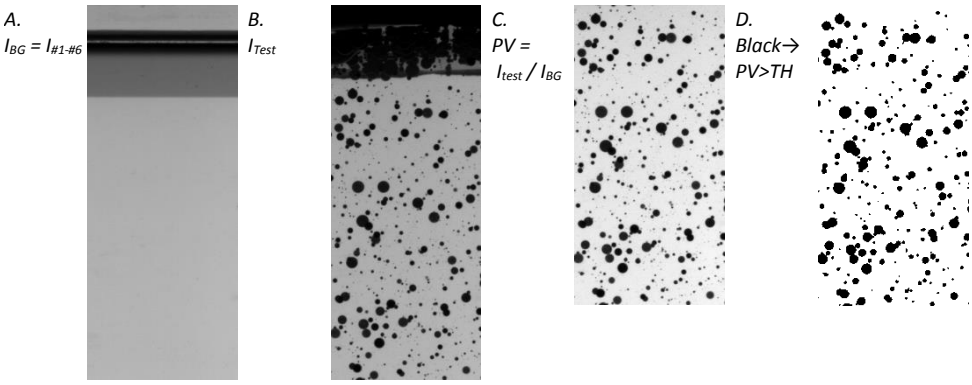

Fig. S3-1. *Image processing, performed on a cut-out of a close-up picture. A= average background image, taken before plunge impact. Notice the oil layer on top. B= test picture, T=5 seconds after impact. C= test picture after background removal. D = binary image of test picture (threshold applied). A slight rise in water level can be observed between A and B, due to a slight delay of the overflow mechanism.*

(Fig. S3-1). First a correction is performed for inhomogeneous illumination; for each experiment a background image is made by averaging the intensity(I) of each pixel in the 6 frames taken of the container prior to plunge impact (Fig. S3-1A). The test picture to be analysed (Fig. S3-1B) is then divided by the corresponding background image, which results in an image of the droplets only, without the background (Fig. S3-1C), in which the value of each pixel (PV) represents how bright(intense) the test picture is compared to the background.

A binary image is created by thresholding; pixels with a value (PV) below selected threshold are considered part of oil droplets (black), pixels with a value above the threshold are background/water (white) (Fig. S3-1D). Setting a lower threshold would incorporate less of the pixels on the edge of the droplet, thus making the droplets smaller, a higher threshold would do the opposite (Fig. S3-2).

The specific thresholds to be applied for the main (0.6) and close up images (0.7), were chosen using a heuristic method; pictures were selected from an experiment where most oil was expected to be present in the tank. The threshold was increased from 0 with increments of 0.05, the threshold was chosen as high as possible, while keeping most of the droplets visible as discrete objects (Fig. S3-2).

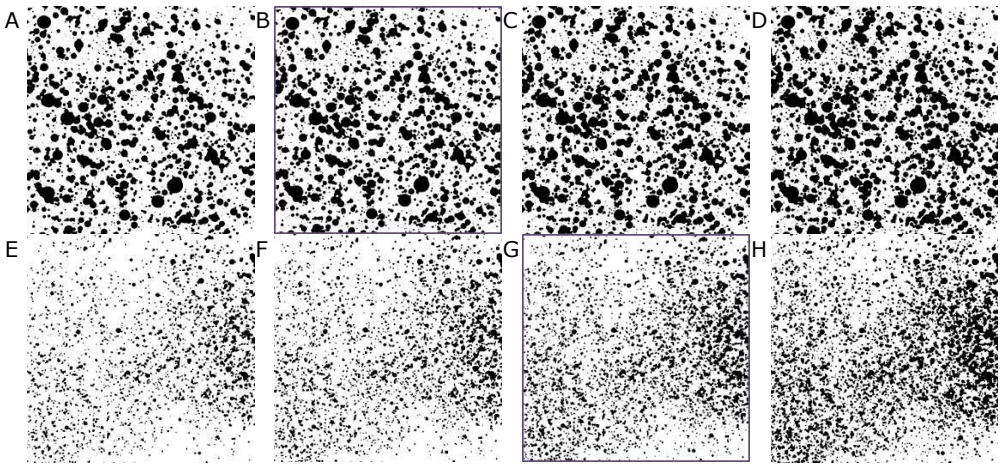

Fig. S3-2. *Result of applying different thresholds (0.5 (A,E), 0.6 (B,F), 0.7 (C,G), 0.8 (D,H)) on the images of case 2 (Table 1) at time T= 2.5 seconds after jet impact. A,B,C,D are cut-outs from the close-up picture (30% of the total width & height) taken from the lower right corner (busiest area). E,F,G,H are cut-outs from the main image (30 % of the width, and 37.5 % of the height) taken from the centre (busiest area). This is a worst-case scenario for amount of oil droplets in the image. Based on such images, the thresholds lined in purple were chosen (0.6 for main images) and (0.7 for close up images).*

Table S3-2. *BLOB features (VisionLab ouput) used in our analysis and calculations. (NHL university of Applied Sciences, 2013, help Files, n.d., chap. Labelling and Blob Analysis).*

Feature	Description	(Virtual) units
Area (ABLOB)	number of pixels in the BLOB	pixels(^{2})
AreaHolesRatio	number of pixels in all holes of the BLOB / number of pixels in the BLOB	-
Breadth	width of the bounding box (smallest possible rectangle that can be fit around the BLOB)	pixels
CoGX	location (Center of Gravity) of the BLOB (X coordinate)	-
CoGY	location (Center of Gravity) of the BLOB (Y coordinate)	-
Eccentricity	[0 = circular .. 1 = line shaped object]	
Ellipsfit	Area / (PI · 0,5 · Length · 0,5 · Breadth)	
ExcircleR	the radius of the smallest circle that encloses the BLOB.	pixels
FormFactor	4 · pi · area/(perimeter · perimeter), so: [0 = line .. 1 = circular shaped object].	
IncircleR	the radius of the biggest circle that is enclosed in the BLOB.	pixels
Hu1 .. Hu7	describe the geometry of the BLOB contour. (the seven Hu moments are position, scale and rotation invariant, because of the high dynamical range of the moments a logarithmical scaling function is used.)	
Length	length of the bounding box	pixels

After segmentation, groups of connected foreground pixels are considered as single objects, called BLOBs (Binary Linked OBject). For each of these BLOBs, the software returns a set of features or properties which are then used for further processing (Table S3-2).

In most cases one BLOB represents one suspended oil droplet. However, in the locations where very much oil is present, especially in short time after plunge impact, single droplets can overlap in the viewing direction. They are recorded as an 'aggregate' on the pictures (also visible in Fig. S3-1D), and observed as one BLOB. It must be understood that although it is obvious to the human eye (and brain) that these are multiple separate droplets, a computer system cannot make this distinction.

Droplet classification

To reliably assess the volume of the oil droplets, a method was developed to estimate the number and size of the oil droplets in a BLOB. Before doing so, a

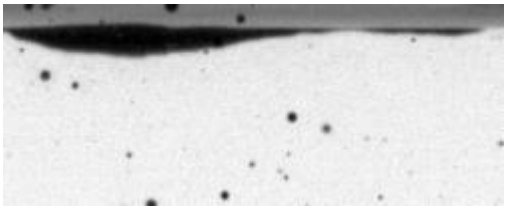

Fig. S3-3. *Example of an oil smear at on the tank glass. As this smear has a large area (in pixels), this would contribute substantially to the oil volume entrained and is therefore subtracted.*

Table S3-3. *Image analysis results for 9 close-images of a plunging jet test performed without oil. Test settings were identical to tests with oil, Hplunge = 15 cm. All objects in these images should be air bubbles.*

Image acquired @ T =	Number of BLOBs per image			Average	Volume of oil per image (px^3)			Average
2.5 sec. after impact	20	23	7	16.7	10473	11779	2414	8222
5 sec. after jet impact	7	2	2	3.7	1747	426	206	793
7.5 sec. after jet impact	0	0	1	0.3	0	0	44	15

For comparison: In the entire dataset of analysed pictures regarding publication "Quantification of the Effect of Oil Layer thickness on Entrainment" the minimum and average number of BLOBS per picture are 2711 and 43463 respectively, the minimum and average volume of oil per picture (in px^3) are 415342 and 4158363.

couple of features in the pictures have to be removed: BLOBs that are too small for reliable calculation are filtered out before further calculations by removing all BLOBS with an IncircleR smaller than 1. (These are 'droplets' smaller than 2 pixels; as they are represented by square pixels information on their precise size and shape is unknown and volume calculation would also not be very accurate or useful.)

To prevent too much impact of a possible oil smear at the glass wall near the water surface, objects in the upper 50 pixels with a Length/Breadth ratio larger than 3, are removed from the analysis (Fig. S3-3, Fig. S3-4).

Although most air bubbles will have left the tank before the time-scale of analysis, some air bubbles are still visible in the pictures as 'rings' (Fig. S3-4). During image processing, these air bubbles are filtered out based on their AreaHolesRatio. The applied limit for exclusion (AreaHolesRatio > 0.4) is relatively conservative, meaning that some of the air bubbles will not be filtered out. Applying a lower limit would increase the probability that oil droplet 'aggregates', mistaken for air bubbles, are erroneously removed from the analysis.

The air bubble recognition process was validated by applying the analysis process to pictures of an experiment without oil (all other settings where

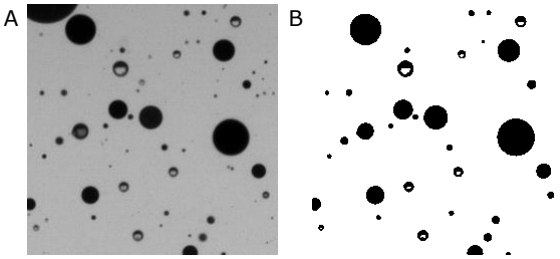

Fig. S3-4. *Air bubbles before (A) and after image processing (B). The software recognizes white pixels inside a black ring as a 'hole'. The area ratio of hole/ black ring (AreaHolesRatio) is used to filter out air bubbles.*

Table S3-4. *Description of the defined BLOB classes, and formulae for calculating number and size of droplets from BLOB features. For explanation of the formulas see text (droplet volume calculation).*

Class #		Diameter of the largest droplet D_1	Diam. of secondary droplet(s) D_n	Number of secondary droplets $n_{drops-1}$
1.	$D_1 \sim D_2$	$2 \cdot (A_{BLOB} \cdot \pi^{-1} \cdot (\text{Breath} / \text{Length}))^{0.5}$	D_1	1
2.	$D_1 \sim D_n$	$2 \cdot (A_{BLOB} \cdot \pi^{-1} \cdot (\text{Breath} / \text{Length}))^{0.5}$	D_1	Length / Breadth [rounded down to an integer]
3.	$D_1 > D_2$	Breadth	Length -Breadth	1
4.	$D_1 > D_n$	$2 \cdot$ IncircleR	the smallest of: $[D_1]$ and $[2 \cdot (\text{ExcircleR} - \text{IncircleR})]$	$(A_{BLOB} - (\pi \cdot \text{IncircleR}^2)) / (\pi \cdot D_n^2)$
5.	undefined/ remaining	$2 \cdot$ IncircleR	the smallest of: $[D_1]$ and $[2 \cdot (\text{ExcircleR} - \text{IncircleR})]$	$(A_{BLOB} - (\pi \cdot \text{IncircleR}^2)) / (\pi \cdot D_n^2)$
6.	$D_{drop} = D_{blob}$	$2 \cdot (A_{BLOB} \cdot \pi^{-1})^{0.5}$	-	0

identical), with the assumption that all objects in the water column are air bubbles. The process described does not remove all air bubbles from the analysis (fig. S3-5), the wrongly added volume of oil, however, is negligible compared to the total oil volume per test picture in our dataset (Table S3-3).

After removing these features, the remaining BLOBs represent oil droplets which need to be classified in order to determine their volume. Six output classes (BLOB types) were defined: two similarly sized droplets ($D_1 \sim D_2$), more similarly sized droplets ($D_1 \sim D_n$), one large with one smaller droplet ($D_1 > D_2$), one large with multiple smaller droplets ($D_1 > D_n$), single discrete droplets ($D_{drop} = D_{blob}$), and a separate class for unrecognizable BLOBs. For each of these six BLOB classes, the droplet size can be computed in a specific way (Table S3-4).

A (tedious) manual classification performed on several images was used as a calibration set for the automatic classification. This set of classifications

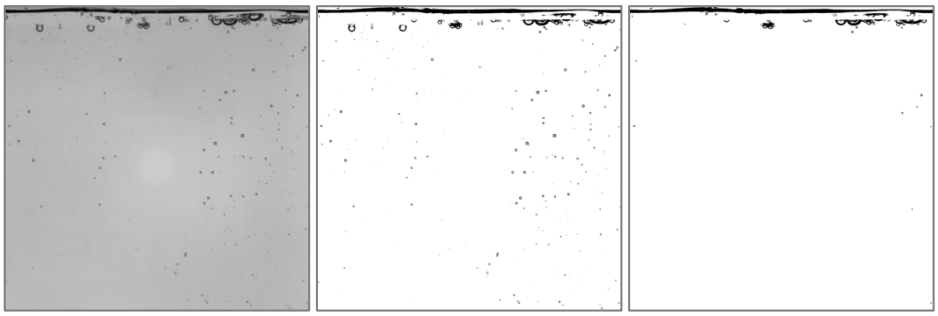

Fig. S3-5. *Air bubble removal process performed on a test without oil (all objects should be air bubbles). From left to right: original greyscale image, segmented image, image after air bubble removal. (Note that objects in the top of the pictures will be removed with the oil smear criterion).*

(prospected output) together with the BLOB features (prospected input),were used to train a linear classifier based on Linear Discriminant Analysis (LDA; Fisher, 1936).

In brief: LDA maps the calibration data in a 5 dimensional space (no. of dimensions = no. of classes - 1), with axes LD1 through LD5. A weighting factor is assigned to each of the BLOB features (Table S3-2), in such a way that, in this 5 dimensional space, the distance between the classes is maximized and the distance (variance) within the classes is minimized. An unknown BLOB, is then mapped using these weighting factors and assigned to the best fitting BLOB class.

Visual assessment was performed on a number of automated class assignments to validate the LDA process, and droplets were found to be classified correctly. Fig. S3-6 shows an example of the classifications of the BLOBs of Fig S3-1.

Most observed BLOBs are classified as single discrete droplets (class 6) (Fig. S3-7); BLOBs in this class will give the most accurate oil volume result. In all cases 'class 6' makes up the largest volume fraction of all classes. As expected, the volume fraction of oil in 'class 6' increases with time after the plunge and decreases for experiments were more oil entrainment is expected (case 2 vs case 1). It must be noted that experimental results with too much droplets in the most unreliable class (class 5), are removed from the analysis as described on page 73.

Droplet volume quantification

The metric used to calculate the volume of oil in a BLOB is specific for the BLOB type. When the BLOB consists of one droplet (class 6), the area of the BLOB is assumed to be a circle with diameter $D = (4 \cdot \pi^{-1} \cdot A_{BLOB})^{0.5}$ and the volume of

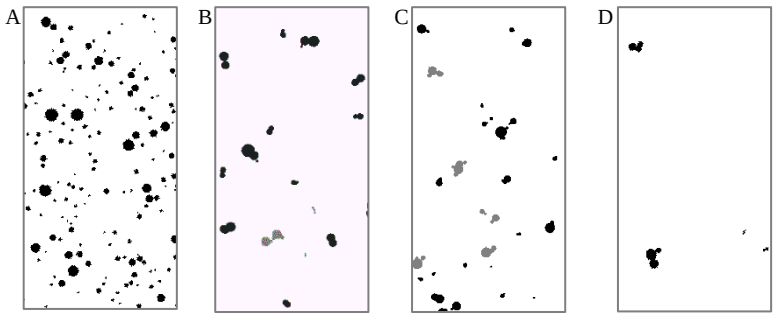

Fig. S3-6. *Example of BLOB classes extracted from Fig. 1D. A= class 6, single discrete droplets. B= class 1&2, 2 (class 1-black) or more (class 2-grey) similar sized droplets. C= class 3&4, one large droplet with 1(class 3-black) or more (class 4-grey) smaller droplets. D= class 5 undefined.*

this theoretical sphere is given by $V_{BLOB} = 1/6 \cdot \pi \cdot D^3$. For BLOBs of type 1 through 5, the volume is calculated by summing up the volumes of the respective droplets found: $V_{BLOB} = 1/6 \cdot \pi \cdot D_1^3 + (n_{drops-1}) \cdot 1/6 \cdot \pi \cdot D_n^3$. The total volume of oil in the picture is then obtained by adding up all the BLOB volumes ($V_{oil} = \Sigma V_{BLOB}$).

Volume of oil entrained

To convert the measures in pixels to ml of oil, a Scaling Factor (SF) is applied. Scaling factors (px/cm) in front and behind the tank were determined using a calibration sheet with a series of black dots. Two outer dots (9 cm apart) at the approximate height of the water surface were used for this analysis. Images of the calibration sheets were acquired using settings for lighting & camera's identical to those in the oil tests. Using the Visionlab software, the coordinates (in pixels) of both dots on the images were obtained (Table S3-5). The scaling factor (cm/px) in the centre of the tank was obtained by averaging the scaling factors in front and behind the tank.

Using the typical test data, comparability between the close-up and the main image was investigated. By only considering the droplets large enough to be observed on the main image (D >1 mm) and only considering the droplets

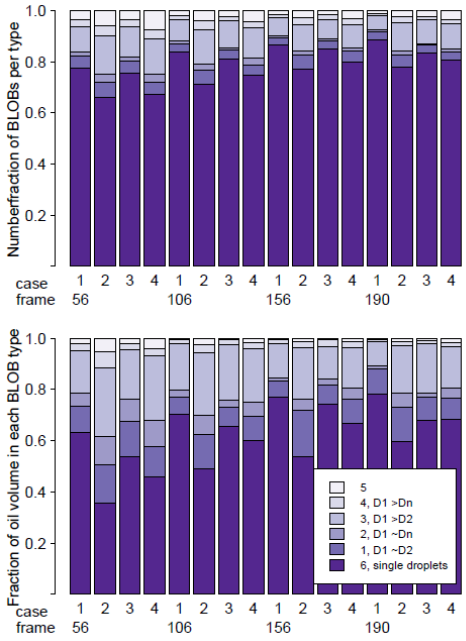

Fig. S3-7. *Number of BLOBs and Entrained oil volume separated per BLOB class, for all 4 test cases (Table S3-1) at 4 time intervals. BLOB classes are listed (top-down) in order of increasing confidence in the calculation accuracy.*

Table S3-5. *Scaling factors as determined from the calibration sheet measurement in front of the tank and behind it.*

View	Calibration sheet location	L (cm)	L (px)	Scalingfactor (um/px)	(ml/px^3)
	In front	9.00	1517		
	Behind tank	9.00	1339		
close				63.0	2.50E-07
	In front	9.00	388		
	Behind tank	9.00	340		
main				248	1.53E-05

located in the overlapping area between both pictures; the results obtained from the main image and close-up image should theoretically be the same. Results of the typical tests (Table S3-1) at all four time intervals show that there is indeed a very strong correlation between these results (Fig. S3-8).

There is a slight offset, the average ratio between the main result and close-up result is 0.848. Slight differences in image quality and processing between the close-up and main picture can be cause for this. However the fact that there is a very strong linearity between the result main and close-up picture means that within this shared 'field of observation' in terms of location and size (droplet size >1mm and location within the overlap region) they capture the same information. As a result, it is considered allowable to extrapolate information outside this shared 'field of observation' based on the available data.

As only with the close-up result also the smaller droplets can be quantified, this view is considered as most reliable. To indicate the total amount of oil in the tank, the volume of oil outside the close-up camera field of view is estimated by means of an Extrapolation Factor (EF) The EF is calculated based on the ratio of the volume of oil in the main picture in the overlapping area with that in the close-up picture of the same area. EF = ∑VBLOB (main, inside overlap with

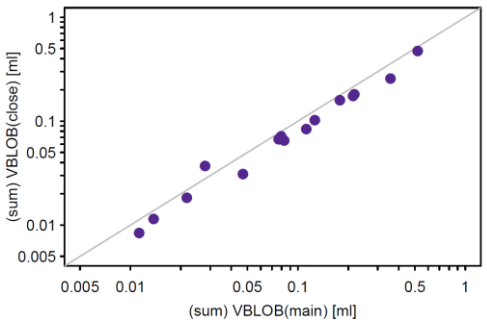

Fig. S3-8. *Correlation between 'volume of oil in the close-up image in droplets with diameters > 1mm' and 'volume of oil in the same area in the main image in droplets with diameters > 1mm' for the typical experiments (Table S3-1) at four time-intervals. Dots are the separate experiments, the solid line is y=x*

close) / ΣVBLOB (main). The oil volume in the main picture is calculated in the same way as for the close-up images, and the BLOBS are grouped as 'inside' and 'outside' the overlap, based on the coordinates known from the close-up picture.

The total volume of oil entrained at time (t) is calculated from the volume of oil in the close up picture, multiplied by the reciprocal of the Extrapolation Factor. The Scaling Factor (SF) is used to calculate the volume from the pixels:

$V_{oil}(t) = \Sigma V_{BLOB\ (close)}(t) \cdot SF \cdot EF(t)^{-1}$.

The results of $\Sigma V_{BLOB\ (close)}(t)$, $\Sigma V_{BLOB\ (main)}(t)$, $\Sigma V_{oil}(t)$ for our typical experiments are shown in fig. S3-9. In most cases the close-up picture observes most oil, as it's viewing area is the busiest area in the tank and the close-up image can observe smaller objects. The ratio between the close up result (green) and the end result (purple) differs in each case, as this is dependent on how much oil is observed outside the close-up viewing area as described above.

Removing unreliable data-points

After these calculations, each entrained oil volume (V_{oil}), calculated from a matching close-up and main picture, makes up one data-point. Some data points were excluded from the analysis, namely if:

- More than 5% of the total volume of oil in the picture is from 'class 5 BLOBs' for which droplet sizes only can be an estimation. This is not a problem as long as the volume of these BLOBs is a small fraction of the total volume of oil.

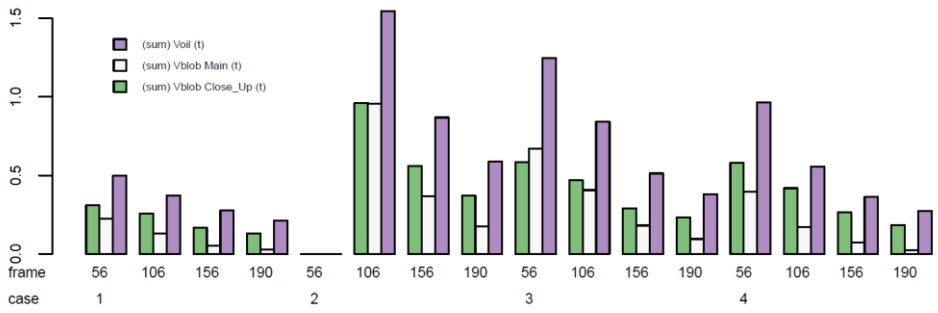

Fig. S3-9. *The results for the 'typical experiments': Oil volume observed in close-up view $\Sigma V_{BLOB\ (close)}(t)$, Oil volume observed in main view $\Sigma V_{BLOB\ (main)}(t)$, Oil volume in the entire tank as obtained by extrapolation $\Sigma V_{oil}(t)$*

- More than 5% of the observed oil volume is within the smallest visible size category (between 4 and 5 pixels in diameter). This would be a strong indication that a relatively large portion of the 'tail' of the droplet size distribution is expected extend below the detection limit of ~4 pixels, without requiring a specific size distribution to be fit for each test.

CHAPTER 4

How oil properties and layer thickness determine the entrainment of spilled surface oil

M. Zeinstra-Helfrich[a,b], W. Koops[a], A.J. Murk[b,c]

Zeinstra-Helfrich, M., Koops, W., & Murk, A. J. (2016). How oil properties and layer thickness determine the entrainment of spilled surface oil. Marine Pollution Bulletin. 110. 184-193

---

[a] NHL University of Applied Sciences, Dept. Maritime, Marine, Environment & Safety
[b] Wageningen University and Wageningen-IMARES, Sub-department of Environmental Technology
[c] Marine Animal Ecology group, Wageningen University, P.O. Box 338, 6700 AH, Wageningen, The Netherlands

Abstract

Viscosity plays an important role in dispersion of spilled surface oil, so does adding chemical dispersants. For seven different oil grades, entrainment rate and initial droplet size distribution were investigated using a plunging jet apparatus with coupled camera equipment and subsequent image analysis. We found that the amount of oil entrained is proportional to layer thickness and largely independent of oil properties: A dispersant dose of 1:200 did not result in a significantly different entrainment rate compared to no dispersants. Oil viscosity had a minor to no influence on entrainment rate, until a certain threshold above which entrainment was impeded.

The mean droplet size scales with the modified Weber number as described by Johansen. The obtained results can help improve dispersion algorithms in oil spill fate and transport models, to aid making an informed decision about application of dispersants.

4.1 Introduction

Oil spilled at sea undergoes a number of weathering processes as a result of its exposure to air (wind), seawater (currents), sunlight and wave energy. These weathering processes change the characteristics of the oil (viscosity, density, surface tension), the oil slick qualities (size, fragmentation, persistence) as well as water column exposure (amount and size of dispersed droplets). Among these processes is natural dispersion, in which wave action mixes oil droplets into the upper layers of the water column enabling dissolution of soluble compounds and biodegradation.

An often-used tool in the spill-response toolbox, application of dispersants (chemical dispersion), enhances this natural dispersion process. This type of response has a number of logistical advantages over other response options such as mechanical recovery of oil from the surface; it can be applied fast (by air) on large volumes of oil and it is less restricted by weather conditions. Resulting increased levels of oil in the water column, however, will enhance acute exposure of local organisms to oil in combination with dispersant. To be able to assess potential adverse effects, the effectiveness of chemical dispersion should be estimated with more accuracy than is currently possible.

For oil spill responders it is very important to be able to predict how the oil mass balance (floating vs dispersed oil) and trajectory will be altered by chemical dispersion. This requires a (surface oil) dispersion algorithm that can calculate natural and chemical dispersion for different oil types and environmental conditions. With such an algorithm we can determine the benefit of dispersants, which is assumed to be limited in either low or very high energy conditions as well as for high viscosity oil types (ITOPF, 2012; National Research Council of the National Academies, 2005) and is unknown for values other than these extremes.

Two main processes in dispersion of surface oil at sea are entrainment and breakup into droplets. Entrainment is the transition of floating to submerged oil, as the oil is pushed down by a breaking wave. Breakup into smaller droplets occurs as a result of this high energy impact. Smaller droplets are favourable for a stable dispersion, as they remain suspended for a longer time due to their lower rise speed.

A plunging jet can be used to simulate the vertical energy input of a breaking wave. Plunging jets are used to study air entrainment by breaking waves (Chanson and Jaw-Fang, 1997; Roy et al., 2013) as well as oil dispersion (Delvigne and Hulsen, 1994; Reed et al., 2009). The size of air bubbles

entrained by a plunging yet can be calculated using the Weber number and impact (turbulence) conditions (Chanson and Cummings, 1994). Oil entrainment differs from air entrainment in two ways; the viscosity and the availability of the 'entrained' medium. Air is much less viscous than oil and abundantly available, whereas oil is only present as a surface film. Of the different air entrainment mechanisms described in literature, two were considered relevant for oil entrainment by jets and waves (Zeinstra-Helfrich et al., 2015a). 1) Oil being sandwiched between the falling jet and the receiving water travels down with it (entrapment). 2) The interfacial shear induced by the impacting jet slightly pulls down the surrounding (water or oil) surface, oil can be dragged into the jet downward movement.

The entrapment process (1) is expected to prevail, due to the intermittent nature of wave breaking that agitates a 'new' area each time.

4.1.1 Consequences of oil properties for dispersion

It is well accepted that oil type is a key variable in both natural and chemical dispersion, especially the oil qualities viscosity and interfacial tension (Lewis et al., 2006; National Research Council of the National Academies, 2005). Chemical dispersants lower the oil water interfacial tension and thereby favour the creation of much smaller oil droplets (Khelifa and So, 2009; Lee et al., 2009; Lunel, 1993). Interfacial tension for fresh oil (and seawater) is usually around 25 mN/m but can range from 8 to 40 mN/m. Weathering of the oil generally slightly increases interfacial tensions (Wang et al., 2003). Application of dispersants can lower interfacial tension by a couple of orders of magnitudes and even for very viscous oils dispersants lower the viscosity (SL Ross Environmental Research and MAR Incorporated, 2010).

Oil viscosity influences the dispersion process in different ways. In colloid and food science, it is well accepted that higher viscosity will create larger droplets (Walstra, 2005). Although similar observations have been made in relation to dispersion of spilled oil, a consistent relationship between viscosity and oil droplet size has not yet been established (Canevari et al., 2001; Fingas et al., 1991; Zeinstra-Helfrich et al., 2015c).

Additionally, a sharp decline of dispersion efficiency with viscosity is reported: Chemical dispersion of oil at sea is considered not feasible for oils with a viscosity above 10 to 20 Pa.s (ITOPF, 2012; National Research Council of the National Academies, 2005) because of 1) the difficulty of the dispersant penetrating and mixing into the oil layer and 2) the resistance of viscous oils to breakup in small droplets.

Wave tank test results indeed indicate a cut off in chemical dispersion effectiveness: oil with a viscosity above 33.4 Pa.s could not be dispersed chemically in the OHMSETT wave tank with a wave height of 0.42m (Trudel et al., 2010). Oil-dispersant mixtures with viscosities above 10 Pa.s (DOR up to 1:20) could not be dispersed In the 0.22 m high waves in the (small scale) SLROSS wave tank, but could be dispersed under the higher waves of the OHMSETT tank (SL Ross Environmental Research and MAR Incorporated, 2010). Further increase of the dispersant dosage resulted in reasonable dispersion for these oils in the smaller SLROSS tank, even though oil-dispersant mixture viscosities still ranged up to 13 Pa.s.

Additional OHMSETT wave tank trials indicated that dispersant incorporation in the oil was no limiting factor in the dispersion of these viscous oils, as oils sprayed with dispersants dispersed better than those pre-mixed with dispersants (SL Ross Environmental Research and MAR Incorporated, 2010).

There is a sharp decline in dispersion efficiency that depends on viscosity, dispersant (interfacial tension) and mixing energy.

4.1.2 Oil properties and layer thickness in dispersion algorithms

The well-known and most used algorithm for dispersion of surface oil, by Delvigne and Sweeney (1988), reduces the properties of an oil type into one constant, C, and does not consider oil layer thickness to be relevant (Zeinstra-Helfrich et al., 2015c).

The (natural) dispersion algorithm suggested by Mackay does include the steps for entrainment and break-up. In this algorithm, the fraction of oil (naturally) dispersed rate per unit of time (D) is calculated by multiplying the fraction of sea surface dispersed per unit of time (D_a) with the fraction of the dispersed oil not returning to the slick (D_b) determined for specific oil qualities (viscosity and interfacial tension) (Nazir et al., 2008):

$$D = D_a \cdot D_b = 0.11[U_w+1]^2 \cdot [1+50 \cdot H_{oil} \cdot \mu^{.5} \cdot \sigma]^{-1} \qquad (4\text{-}1)$$

with, the fraction of sea surface subject to dispersion (fraction of oil entrained) per hour, D_a, depending on wind speed (U_w) and independent of oil properties. The fraction of oil permanently dispersed (D_b), i.e. fraction of oil in small droplets, decreases with increasing viscosity (μ) and interfacial tension (σ). In this formula, an increasing oil layer thickness (H_{oil}) results in a smaller fraction of oil permanently dispersed, yet the absolute oil volume permanently dispersed ($H_{oil} \cdot D_a \cdot D_b$) does increase with layer thickness.

In more recent work, oil droplet size created by a plunging jet was related to oil (layer) characteristics and impact conditions using an algorithm based on the non-dimensional Weber and Reynolds numbers (Johansen et al., 2015). In their work, two breakup regimes are considered depending on the dominant opposing force; 1) interfacial tension-limited regime, in which case droplet size correlates with the Weber number ($\rho \cdot U_h^2 \cdot H_{oil}/\sigma$) and 2) viscosity-limited regime, in which case droplet size correlates with the Reynolds number ($\rho \cdot U_h \cdot H_{oil}/\mu$). The model formula $D_{50}/H_{oil} = A \cdot We^{-a} + B \cdot Re^{-a}$ combines these both regimes.

The exponent a = 0.6 and constants A = 2.251 and B = 2.251·0.027, fitted from their plunging jet test data, make the final equation:

$$\frac{D_{50}}{H_{oil}} = 2.251\left(\frac{\rho\, U_h^2\, H_{oil}}{\sigma}\right)^{-0.6} + 0.607\left(\frac{\rho\, U_h\, H_{oil}}{\mu}\right)^{-0.6} \quad (4\text{-}2)$$

with; the number median droplet size (D_{50} in m), the oil layer thickness (Hoil in m), oil density (ρ in kg/m^3), oil-seawater interfacial tension (σ in N/m), oil dynamic viscosity (μ in kg/ms) and Uh the plunge impact speed (m/s) calculated from the plunge height (in m): $U_h = \sqrt{2gH_{plunge}}$.

This means, relative droplet size scales with the modified weber number D/Hoil = A · We*-a. The modified weber number, written in full:

$$We^* = \frac{\rho\, U_h\, H_{oil}}{\sigma}\left(1 + \frac{B}{A}\left(\frac{U_h\, \mu}{\sigma}\right)^a\right)^{-1/a} \quad (4\text{-}3)$$

The approaches by Mackay and Johansen both incorporate the effect of oil properties and layer thickness on droplet size more explicitly than the widely used Delvigne algorithm. The entrainment process as incorporated by Mackay, however, is independent of oil properties.

4.1.3 Aim and approach

In this paper, we aim to quantify the consequences of the oil layer thickness, the oil viscosity and the effects of dispersants on the entrainment process and initial breakup into droplets. The entrainment of oil is determined using a plunging jet apparatus. We quantify amount of oil entrained and initial droplet size distribution by performing image analysis on pictures obtained with a set of cameras coupled to this test system. This procedure was used for a set of experiments comprising a series of oil types (with assessed viscosity) and layer thicknesses. Additionally, a small set of chemical dispersion experiments is performed, using the same set-up.

4.2 Materials and methods

4.2.1 Materials

Our experiments cover 7 different oil types. Two main oil types: A, surrogate MC252 oil obtained through the GoMRI programme (Pelz et al., 2011) and B, a more viscous North Sea oil. To obtain a viscosity range, 3 different mixtures of A & B oils were made. Additionally, oils A and B were weathered by evaporation by placing them on a heated stir plate for three days, resulting in 27.6% and 8.2% evaporative loss respectively.

Dispersant used was Corexit EC9500A, kindly provided by NALCO (Nalco, 2011).

Artificial seawater for the experiments was prepared from demineralised water with artificial sea salt mix (Coralsea Salt, AquaHolland Dordrecht). The seawater was aerated for at least 20 h before use and the seawater conductivity was adjusted to between 41 and 42 mS/cm at 25 °C, by either adding demineralised water or sea salt. After sufficient mixing, the water was filtered (pore size 0.053 mm) to remove possible suspended particles.

4.2.2 Viscosity measurements

The viscosity was determined using a Physica MCR301 rheometer with coaxial double gap geometry (DG26.7-SN11575). A coupled Peltier temperature control unit (C-PTD 200) ensured a constant oil temperature of 18 °C during the measurements.

Before the start of the measurement, the oil samples are subjected to a shear rate of 10 /s for 60 s to ensure homogeneous filling of the cup and remove possible air bubbles, followed by a stagnant period of 30 s. Viscosity measurements were performed with a shear rate measuring range from 5 to 5000 s^{-1} in 30 logarithmic increments.

Between measurements, the cup and spindle were cleaned with the following procedure: rinse off visible oil with plenty of running water, wipe all surfaces with an ethanol-soaked cloth, and rinse with demineralised water and air-dry.

4.2.3 Entrainment quantification

The entrainment process and initial droplet size distribution were investigated using a plunging jet test with a coupled camera system and subsequent image analysis. Full details can be found in the method paper and its supplementary information (Zeinstra-Helfrich et al., 2015a), in brief the plunging jet procedure

is as follows (Fig. 3-1): The holding tank(1) is filled with just over 9 l of artificial seawater, the overflow(5) connected to the bottom of the tank ensures the water level is constant between tests. The amount of oil required to produce a certain oil layer thickness is distributed across the water surface by drop-wise addition. Every 0.1 mm of oil height requires 3 ml of oil, which is inversely pipetted using a 5 ml pipette with tip. The oil layer is left to 'settle' for 10 min. To execute the plunge test, the plunge container (2) is tilted backwards until the upper bracket (3) and filled with 100 ml of artificial seawater. Upon release, the container tilts back to its horizontal position onto the lower bracket (4) thereby pouring its contents onto the holding tank.

A small lever (7), hit by the dropping plunge container, makes a microcontroller (8) trigger the two industrial grade IDS cameras to record overview (9) and close-up (10) images of the events underwater at set periods of time. The LED back light (6) (Smart Vision Light, SOBS-450 300, Stemmer Imaging), ensures optimal droplet visibility and contrast in the images. Camera set-ups are optimised to reduce motion blur (shutter speed), optimise depth of field (diaphragm and focus) and minimise perspective distortion (lens focal length).

After a test, the oil is removed from the water surface with oil-only-absorbent sheet. The glass walls of the tank are cleaned in the same manner. Once the tank and water surface are visually clean, the procedure is repeated with a clean absorbent sheet. After a maximum of 10 tests and after every test with dispersants, the tank is fully drained, washed with water and detergent and rinsed with demineralised water before further use.

4.2.4 Quantification of entrainment and droplet size

For quantification of the results, the same software for image acquisition (Vision Lab) is used to perform image analysis on 3 separate images taken at 4.9, 5 and 5.1 s after plunge impact.

The background image of the test tank before plunge impact is subtracted from the test image, yielding a relative brightness/intensity value for each pixel. The image is transformed into black and white by applying a threshold for this pixel value (0.6 and 0.7 for main and close-up images resp.): Dark pixels with a pixel value below the threshold are considered part of oil droplets (black), brighter pixels with high values are background/water (white). In the black and white image, each group of connected black pixels is considered an object, a BLOB (Binary Linked Object). Each BLOB has designated features such as location, length, width, area. Most BLOBs represent single spherical oil droplets and are easy to quantify. However, in locations with large amount of oil droplets,

droplets will overlap in the viewing direction and are recorded as an aggregate on the images. Six BLOB categories were defined (ranging from single spherical droplets, to multiple similarly sized droplets to undefined blobs, (Zeinstra-Helfrich et al., 2015b), each with its own calculations for number of droplets and diameters of those droplets. Using Linear Discriminant Analysis and a hand-made training-set, the BLOB-features were used to classify the BLOBs into the different categories, after which the individual droplet diameters could be calculated.

Using the diameter of the main droplet (D_1) as well as the number ($n_{drops-1}$) and diameter (D_n) of the secondary droplets, the volume of oil in each BLOB is determined with: $V_{BLOB} = 1/6 \cdot \pi \cdot D_1^3 + (n_{drops-1}) \cdot 1/6 \cdot \pi \cdot D_n^3$.

The total volume of oil in the picture is obtained by adding up all the BLOB volumes. The close-up image is most reliable, but cannot account for all the oil in the tank. The total volume of oil entrained is calculated by combining the data from the close-up image with that of the matching main image (taken at the same time). $V_{oil}(t) = \Sigma V_{BLOB\ (close)}(t) \cdot SF \cdot EF(t)^{-1}$. In which $\Sigma V_{BLOB\ (close)}$ is the total volume of oil in the close up picture, SF is a scaling factor from pixels to ml and EF is an extrapolation factor for the amount of oil outside the close up view: $EF = \Sigma V_{BLOB\ (main\ view,\ inside\ overlap\ with\ close\ view)} / \Sigma V_{BLOB\ (main)}$.

For each close-up image, a (left truncated) log normal droplet size distribution was fit to the density distribution of the individual droplet diameters (Zeinstra-Helfrich et al., 2015a). Lognormal distributions are very common in this field of study (Johansen et al., 2013; Lee et al., 2009; Li et al., 2009b), the truncation takes into account that there is no data below the measurement limit of 4 pixels.

The obtained droplet size distribution parameters (log mean and log sd) were used to calculate the mass median diameter (using Hatch-Choate equations) and the volume fraction of oil in the small size classes (< 500 μm).

Data points are removed from the analysis if there is suspicion that they do not comply with our assumptions: If more than 5% of the oil in either the close up or the main image originates from BLOBs with an undefined shape as, for these BLOBs, the oil volume is a rough estimate. Also if the smallest visible size category in the close up image (4-5 pixels in diameter) makes up more than 5% of the observed oil volume this would mean a too large portion of the droplet size distribution extends below our detection limit.

In post-processing, the actual oil layer thickness for each test is calculated from the volume of oil applied and the actual area covered by oil. The latter is

Table 4-1. Number of experiments performed per test setting and symbol and colour designation used throughout this paper. Italic numbers are not used in the ANOVA's, but are used in graphics, tables and interpretation of the results.

	(nominal) Oil layer thickness (mm)				
Oil type	0.2	0.4 (Chem)	0.6	0.8	1.0
A (MC252)	*2* ▼	2 ●	*2* ◆	2 ▲	*2* ■
B		2 ● 1 ○	*2* ◆	2 ▲	*2* ■
75/25 A/B		2 ● 1 ○		2 ▲	
50/50 A/B		2 ● 1 ○		2 ▲	
25/75 A/B		2 ● 1 ○		2 ▲	
Aevap		2 ● 1 ○		2 ▲	
Bevap		2 ● 1 ○		2 ▲	

obtained by estimating the surface area not covered by oil from the frames before test impact.

4.2.5 Experimental design

In this investigation, we worked with one plunge height (15 cm), selected based on previous experiments (Zeinstra-Helfrich et al., 2015a). The majority of the experiments was performed with layer thicknesses of 0.4 and 0.8 mm (Table 4-1). For oil types A and B some additional layer thicknesses were investigated.

Chemical dispersion tests were performed with an oil layer thickness of 0.4mm and for all oil types except oil type A which dispersed into too small droplets for our analysis (Zeinstra-Helfrich et al., 2015a).

For chemical dispersion tests, oil was pre-mixed with dispersants prior to application on the water surface to be able to standardise dosing. Dispersant was used in a dispersant to oil ratio (DOR) of 1:200. This dose is well below the recommended (1:20) for two reasons: First of all, higher dosages have shown to create such dense plumes of small droplets that they are not quantifiable in our system. Secondly, dispersant losses can occur between spraying from an aircraft and incorporation in the oil layer at sea (spray drift, washing off of the slick, fall through, leaching). Therefore we assume the recommended dosage is rarely achieved in real application of dispersants.

4.2.6 Statistical procedures

The significance of the effects of the variables on the entrainment results were tested with type III ANOVA, as it can deal with unequal 'sample sizes' that can occur due to removal of unreliable data points. This analysis was performed on the .4 and .8 mm layer thickness experiments. The more limited results of the

other thicknesses (italics in Table 4-1) are shown in the graphs and tables and are used in the interpretation of the results.

All ANOVA's were first performed including interactions between variables. When the interaction did not have a significant effect on the response variable, the ANOVA was repeated without interactions.

4.3 Results

4.3.1 Oil viscosity

The viscosities of the oils and mixtures thereof are evenly distributed between the viscosities of the 'original' oils A and B (Fig. 4-2). At shear rates exceeding 500 /s, these oils are slightly less viscous, so they show slightly pseudo-plastic behaviour. The oils weathered by evaporation (Aevap, Bevap) have much greater viscosity and also show more pseudo-plastic behaviour at greater shear rates than the original oils.

Viscosities measured at a shear rate of 10 s^{-1} are used in further comparison, as this is common oil dispersion studies, including Johansen's work. It should be noted that the relative differences in viscosity between the oil types change with shear rate.

4.3.2 Entrainment

Based on the reliability criteria given at the end of paragraph 4.2.3, all of the results of the 38 experiments performed without dispersants are acceptable for further analysis. For the seven chemical dispersion experiments, the results with oil type Bevap had to be removed, as the analysed images had a too large

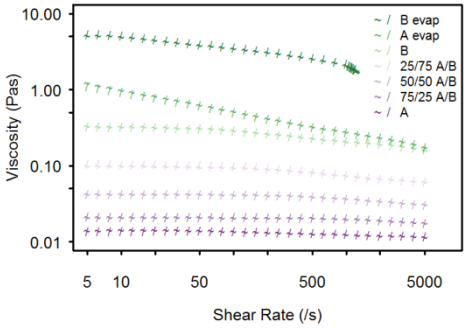

Fig. 4-2. Viscosity (y axis) of the different oil types (colours) at different shear rates (x-axis). The two replications are shown with separate symbols (/,~) but mostly overlap. High viscosity of the weathered oil type B made measurements above 1000/s in this setup impossible, as the torque limit of the measurement system (0.2 N) was reached.

percentage of oil in BLOBs with unidentified shapes.

Oil volume entrained

Analysis of variance on the balanced dataset comparing natural dispersion results for the different oil types at the layer thicknesses 0.8 and 0.4 mm, indicates that the volume of oil entrained is significantly influenced by both oil layer thickness ($P < 2.2E-16$) and oil type ($P < 2.2E-16$), independent of their combination (no interaction) (S4.1 - ANOVA tables).

As can be seen in Fig. 4-3, the slope of the relationship between oil layer thickness and volume of oil entrained is quite similar for all oil types (slope 1.035). Oil types A and B have been tested at greater layer thickness; for oil type B with layer thickness > 1 mm the entrained volume seems to become less.

The absolute amount of oil entrained clearly is less for oil Bevap than for the other oils (Fig. 4-3), the results with the other oil types appear to be very similar to each other. A fitted linear model (S4.1) shows that the volume of oil entrained for oil type Bevap indeed differs significantly ($P < 2.2E-16$) from the others, as does oil type B ($P=0.007$). The corresponding coefficients, indicate that for oil type Bevap entrainment is much lower, and for oil type B it is slightly higher than the other oil types (S4.1).

The images of the oil layer during plunging jet impact also show a different behaviour of oil type Bevap compared to the other oils (Fig. 4-4): The jet impact itself (left column) creates an indentation in the receiving pool, this 'cusp' is typical for impact of translating (moving) jets (Gómez Ledesma, 2004; Kiger and Duncan, 2012). When oil is present on the water surface (middle columns), the cusp is similarly shaped and 'lined' with oil. At the bottom of the cusp, oil

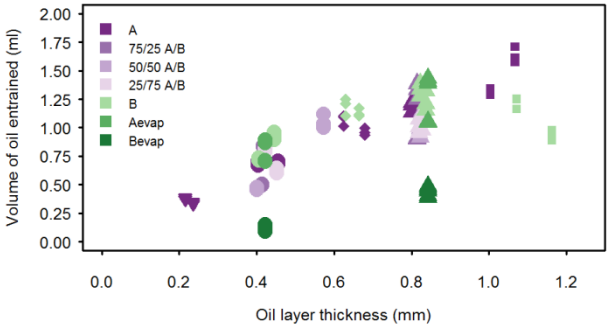

Fig. 4-3. Volume of oil entrained for the 7 oil types (see table 4-1), at 5 s after jet impact (natural dispersion). Results other than 0.4 and 0.8 mm (excluded from the ANOVA) have slightly smaller markers.

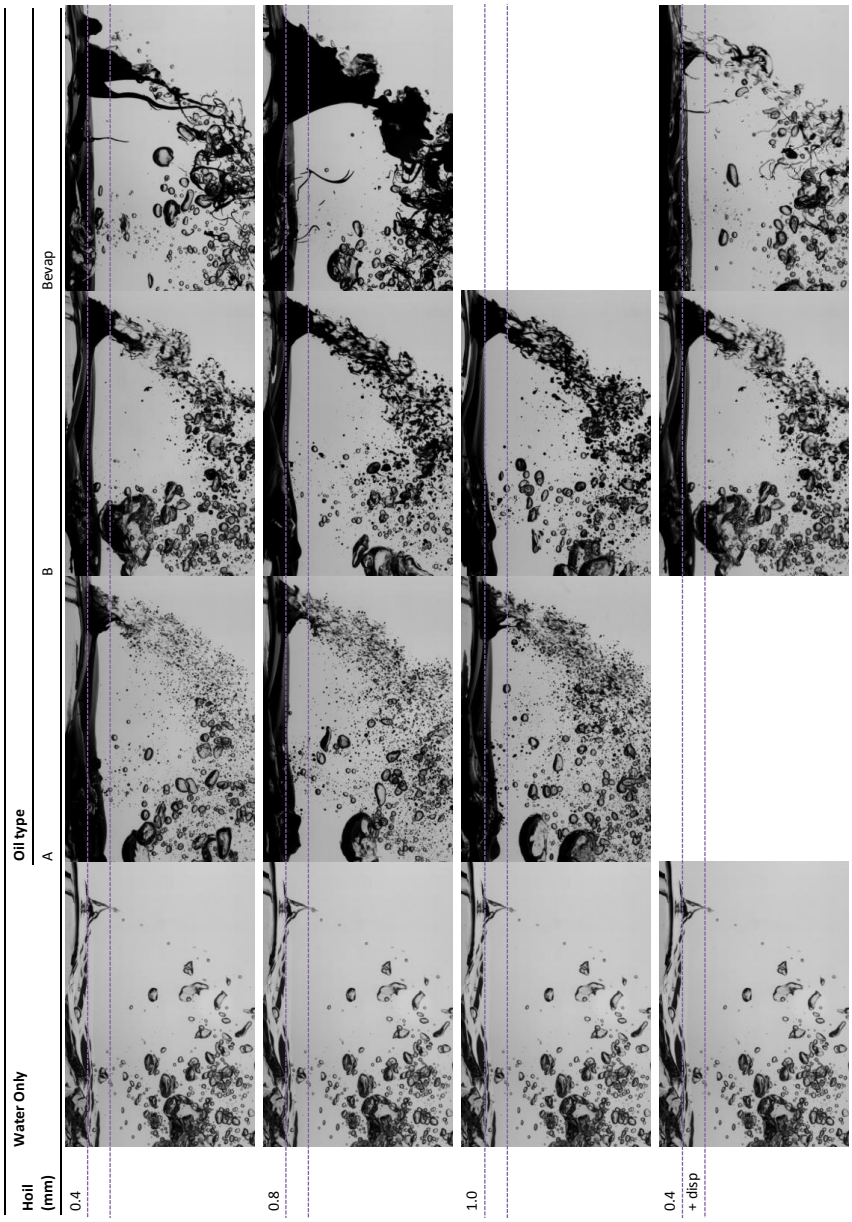

Fig. 4-4 Flow profile under water of the incoming plunging jet (on the upper right the jet is visible above the water surface). With no oil, and oil types with increasing viscosity: A, oil type B, and oil type Bevap. The flow profile for most of the tested oils (including those not shown) is similar to the impact without oil; The depth of the intrusion ('cusp') created by the jet impact on a layer is indicated with a purple dashed line. In the test of oil type Bevap, the cusp extends deeper.

droplets are continuously sheared off of the oil layer. The cusp at the jet impact on an oil layer of oil Bevap (left column) extends much deeper and irregularly shaped (stretched, sometimes even fibre-like) 'droplets' are broken off.

Direct comparison of the test results of oil treated with a 1:200 dose of dispersants with the results of the same untreated oil, indicates that the applied dosage of dispersants (P=0.0785) does not have a significant effect on the volume of oil entrained (S4.1).

Entrained oil droplet sizes

Oil droplet size distributions from different frames within each experiment are very similar, and show a good fit with the (left truncated) lognormal distribution (example Fig. 4-5). As can be seen, addition of dispersant creates a shift in the droplet size distribution to the left. All droplet size distribution data (number mean diameter, standard deviation) are provided in the annex (S4.2), our elaboration here focusses on the inferred data that are most relevant for the dispersion process.

The mass median diameter of the droplet size distribution, is significantly influenced by oil type (P<2.2E-16) and oil layer thickness (P=0.0024) (S4.1). The mass median diameter ranks with viscosity to a large extent, except for oil type Aevap. Mass median diameter slightly increases with oil layer thickness, except for oil type B (Fig. 4-6). The results of the experiments with oil type Bevap show a much larger variation between mass median diameters (also within the same experimental settings).

The fraction of oil in the small inferred size classes (< 500 μm), is significantly

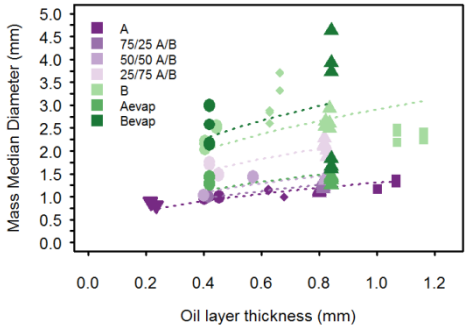

Fig. 4-5. Mass Median Diameter 5 s after plunge impact as a function of oil layer thickness. Dotted lines represent D~Hoil$^{0.4}$ for each oil type (this relation between droplet size and layer thickness results from rewriting eq. 4-1).

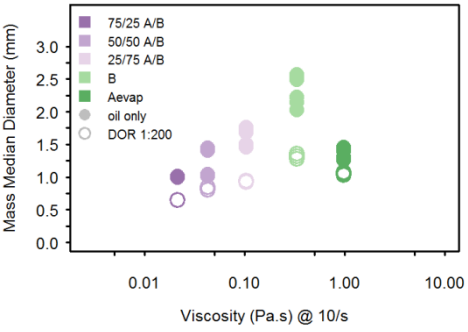

Fig. 4-6. The effect of dispersants (open circles) on the droplet sizes for the different oil types 5 s after plunge impact.

influenced by oil layer thickness (P=8.73E-11), oil type (P<2.2e-16) and their interaction (P=1.15E-08) (S4.1). Although the fraction of oil in small volume droplets decreases with oil layer thickness, the (absolute) volume of oil in small droplets increases slightly with layer thickness because of the increased entrainment (S4.2).

Treatment of the oil with a 1:200 dose of dispersants, results in a significant reduction of droplet size (P=9.93E-13) and the change in droplet size is clearly oil type dependent (Oil type: P<2.2E-16, Interaction: P=1.52E-05) (S4.1). The mass median oil droplet diameter decreases by 20 to 50% upon addition of dispersant (Fig. 4-6) and ranks in the same way with original oil viscosity as for naturally dispersed oils, with Aevap being the odd one out again.

4.4 Discussion

The aim of this study was to quantify the effect of oil viscosity, layer thickness and the addition of dispersants on oil entrainment and initial droplet breakup. We reveal that in our setup the oil volume entrained is proportional to the layer thickness and largely unaffected by oil viscosity up to 5 Pa.s as well as presence of dispersants. The droplet size increases slightly with oil layer thickness and more with oil viscosity, and greatly decreases with application of dispersants. The results with oil type Aevap, however are consistently lower than the observed trends would suggest.

Of the 45 test performed, images of 44 comply with the criteria for reliable quantification as given in paragraph 4.2.3. Only the test results for chemical dispersion of Bevap are excluded because this oil does not breakup into droplets but forms fibre-like strings for which the image analysis is not validated.

4.4.1 Volume of oil entrained

In our test set-up, due to the timing between the impact and the analysis (5 s), some settling of the larger droplets occurs. As the smaller droplets in the droplet size distribution are the most relevant ones in the dispersion process, this potential deviation is not considered a threat for our results. This settling of the larger droplets could be the cause for the (largely insignificant) spread in the entrainment-results between the oil types other than Bevap (Fig-4.3).

Effect of oil layer thickness

The volume of oil entrained follows a linear trend with layer thickness but the entrainment decreases again for thickest layers (> 1 cm) of oil type B (Fig. 4-3). This could be explained by the much larger droplets formed for oil type B,

especially at higher layer thicknesses. The images taken sooner after plunge impact unfortunately are 'too busy' to perform our image analysis on, but it can be clearly seen that oil type B forms much larger oil droplets (or even pockets of irregular shapes) than oil type A at the same thicknesses (Fig. 4-4). These larger droplets may already have risen out of the water column at the time the photo is taken, 5 s after impact. This would also explain why the median droplet size for this thick layer of oil type B is lower than expected (Fig. 4-6).

The deviation of oil type B at thick layers from the trend is considered an artefact, which is the consequence of the measurement method.

Influence of oil viscosity

In our study, the volume entrained is largely independent of oil type. Entrainment is not significantly different between 5 of the 7 oil types.

High viscosity, above 5 Pa.s, impedes the entrainment. The volume of oil entrained for oil type Bevap is much lower than for the other oil types. The images suggest that the oil layer withstands droplets shearing off by the jet (Fig. 4-4). Oil entrapped by the jet does not detach from the 'bulk of the layer' and the impact flow pattern is altered by the resistance of the oil layer.

Oil type B is an exception to the rule that entrainment below the threshold is oil-type independent: This oil type is entrained slightly more than the other oil types. From the images (Fig. 4-4) it is clear that the depth of the indentation is equal, but droplets formed are large and irregular. Where other oil types produce single spherical droplets shortly after being propelled downwards, oil type B forms elongated droplets indicating resistance to breakup. Possible explanation for the increased entrainment could be that due to this resistance to break-up oil directly outside the agitated area is pulled into the jet flow and entrained too.

Stretching of oil droplets into elongated shapes prior to breakup, has been observed earlier in relation to crude oil dispersion (Katz, 2009). In situations where the interfacial stress is dominant, the droplet will remain semi-spherical and break-up into smaller drops after little deformation (Janssen, 1993). Such situations are characterised with a low capillary number ($Ca=\mu_c YD/2\sigma$). For high capillary numbers further elongation can take place before breakup (into multiple drops) occurs.

The formation of the filaments of oil type B in our test indicates low (relative) influence of interfacial stress.

Influence of dispersants on volume of oil entrained
For the oil types with viscosities below 5 Pa.s, dispersants do not significantly alter the volume of oil entrained.

The influence of dispersants on the entrainment above 5 Pa.s, cannot be quantitatively assessed; test images for the very viscous oil Bevap treated with dispersants cannot be analysed because too many non-spherical blobs were formed. As can be seen in the images for the dispersant treated oil Bevap (Fig. 4-4), the plunging jet impact does create a normal cusp shape. Below the cusp, however, a large portion of the oil forms long threads of oil instead of breaking up into droplets, the same phenomenon as can be observed in the pictures of the untreated oil type Bevap. The elongation induced by the plunge impact, is not sufficient to result in breakup into droplets. After the impact, instead of retracting to spherical shape to attain the smallest relative surface area, these strands persist until they resurface. As explained earlier, this indicates that viscosity is a much more dominant feature than interfacial tension in the deformation and break-up of this oil.

Entrainment process
Our observation that in most conditions entrainment volume is independent of oil type (and dispersants) and linearly dependent on oil layer thickness, suggests that in case of an excess of energy, entrainment is only limited by oil availability. Exceptions are conditions where oil properties are such that the jet impact energy is not sufficient to shear off affected oil.

This theory might explain the viscosity limit for (chemical) dispersion at sea; at a certain viscosity entrainment is impeded and the 'dispersion effectiveness' decreases sharper than would be expected based on a correlation between viscosity and droplet size. The observed entrainment threshold is between 1 and 5 Pa.s, in our system with a plunge height of 15 cm. Reed and colleagues (2009) indicate viscosity limit for entrainment at 10 Pa.s, in a plunging jet that is adjustable up to 30 cm. Taking into account that the viscosity limitation increases with dispersant dosage (SL Ross Environmental Research and MAR Incorporated, 2010), our observations could correlate with the observed limiting viscosities for (chemical) dispersion in other conditions (Table 4-1).

In addition to the entrainment threshold above which entrainment is seriously declined, we observed that when there is a slight increase in entrainment in a condition where oil droplets are not easily sheared off.

Further research should reveal whether this needs incorporation in modelling: The influence of this phenomenon on the entrainment volume is slight, and the

Table 4-2. Reported viscosity thresholds for oil entrainment determined under different conditions.

Source	Wave height (m)	Viscosity threshold (Pa.s)
Entrainment threshold (natural dispersion):		
Present work	H_{plunge}: 0.15	1 - 5
(Reed et al., 2009)	H_{plunge}: 0.30	10
Limiting viscosity for chemical dispersion:		
(SL Ross Environmental Research and MAR Incorporated, 2010)	SL Ross wave tank H_{wave}: 0.22	10 (DOR 1:20) >13 (DOR 1:5)
(Trudel et al., 2010)	Ohmsett $H_{sign.wave.}$: 0.42	33.4
(ITOPF, 2012; National Research Council of the National Academies, 2005)	At sea	10-20

large droplets inherent to this condition could mitigate the effect on the mass balance quite fast.

4.4.2 Droplet size

The mean droplet size formed of the oil type Aevap, both with and without dispersants, is consistently smaller than expect based on its viscosity ranking (Fig. 4-6 & 4-7). Droplets originating from oil type Aevap are smaller than those created from the less viscous oil type B. The pseudo plastic behaviour of oil type Aevap (Fig. 4-2) might be an explanation for this. Our ranking is based on the viscosity measured at shear rate 10/s. However, it is clear that oil type Aevap becomes less viscous at higher shear rates (Fig. 4-2), and it would not be unthinkable that it's viscosity ranking would drop to a level between the viscosities of oil types 50/50 A/B and 75/25 A/B, at higher shear rates.

The observed pseudo plastic behaviour is not uncommon in weathered oils, and this phenomenon reaffirms that dispersion testing needs to be performed with field-relevant shear rates to enable translation of the results to field-conditions. Further research should indicate suitable viscosity measurement settings.

Measured droplet sizes in our set-up, are formed by the shearing action of the plunge (breaking wave) on the oil layer. At sea, droplet breakup is also expected to occur during breaking wave occurrence, as this is the most energetic event. It is not clear whether breakup of oil droplets at sea is due to the shearing of the plunge or oil droplets or broken up (further) due to the turbulence generated underwater. Of course the jet energy levels in our test are lower than at sea, yet this scale is very suitable to gain a mechanistic understanding (provided the oils are near-Newtonian).

Fit droplet sizes to existing algorithms

When assuming an interfacial tension of 25 mN/m for untreated oils and an interfacial tension of 3 mN/m for DOR 1:200, the theoretical fraction permanently dispersed at sea can be calculated according to Mackay's formula (eq. 4-2).

The droplet size distribution output calculated with Mackay's formula (fraction of oil permanently dispersed) is independent from energy input. As the calculation is aimed at the energy levels present at sea, a direct comparison is impossible. Still there is a correlation between the experimentally determined volume fraction of small droplets and the calculated theoretical fraction permanently dispersed at sea (Fig. 4-8), meaning that test conditions (H_{oil}, DOR, viscosity) that generate a large fraction of small oil droplets in our test system, would also generate a large fraction of permanently dispersed droplets at sea.

Using the interfacial tension estimates given above, the modified weber number is calculated with eq 4-3. Relative droplet sizes are clearly much larger than the data this equation was based on (Johansen et al., 2015) (Fig. 4-9), whereas modified Weber numbers are much smaller. Both can be attributed to the fact that the layer thicknesses in our study are smaller than those in Johansen's work. The (relative) droplet sizes found in our natural dispersion experiments, follow the overall trend, but do not collapse on the curve of predicted values by Johansen's formula. Variation of the IFT's within the expected range (8 – 40 mN/m) does not make the fit substantially better.

The similar slope in the log-log graph (Fig. 4.9) indicates that the chosen exponent, a=0.6 (Johansen et al., 2015), is valid for our data. This is confirmed by the fact that the relationship; diameter ~ $H_{oil}^{0.4}$ (which results from rewriting eq. 1), matches the increase of MMD with oil layer thickness in our data: The

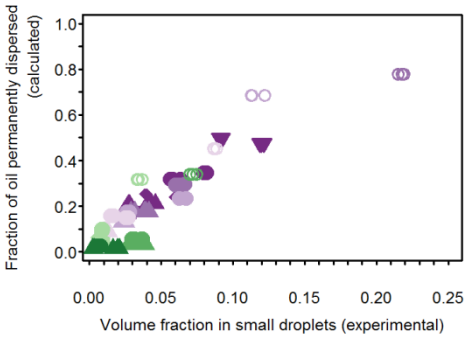

Fig. 4-7. Fraction of oil volume in small droplets observed in our experiments (x-axis) compared to Mackay's theoretical fraction of oil permanently dispersed (for at sea conditions) (y-axis). Pearson's correlation coefficient: R 0.92.

lines in Fig 4-6 are MMD = C * $H_{oil}^{0.4}$, with oil-type-specific constants.

In our results, number mean droplet size is not very representative for the distribution behaviour: Mass median diameter is much more exemplary for the dispersion outcome (mass in small droplets), and it also shows better (more logical) correlation with input parameters (oil type and layer thickness). In order to adapt the modified Weber number to predict the mass median diameter, new constants need to be fitted to the model formula $MMD/H_{oil} = A\ We^{-.6} + B\ Re^{-.6}$. Øistein Johansen kindly provided mass median diameters obtained by direct measurements in his experiments. New constants for the modified Weber number fitted to only his data, result in a relationship that extrapolates into our dataset much better (Fig. 4-10).

Although not yet perfect, the fit between our mass median diameter and the modified weber number based on Johansen's data is promising. Deviations could be caused by differences between the two different test systems, measurement

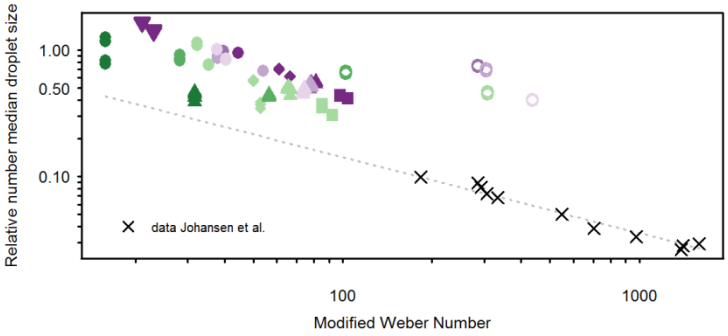

Fig. 4-8. Relative number median droplet size as a function of modified Weber number (eq.3) with Johansen's constants; A=2.251, B=0.06, a=0.6 (calculated with assumed interfacial tension).

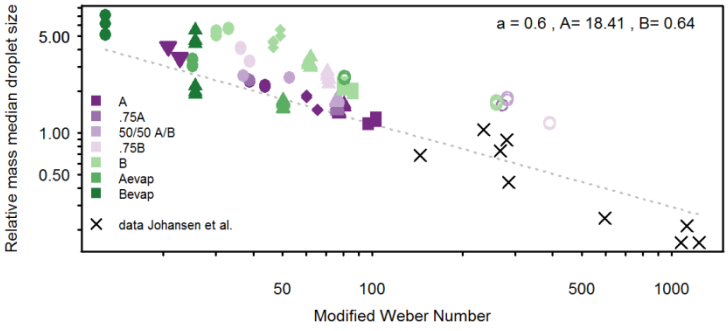

Fig. 4-9. Relative mass median droplet size as a function of modified Weber number (eq. 3) with adapted constants. The new constants, given in the upper right, were obtained by fitting mass median diameter for the Johansen data to the model equation (eq. 4-2).

errors, potential settling bias, viscosity shear rate, and the assumed interfacial tensions.

Validating such droplet size algorithm with field or wave tank results is not straightforward; Predicted droplet size averages are those initially formed at entrainment, direct validation would require droplet size measurement during or right after entrainment.

Most droplet sizes measurements in large scale systems are time-averaged and often occur deeper than initial entrainment would bring the droplets. This means these measurements mainly observe the smaller droplets, which remain in suspension for a longer time. Although the droplet size distribution is a highly dynamic parameter due to size fractionation, the measured average droplet size stabilises over time (Li et al., 2010, 2009a, 2008), as a result of 'accumulation' of small droplets. Such measurements are useful in understanding dispersion as a whole, but are not suitable for validation of our model for dispersion by an individual breaking wave event.

4.4.3 Implications of the results for oil fate modelling

The present work confirms the importance of oil layer thickness in entrainment of oil by breaking waves as recently proposed (Zeinstra-Helfrich et al., 2015a) with different oil types.

Up to the viscosity threshold (depending on dispersant application), entrainment is largely independent of oil type. In addition, the (relatively low) dispersant dosages used, did not significantly influence entrainment. This means that below the viscosity threshold, volume entrained (m^3) is simply calculated by multiplying area agitated (m^2) with oil layer thickness (m).

The oil viscosity (with & without dispersants) at which entrainment will be impeded in at sea conditions is suspected to coincide with the limiting (chemical) dispersion viscosity. Further studies are necessary to determine the threshold for entrainment at sea, expressed either as oil viscosity or yield stress.

Dispersed droplet size averages appear to follow a Weber and Reynolds number correlation, further investigation is required to test its validity in large scale.

4.5 Conclusions

This study confirms that the entrainment of oil and the breakup into droplets are separate processes governed by separate parameters that can and should be included in spilled oil fate modelling.

The results presented demonstrate that in most conditions, entrainment rate is independent of the oil properties. Even pre-mixing dispersants (DOR 1:200) did not significantly influence entrainment. In such cases entrainment rate at sea is simply the product of oil layer thickness and breaking wave coverage. Exception was high viscosity oil, for which entrainment was less than expected as the oil layer could not be broken up by our jet.

The influence of oil properties on the dispersion process is more pronounced in the second step, the process of droplet breakup: in our system, entrained oil droplet sizes are correlated with the Weber and Reynolds number as a result of the influence of viscosity, oil layer thickness, oil density, interfacial tension and plunge height.

These findings reveal another piece of a puzzle of understanding and predicting the efficacy and limitations of chemical dispersants application at sea.

S4. Annex to chapter 4 (supplementary information)

Data are publicly available through the Gulf of Mexico Research Initiative Information & Data Cooperative (GRIIDC) at https://data.gulfresearchinitiative.org (doi: http://dx.doi.org/10.7266/N7RF5S04).

S4.1 - ANOVA tables for the analysis performed on presented data

*Output ANOVA (type III) on **Volume of oil entrained** @ T= 5 sec after jet impact (natural dispersion) as function of oil layer thickness and oil type*

	Sum Sq	Df	F value	Pr(>F)	Sum Sq	Df	F value	Pr(>F)
(Intercept)	2.877	1	140.5	**< 2.2E-16**	5.925	1	287.1	**< 2.2E-16**
H_{oil} (nominal oil layer thickness)	0.789	1	38.5	**3.38E-08**	3.283	1	159.1	**< 2.2E-16**
Oil type	2.028	6	16.5	**9.49E-12**	4.801	6	38.8	**< 2.2E-16**
H_{oil}:Oil (interaction)	0.135	6	1.1	0.3735	without interaction			
Residuals	1.433	70			1.568	76		

*Coefficients for a linear model fit on **Volume of oil entrained (ml)** @ T= 5 sec after jet impact (natural dispersion) as function of oil layer thickness (mm) and oil type. (no interaction)*

Coefficients:	Estimate	Std. Error	t value	Pr(>|t|)
(Intercept):				
Oil 75A	0.257	0.058	4.45	**2.85E-05**
Hoil	1.035	0.071	14.53	**< 2E-16**
Oil. 75B	-0.033	0.053	-0.61	0.54
Oil 50/50 A/B	-0.029	0.053	-0.56	0.58
Oil A	0.048	0.053	0.91	0.37
Oil Aevap	0.102	0.053	1.92	0.06
Oil B	0.148	0.053	2.80	**0.0065**
Oil Bevap	-0.623	0.053	-11.74	**< 2E-16**

Residual standard error: 0.13 on 76 degrees of freedom
Multiple R-squared: 0.867, Adjusted R-squared: 0.8548
F-statistic: 70.78 on 7 and 76 DF, p-value: < 2.2e-16

*Output ANOVA (type III) on Volume of oil entrained @ T= 5 sec after jet impact with layer thickness .4 mm and **with and without dispersants**.*

	Sum Sq	Df	F value	Pr(>F)	Sum Sq	Df	F value	Pr(>F)
(Intercept)	4.11	1	166.9	**7.02E-15**	6.531	1	252.9	**2.00E-16**
Oil type	0.09	4	0.9	0.4500	0.383	4	3.7	**0.0119**
DOR (none vs 1:200)	0.02	1	0.9	0.3450	0.084	1	3.3	0.0785
Oil:DOR (interaction)	0.15	4	1.5	0.2286	without interaction			
Residuals	0.86	35			1.007	39		

*Output ANOVA (type III) on the **Mass Median Diameter** @ T= 5 sec after jet impact (natural dispersion).*

	Sum Sq	Df	F value	Pr(>F)	Sum Sq	Df	F value	Pr(>F)
(Intercept)	5.63	1	36.3	**7.09E-08**	9.62	1	64.9	**8.55E-12**
H_{oil} (nominal oil layer thickness)	0.17	1	1.1	0.2932	1.46	1	9.9	**0.0024**
Oil type	13.86	6	14.9	**6.81E-11**	31.06	6	35.0	**< 2.2E-16**
	0.40	6	0.4	0.8532	without interaction			
Residuals	10.85	70			11.26	76		

*Output ANOVA (type III) on the **volume fraction of droplets smaller than 500 μm** @ T= 5 sec after jet impact (natural dispersion).*

	Sum Sq	Df	F value	Pr(>F)
(Intercept)	0.0293	1	479.4	**< 2.2E-16**
H_{oil} (nominal oil layer thickness)	0.0036	1	58.2	**8.73E-11**
Oil type	0.0232	6	63.1	**< 2.2E-16**
H_{oil}:Oil (interaction)	0.0041	6	11.1	**1.15E-08**
Residuals	0.0043	70		

*Output ANOVA (type III) on the **Mass Median Diameter** @ T= 5 sec after jet impact with layer thickness .4 mm and **with and without dispersants.***

	Sum Sq	Df	F value	Pr(>F)
(Intercept)	8244	1	1861.1	**< 2.2E-16**
Oil type	1584	4	89.4	**< 2.2E-16**
DOR (none vs 1:200)	520	1	117.4	**9.93E-13**
Oil:DOR (interaction)	179	4	10.1	**1.52E-05**
Residuals	155	35		

S4.2 Droplet size distribution data

Oil	H_{oil} (nom.)	DOR	Viscosity	Density	H_{plunge}	Volume entrained	sd Ventr	Mean droplet diameter	sd mean	SD of the drop size distribution	sd sd	Mass Median Diameter	sd MMD	Fraction of oil in small droplets	sd SmallVolF	Volume of oil in small droplets
	mm		Pa.s		cm	ml		mm		mm		mm		-		ml
75A	0.4	0	0.02135	0.853	15	0.6707	0.1848	0.3910	0.0176	0.1105	0.0015	1.0048	0.0078	0.0637	0.0030	0.0427
75A	0.4	0.005	0.02135	0.853	15	0.5119	0.0370	0.3055	0.0037	0.1042	0.0005	0.6522	0.0028	0.2177	0.0020	0.1115
75A	0.8	0	0.02135	0.853	15	1.1141	0.2323	0.4148	0.0135	0.1156	0.0011	1.2500	0.0602	0.0352	0.0051	0.0392
75B	0.4	0	0.1025	0.873	15	0.7153	0.0981	0.4030	0.0260	0.1241	0.0007	1.5974	0.1316	0.0208	0.0055	0.0149
75B	0.4	0.005	0.1025	0.873	15	0.4640	0.0170	0.3213	0.0041	0.1147	0.0007	0.9420	0.0085	0.0874	0.0012	0.0405
75B	0.8	0	0.1025	0.873	15	1.0367	0.0664	0.3897	0.0222	0.1330	0.0036	2.0762	0.1420	0.0114	0.0012	0.0118
50/50 A/B	0.4	0	0.0428	0.873	15	0.7596	0.3240	0.3729	0.0223	0.1180	0.0038	1.2272	0.2155	0.0464	0.0211	0.0352
50/50 A/B	0.4	0.005	0.0428	0.873	15	0.6411	0.0251	0.3254	0.0094	0.1104	0.0018	0.8349	0.0205	0.1162	0.0052	0.0745
50/50 A/B	0.8	0	0.0428	0.873	15	1.0514	0.0928	0.4342	0.0137	0.1182	0.0019	1.4243	0.0418	0.0240	0.0009	0.0252
A	0.2	0	0.0141	0.867	15	0.3607	0.0256	0.3446	0.0129	0.1094	0.0010	0.8587	0.0442	0.1057	0.0157	0.0381
A	0.4	0	0.0141	0.867	15	0.6925	0.0155	0.3935	0.0397	0.1091	0.0025	0.9685	0.0321	0.0699	0.0121	0.0484
A	0.6	0	0.0141	0.867	15	1.0168	0.0703	0.4295	0.0141	0.1094	0.0019	1.0725	0.0864	0.0501	0.0116	0.0510
A	0.8	0	0.0141	0.867	15	1.2052	0.0361	0.4472	0.0146	0.1120	0.0023	1.2093	0.1060	0.0354	0.0088	0.0427
A	1	0	0.0141	0.867	15	1.4750	0.1776	0.4378	0.0045	0.1137	0.0024	1.2490	0.0364	0.0333	0.0063	0.0491
Aevap	0.4	0	0.968	0.920	15	0.7946	0.0938	0.3605	0.0190	0.1225	0.0036	1.3573	0.0872	0.0336	0.0034	0.0267
Aevap	0.4	0.005	0.968	0.920	15	0.7581	0.0216	0.2787	0.0074	0.1228	0.0015	1.0586	0.0228	0.0725	0.0025	0.0549
Aevap	0.8	0	0.968	0.920	15	1.2306	0.1945	0.3666	0.0075	0.1221	0.0021	1.3630	0.0828	0.0328	0.0048	0.0404
B	0.4	0	0.3285	0.883	15	0.8274	0.1150	0.3944	0.0608	0.1363	0.0074	2.3361	0.2253	0.0086	0.0004	0.0071
B	0.4	0.005	0.3285	0.883	15	0.9336	0.0320	0.3670	0.0090	0.1211	0.0015	1.3197	0.0366	0.0350	0.0019	0.0327
B	0.6	0	0.3285	0.883	15	1.1596	0.0622	0.3010	0.0637	0.1532	0.0104	3.1781	0.4733	0.0059	0.0008	0.0069
B	0.8	0	0.3285	0.883	15	1.2812	0.0873	0.4024	0.0199	0.1389	0.0032	2.6242	0.1616	0.0064	0.0005	0.0082
B	1	0	0.3285	0.883	15	1.0711	0.1692	0.3683	0.0188	0.1381	0.0022	2.3308	0.1248	0.0094	0.0012	0.0100
Bevap	0.4	0	5.115	0.937	15	0.1330	0.0219	0.4215	0.0922	0.1364	0.0112	2.5069	0.4108	0.0068	0.0009	0.0009
Bevap	0.8	0	5.115	0.937	15	0.4415	0.0385	0.3647	0.0248	0.1418	0.0152	2.8973	1.3449	0.0109	0.0090	0.0048

CHAPTER 5

How wind speed and oil properties determine oil slick elongation via entrainment and resurfacing.

M. Zeinstra-Helfrich[a], W. Koops[a], A.J. Murk[b]

Submitted

---

[a] NHL University of Applied Sciences, Dept. Maritime, Marine, Environment & Safety
[b] Marine Animal Ecology group, Wageningen University

Abstract

Oil slick at sea are observed to attain elongated, comet-like, shape. This has been explained by temporary entrainment and resurfacing of oil upwind. We investigate the influence of wind speed, oil viscosity and dispersant application on the oil slick surface development. Assuming a constant mixing by breaking waves, entrainment and resurfacing are modelled to obtain the oil slick mass distribution across a transect through the slick over time. This reveals how the surface oil mass changes from a large comet shaped slick for sub-optimal dispersion, to a small surface oil mass with a large suspended oil mass for optimal dispersion. These outcomes largely depend on wind speed and to a lesser extent oil properties determining dispersability. This relationship follows a concave trend, with a region of sub-optimal dispersion that is very sensitive to changes in oil properties and wind speed. Dispersants mainly have added benefit in situations with sub-optimal dispersion, with the exception of very viscous oils.

5.1 Introduction

The decision making concerning the application of chemical dispersants remains a complex trade-off between the adverse effects of floating oil and those of suspended/dissolved/sunken oil. Current dispersion algorithms require expert input on dispersant effectiveness and do not provide information on the NET effectiveness of dispersants (National Research Council of the National Academies, 2005; Zeinstra-Helfrich et al., 2015c).

Chemical dispersants can enhance the natural dispersion process by reducing the oil-water interfacial tension. This stimulates oil entrained by breaking waves to be broken up into smaller droplets. The droplet size effects the fate of the oil, as smaller droplets stay longer in the water column before resurfacing. Generally, droplets with sizes below 70μm are considered to remain in the water column indefinitely (French-McCay, 2004).

As the main goal of dispersant application is to remove the oil from the water surface as fast as possible, the success of such action should be defined from its effectiveness in reducing surface slick area over time. The surface area of an oil slick is determined by the mass of oil still floating (as opposed to evaporated, dissolved or suspended), the gravitational spreading of the oil slick and the wind shear. Wind shear causes the slick to elongate as entrained oil resurfaces upwind of the original slick (Elliott, 1986; Elliott et al., 1986). As this wind shear process is dependent of dispersion, an understanding of how a dispersant response impacts is crucial. The wind-shear mechanism is not/hardly described in the literature, as it can only be observed in sea-trials, as the differential transport between floating and suspended oil is not present in any of the other test systems. Unfortunately, sea-trials are hard to perform and control. Therefore, in this paper we develop a model for simulating the oil slick elongation and lengthwise mass distribution resulting from dispersion and wind shear. Based on the presented model, the influence of key parameters in dispersion (wind speed, oil type and interfacial tension) on the mass balance and oil slick appearance is investigated for 3 wind speeds, 3 oil types and with or without dispersants added.

5.2 Methods

We consider a lengthwise cross-section of an oil slick, moving across a 'grid' at a speed depending on the wind speed. At any given time, an area (fraction) A_{mix} of the oil slick is (newly) hit by breaking waves. Upon impact, the floating oil is entrained, broken up into droplets and assumed to be distributed evenly across

mixing depth z_i. During the following quiescent period (while other areas are mixed/entrained) part of the oil resurfaces. After a time period T_{bw}, the same location is hit by a breaking wave again, redistributing the oil droplets still suspended across z_i together with newly entrained oil.

Following these steps, we calculate the evolution of the oil slick thickness by estimating the mass entrained and resurfacing as a function of time and location.

Wave Field Characteristics. Simulating the intermittent entrainment and resurfacing of oil requires two parameters for the timing of breaking waves: the area agitated by breaking waves per unit of time and the time period between successive breaking waves.

Whitecap area formation, in short **agitated area fraction** (A_{mix}, s^{-1}), can be obtained by dividing the total area fraction covered by breaking waves (Whitecap Coverage) by the lifetime of each breaking wave(τ) (Monahan, 1971; Monahan and Callaghan, 2015) (Eq. 5-1). As this area agitated also expresses the number of breaking waves passing a given location per unit time (Kleiss and Melville, 2011; Phillips, 1985), the time between two 'mixing incidents' in one location is $T_{bw}=1/A_{mix}$ (Eq. 5-2).

Whitecap coverage is often investigated as an important parameter in climatology, determining visible albedo, Sea Salt Aerosol flux and air-sea gas exchange. Direct parameterization with wind speed, however, proves to be difficult (Anguelova and Webster, 2006) due to differences in measurement techniques and the influence of parameters other than wind speed (Salisbury et al., 2013) causing variation in whitecap lifetime (Callaghan et al., 2012). In this paper, whitecap coverage is calculated based on a recent parameterization for active breaking waves (Eq. 5-3) (Salisbury et al., 2014, 2013), as this is valid for a wide range of conditions. Based on field-observations, we approximate the characteristic lifetime (τ) of this breaking wave phase at 1 second (Callaghan, 2013; Monahan and Woolf, 1989).

The **breaking wave jet free fall height**, is required as input for the droplet size equation. Taking into account that this jet falls partly on the wave's own front face, the free fall height is less than the wave height. Photographic measurements indicate fall height is between 0.2 to 0.5 H_{bw} (Chanson and Cummings, 1994), of which we take the median value of 0.35 in our plunge height (Eq. 5) with the breaking wave height based on a fully developed Pierson and Moskowitz wave spectrum (Galt and Overstreet, 2009) (Eq. 5-4).

The mixing depth, or the thickness of the layer below the water surface over which the droplets are distributed, determines how long it takes for suspended oil droplets to resurface. Generally (National Research Council of the National Academies, 2005) a value of 1.5 times the wave height is assumed based on two sources: Delvigne and Sweeney (1988) who found their smaller droplet sizes to be homogeneously distributed across a depth of (1.5 ± 0.35) H_{bw} below the water surface. Li and Garrett (1998) define a surface layer of constant turbulent dissipation rate(ε) with a thickness 1.4 H_{sign}, yet do not necessarily relate this to droplet entrainment depth. These values might seem high, yet literature regarding air bubble entrainment suggests values in the same order of magnitude: Air bubble injection by breaking waves is estimated to occur in a layer of thickness up to 0.25 to 2 times the wave height (Chiba and Baschek, 2010; Gemmrich, 2009).

We base our mixing depth (Eq. 5-7) on the Li and Garrett's turbulent dissipation rate layer (Li and Garrett, 1998), with the so-called significant wave height based on a fully developed Pierson and Mosckowitz wave spectrum (Eq. 5-6) (Galt and Overstreet, 2009).

Wind induced velocity of floating slick and suspended droplets. The most common mechanisms causing differential movement between the (floating slick on the) water surface and the underlying water are; the vertical structure of the tidal currents, stokes drift, and wind forcing (Elliott, 1986; Elliott et al., 1986). Elliot's work on elongation of oil slicks as a result of near-surface velocity shears (Elliott, 1986; Elliott et al., 1986), considers a 3.5 % wind induced surface velocity additional to the stokes drift induced velocity. Others add a smaller wind driven-transport factor to the stokes drift (Ardhuin et al., 2009; Hénaff et al., 2012; Lehr et al., 2002). The latter option results in a total contribution of wind (via stokes and direct forcing) on the oil slick transport, closer to the commonly assumed wind drift factor of 3 to 4 % of the wind speed (Lee et al., 2015).

We calculate the forward velocity of the slick and suspended particles due to stokes drift based on the approximation by Li & Garrett (Ming et al., 1993). The stokes drift on the water surface equals $u(z_0) = 0.016\ U_w$. The exponential decline of velocity with depth is characterized by the so-called e-folding depth in relation to wind speed: $0.12\ U_w^2 / g$. The forward velocity on account of the stokes drift, as a function of depth (below the water surface), is then: $u_s(z) = 0.016\ U_w\ e^{-kz}$, with $k = 8.33\ g / U_w^2$ (Eq. 5-8).

The additional wind drift factor (wind-driven surface transport other than stokes drift) in our model is set to 0.03 at the water surface, and decays logarithmically

Table 1. *Formulas introduced and referred to in the text.*

Eq.	Quantity	units	formula	source
5-1	Area fraction agitated	s^{-1}	$A_{mix} = \frac{WCC}{\tau}$	(Kleiss and Melville, 2011; Phillips, 1985)
5-2	Breaking wave period	s	$T_{bw} = \frac{1}{A_{mix}}$	(Kleiss and Melville, 2011; Phillips, 1985)
5-3	WhiteCap Coverage (fraction)	s^{-1}	$WCC = 0.46\, U_w^{2.26}$	(Salisbury et al., 2014)
5-4	Breaking wave height	m	$H_{bw} = 0.02854 U_w^2$	(Galt and Overstreet, 2009)
5-5	Free Fall Height	m	$H_{pl} = 0.35 H_{bw} = 0.009989 U_w^2$	Own observations + (Eq. 4)
5-6	Significant wave height	m	$H_{sign} = 0.02244\, U_w^2$	(Galt and Overstreet, 2009)
5-7	Droplet injection depth	m	$z_i = 1.4\, H_{sign}$	(Li and Garrett, 1998)
5-8	Stokes induced velocity	m s^{-1}	$u_{stokes} = 0.016 U_w e^{-kz}$, with $k = 8.33 \frac{g}{U_w^2}$	(Ming et al., 1993)
5-9	Wind induced velocity	m s^{-1}	$u_{wind} = 0.03 U_w \left(1 - \frac{\log(z/z_o)}{\log(z_c/z_o)}\right)$, with z_0 = 0.0001, and z_c=20	(Elliott, 1986)
5-10	Total slick velocity	m s^{-1}	$U_{slick} = u_{stokes}(0) + u_{wind}(0) = 0.046 U_w$	Eq. 8, 9
5-11	Relative velocity of a droplet at depth z compared to the surface slick	m s^{-1}	$U_{d\|s}(z) = \left(u_{stokes}(z) + u_{wind}(z)\right) - U_{slick}$ $U_{d\|s}(z) = 0.03 U_w \left(\frac{\log\left(\frac{z}{z_o}\right)}{\log\left(\frac{z_c}{z_o}\right)} - 1\right) + 0.016 U_w (e^{-kz} - 1)$	Eq. 8, 9
5-12	Mass Median Diameter	m	$MMD = h_{oil}\left[18.41\left(\frac{\rho H_{oil} 2gH_{pl}}{\sigma}\right)^{-0.6} + 0.64\left(\frac{\rho H_{oil}\sqrt{2gH_{pl}}}{\mu}\right)^{-0.6}\right]$	(Johansen et al., 2015; Zeinstra-Helfrich et al., 2016)
5-13	Bouyant rise velocity	m s^{-1}	$v = d^2 g(1 - \frac{\rho_o}{\rho_w})/18\nu_w$, for $d < 9.25\nu_w^{2/3}/g^{1/3}\left(1 - \frac{\rho_o}{\rho_w}\right)^{1/3}$	Stokes' law

down from a depth of 0.1 mm to 20 meters (Eq.5-9) (Elliott, 1986). This makes the total wind-induced velocity of our floating slick 4.6 % of U_w (Eq. 5-10).

Tidal currents are not included in this calculation as they affect suspended and floating oil in the same way, and our interest is in the differential movement by the wind. (Our grid moves along with the tidal currents.)

Oil Droplet Breakup. The droplet size distribution is calculated with the Weber and Reynolds relationship developed by Johansen and colleagues (Johansen et al., 2015), with adapted constants (A=18.41, B=0.64) to yield Mass Median Diameters (Zeinstra-Helfrich et al., 2016) (Eq. 5-12). The standard deviation for this lognormal droplet size distribution is $\log_{10}(0.38)$.

This particular algorithm is based on measurements of instantaneously formed droplet sizes, making validation with field-measurements extremely difficult (Zeinstra-Helfrich et al., 2016). The calculation results do follow expected trends with oil properties.

Resurfacing. An individual droplet with a diameter d, rises back to the surface with a velocity as dictated by Stokes' law (Eq. 5-13). The mass of oil entrained in larger droplets ($v(d) > z_i/T_{bw}$), will entirely resurface before the next breaking wave impact. Of droplets that are smaller, a fraction $1- T_{bw}v(d)/z_i$ will still be suspended when the next breaking wave hits. As the remainder of oil mass is re-distributed across z_i with each new breaking wave, the resurface rate of these smaller droplets at time periods exceeding the first breaking wave periods can be based on exponential decay.

Implementation in a model. A 1d grid is defined by the total length that accommodates the oil slick maximum travel distance in the given timeframe. The grid cell length, Δx, is set to be around 10 meters, and adjusted for each case so that the number of grid cells traveled in one breaking wave period T_{bw} is an integer. The time step length, Δt, is set equal to the time it takes the slick to travel exactly one grid cell.
In one time step, the oil layer moves exactly one grid cell downwind, an oil volume $\Delta t\ A_{mix}\ H_{oil}$ is removed by entrainment, an oil volume V_{res} resurfaces (back) into the cell. This V_{res} is an addition of linear resurfacing of droplets entrained for periods < T_{bw} from the same grid cell and near upwind cells ($V_{res\ l}$) and resurfacing as a result of quasi-exponential loss of the mass of oil in suspension for longer periods of time ($V_{res\ e}$).

To avoid calculating the droplet size distribution in each time step and each location, some relations between droplet size distribution and oil layer thickness (with the constant oil properties and wind speed) were calculated at the start of the simulation.
Twenty droplet size classes were defined to properly display the different resurfacing characteristics between small and large droplets. Nineteen of these classes are evenly distributed between $MMD(h_{min})$ - 2.326 σ_{DSD} and the droplet size that resurfaces within a quarter of the breaking wave period (0.25 T_{bw}). Mass in droplets larger than that, is bunched into a 20^{th} size class, as this oil will all resurface very fast and not far from the point of entrainment.
The oil mass entrained per droplet size class is calculated with the probability density function for the lognormal distribution around MMD (as a function of H_{oil}) from the lower limit of the size class to the upper limit (Eq. 5-14).

Table 2. *Implementation of the processes in the oil slick model*

Eq.	Quantity	units	Formula
5-14	Oil layer thickness after a time step.	m (m^3m^{-2})	$\mathrm{H}_{oil}[\mathrm{t},\mathrm{x}] = (1 - \Delta\mathrm{t}\ \mathrm{A}_{mix}\ \mathrm{H}_{oil}[\mathrm{t}-,\mathrm{x}-\Delta\mathrm{x}]) + V_{res\,l} + V_{res\,e}$
5-15	Entrainment rate per size class D(ranging from d_{low} to d_{up})	$m^3m^{-2}s^{-1}$	$Q_{entr}(D) = F_v(D)\ A_{mix}\ H_{oil}$
5-16	Maximum length (/distance) of resurfacing	m	$dx\ (d,z) = \int_{z_i}^{0} U_{d\|s}\ /v(d)$, for d > d lim
5-17	Mass resurfacing per time step per up-wind grid cell	m^3m^{-2}	$V_{res\,l}[\mathrm{x},\mathrm{t}] = \sum_{D1}^{D20}\ Q_{entr}(D,h) \int_{z_i}^{0}(F_{res}[x]\ F_{res}[t])\ /z_i$, with
5-18	Volume still suspended after 1 T_{bw}	m^3s^{-1}	$\mathrm{V}_{susp\,T_{bw}}(\mathrm{D}) = Q_{entr}(D)[t - T_{bw}, x]\left(1 - \frac{T_{bw}v(d)}{z_i}\right)$
5-19	Volume suspended after time step	m^3m^{-2}	$V_{susp\,e} = \sum_{d\,1}^{d\ lim} V_{susp(t-1)}e^{-k\Delta t} + V_{susp\,T_{bw}}(D)\int_0^{\Delta t} e^{-kt}$, with $k(D) = \frac{-\ln\left(1-\frac{T_{bw}v(d)}{z_i}\right)}{T_{bw}}$
5-20	Volume resurfacing in one time step	m^3m^{-2}	$V_{res\,e} = \sum_{d\,1}^{d\ lim} V_{susp(t-1)}(1 - e^{-k\Delta t}) + V_{susp\,T_{bw}}(d)\int_0^{\Delta t} 1 - e^{-kt}$
5-21	Fraction of suspended oil droplets that moves to the downwind grid cell during one time step.	-	$F(D) = \Delta x^{-1}\int_{z_i}^{z(\Delta t)}\int_{z}^{z-z(\Delta t)} U_{d\|s}\ /v(d) + \Delta x$, with $z(\Delta t) = v(d)\Delta$t
5-22	Largest droplet diameter that can remain suspended for T_{bw}	m	$D_{lim} = 5.1 \cdot 10^{-5}\ (\rho_w - \rho_o)^{-0.5}\ U_w^{2.13}$

One oil droplet of size d, initially entrained to depth z, resurfaces $z/v(d)$ seconds after entrainment. The water column velocity relative to the slick velocity integrated over depth z, with rise velocity as residence time in each location, yields the distance behind the entrainment location in the (moving) slick that this droplet resurfaces (Eq. 5-15).

As the mass of oil entrained is assumed evenly distributed across the top water depth z_i, the mass distribution due to resurfacing within the first breaking wave period after entrainment was obtained by numerically integrating (Eq. 5-15) for entrainment across the time step and across the grid cell length. At the start of each simulation, this mass resurfacing per time step per (upwind)location is pre-calculated based on the droplet size distributions resulting from 20 layer thicknesses. This number of classes is chosen to show the differences in results as a function of layer thickness. A linear interpolation of these results yields mass resurfacing per time step per (upwind)location as a function of the oil layer thickness (H_{oil}). During each step of the simulation, $V_{res\ l}$ is obtained from these

interpolations performed on the layer thicknesses of the grid cells passing the location in the previous time steps.

The calculation of $V_{res\ l}$ includes the large droplets resurfacing within a breaking wave period and a portion of the smaller droplets that resurfaces due to its shallow intrusion depth. The mass still suspended after 1 breaking wave period is now dealt with per droplet size class $d<d_{lim}$.
$V_{susp\ Tbw}$ is also pre-calculated for 20 oil layer thicknesses (Eq. 5-18) and linearly interpolated for the actual layer thickness in the time step. As a fixed fraction of the oil volume resurfaces per breaking wave period, the resurfacing rate of these longer suspended droplets can be estimated based on exponential decay (Eq. 5-19). As entrainment occurs during the whole time step, the first time step needs to account for the time difference between the start and end of the time-step (as shown by the right hand term in Eq. 5-19&5-20).
As the horizontal movement of the quickly resurfacing droplets is included in the calculation for $V_{res\ l}$, the mass suspended for longer periods is also subjected to forward movement in the water column. Per droplet size class, the fraction of the suspended volume transferred to the next downwind grid cell during the course of one time step, is calculated based on the velocity profile a droplet d at depth z passes during its journey to depth $z-v(d)\Delta t$ (Eq. 5-21).

Using the described model, the oil slick evolution of time was analyzed for three wind speeds (U_w = 5, 10 & 15 m/s), three oil types, and 2 dispersant conditions (natural & chemical dispersion), yielding 18 cases in total. The three oil types considered have the following physical properties:

Oil type	ρ_{oil} (kg/m^3)	μ_{oil} (Pas)
Light	886	0.1
Medium	936	1
Heavy	986	10

These properties are assumed to remain unchanged after dispersant dosage; the application of dispersants only affects the oil-water interfacial tension, this is 0.03 N/m for natural dispersion and 0.003 N/m for chemically treated oil. For the above tests, the slick is set to be 250 m long and 1 mm thick at the start of the simulation, and the simulation lasts for 24 hours.
In addition, for the medium oil type with 5 m/s wind, a set of initial lengths and thicknesses is tested (L_0 250 m, with H_0 0.5 and 2 mm; L_0 500 m, with H_0 0.5 and 1 mm).

5.3 Results and discussion

Each of the simulations results in a graph of the slick evolution over time (Fig. 5-1) and some characteristic metrics of the slick after 24 hours (Fig. 5-2). (The output data & slick graphs for all simulations can be found in S1.)

The slick behaviour shows two distinctly different regimes for favourable and unfavourable dispersion (Fig. 5-1): Conditions least favorable for dispersion are the heavy oil combined with the low wind speed (Fig. 5-1, left). The oil slick clearly develops a tail over time (lower panel). After 24 hours, the downwind edge is formed by a patch of 'true oil color' of a length just over twice the initial slick length (506m), followed by an upwind tail that decreases in thickness as we move further from the thick patch. The total slick length after 24 hours is 10.2 km, and still increasing (although the growth levels off slightly). The fraction of oil suspended in the water column (upper panel) shows a sharp initial increase (0.5 h), after which it continues to steadily increase (almost linear).

Conditions most favorable for dispersion are the light oil, treated with dispersants, combined with the high wind speed (Fig. 5-1, right). A very large portion of the oil mass, is transferred to the water column in only the first half hour, and slowly increases after that (upper panel). Consequently, the surface expression of the remaining mass is very limited. The 'true oil color' is only

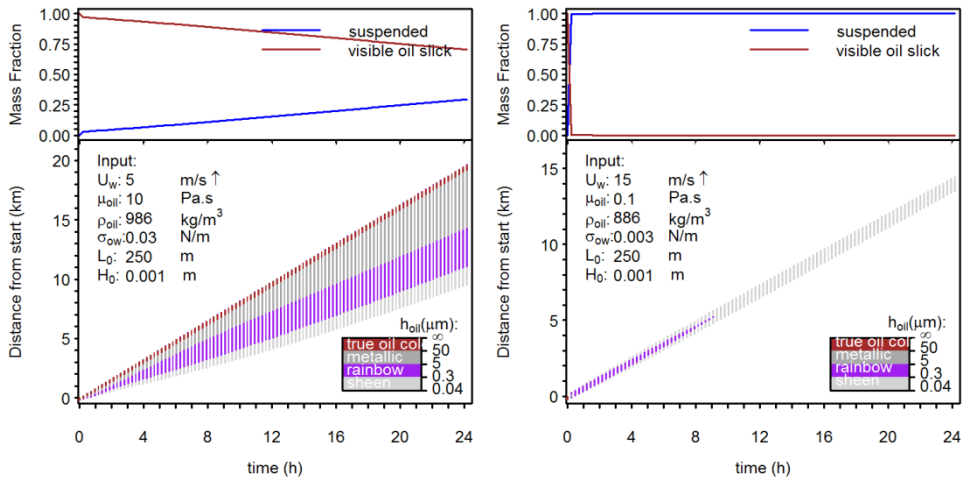

Figure 5-1. Simulation results for the least (left) and most (right) favorable conditions for dispersion. Upper panels: the distribution of oil mass over time. Lower panels: slick lengthwise mass distribution (thickness shown as appearance according to the Bonn Agreement Appearance Code (Bonn Agreement, 2011, 2009)*) and wind-induced displacement over time. Wind direction is upwards.*

visible in the first 15 minutes, followed by a brief flash of 'metallic' and a period of 'rainbow color' transitioning to 'sheen' from the front and back edge of the slick. The length of the oil slick has slowly increased over time, but appears to stabilize at 1.0 km after 24h. We expect that this remaining sheen will diminish into an invisible oil layer (<0.04μm) in a similar way as the change from rainbow to sheen (from the up and down-wind edges towards the middle). The wind driven transport has moved the downwind edge 15.3 km in 24 hours, this is very little compared to the 59.6 km that would result from (Eq.5-10) without entrainment. This is consistent with earlier observations oil slick wind driven transport being reduced in conditions with a lot of entrainment (Reed et al., 1994). In such cases, the surface slick is only a (temporary) expression of the underwater plume, repeated mixing ensures an oil packet is not available on the surface long enough to be transported. The resulting effective (wind & stokes) drift factor for this simulation, 1.18%, does match with the lowest observed wind drift factor in the field of 1% (Lehr and Simecek-beatty, 2000).
The slick of the first, least favorable case spreads much further than can be explained by circular slick gravity-spreading: When assuming an oil volume based on an initial circular slick $V=(0.25\pi L_0^2)h_0$, spreading according to Fay's(Lehr et al., 1984) formulae would result in a maximum slick diameter of 1.5 km (with an average thickness of $H_{oil}\approx 26\mu m$) in just over 8 hours. The least favorable case exceeds this spreading by 6 times. The 'optimal' dispersion case does not reach this predicted diameter, the oil mass remaining on the surface is not sufficient to form such a slick. Additionally, one can question whether such a gravity-spreading phenomenon would take place on this slick where continuous mixing also prevents wind drift to occur.
It must be noted that in this simulation, all mass is assumed to be preserved in a 1D stretch. In reality, mass will also disappear from the slick by the lateral spreading, and be lost from the slick by evaporation and dissolution. Suspended droplets can also be lost from the mass balance by turbulent diffusion outside the 'area of interest' or sinking to the sediment after interaction with particles or sea snow (van Eenennaam et al., 2016; Vonk et al., 2015).

Based on the input parameters, we can quickly calculate how susceptible for dispersion each of the combinations of conditions is. Using the oil properties, the environmental conditions and the initial thickness, the volume fraction of oil droplets smaller than the limiting diameter (largest diameter that can stay suspended for longer than T_{bw}) is calculated. This parameter indicates the oil fraction that is relatively stable suspended; the dispersability factor (DF):

$$DF = \int_0^{d_{lim}} \frac{1}{d\sigma\sqrt{2\pi}} e^{-\frac{(\ln(d)-MMD(H_{oil}))^2}{2\sigma^2}} \quad \text{(Eq. 5-23)}$$

As this factor considers both the oil as the mixing conditions, it provides an overview of the situation at hand.

The dispersability factor (DF), provides a good indication of the four main output parameters after 24 hours (Fig. 5-2): 1) Volume fraction of oil in the visible slick, 2) Effective drift factor, 3) Visible slick length, 4) Lifetime of the thick, 'true oil color' slick.
For cases with high DF (>0.4), outputs after 24 hours do not differ much between settings. For cases with lower DF all 4 shown output parameters are much more sensitive to changes in DF, in this region, dispersion is not optimal.
Slick length after 24 hours generally increases with decreasing DF, but decreases again for very low DF values. If there is little entrainment of fast resurfacing droplets slick elongation is maximal. In even less favorable conditions with very little entrainment and very fast resurfacing droplets, the slick elongation mechanism occurs slower.
The wind speed (5□, 10○, 15Δ m/s in Fig. 5-2) clearly has a large influence on the slick fate. The medium and high wind speed leave hardly any (>5%) oil on the surface (Fig. 5-2A), where with the low wind speed 10 to 70 % of oil remains afloat. Slick length, effective drift factor and life time of the 'thick' slick decrease with increasing wind speed (Fig. 5-2. B,C&D).

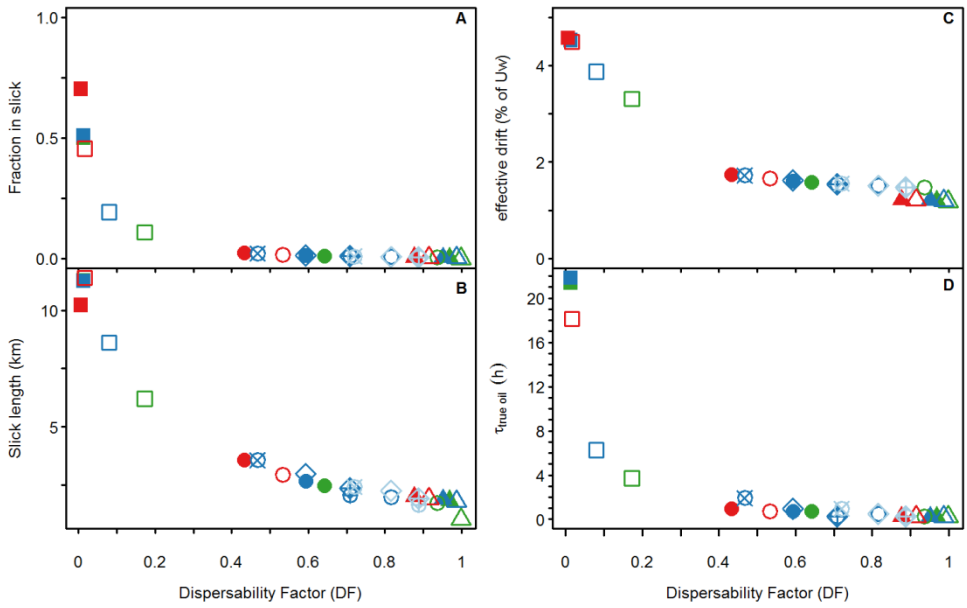

Figure 5-2. Oil slick metrics after 24h as a function of dispersability factor (Eq. 23). Symbol shape indicates wind speed: (□ 5, ○ 10, Δ 15 m/s), color indicates oil type (■ heavy, ■ medium, ■ light oil) in which unfilled symbols represent dispersant treated and filled symbols untreated. Other symbols indicate variation in lengths and layer thicknesses (Fig. 5-3).

The effect of oil type on the oil slick thickness and length after 24 hours is less obvious than that of wind speed. At low wind speed, the influence of oil type best visible, yet the absolute difference in outcome after 24 hours is very limited. Although the light oil type clearly has a higher DF than the heavy oil type, the influence of oil type on the slick length, transport and oil mass, is hardly noticeable (Fig. 5-2, S1). Although increasing oil viscosity does increase the mean droplet size (Eq.5-1), the effect on the droplet's rise-speed is largely compensated by the intrinsic higher density of this oil.

With the same layer thickness, doubling the slick length (in otherwise identical conditions) has no noticeable effect on the fraction of oil in the slick nor on wind drift. Slick length increase (L_{24h}-L_0) is at maximum a factor 1.03, with only a very small effect on the lifetime of the thick slick (Fig. 5-3).

The initial oil slick thickness has a larger effect on the slick evolution (Fig. 5-3) than slick length. It is clear that thicker slicks are harder to disperse; a larger fraction of oil remains in the slick, slick length is larger, and the lifetime of the black slick is longer. As a result, the effective wind drift remains larger.

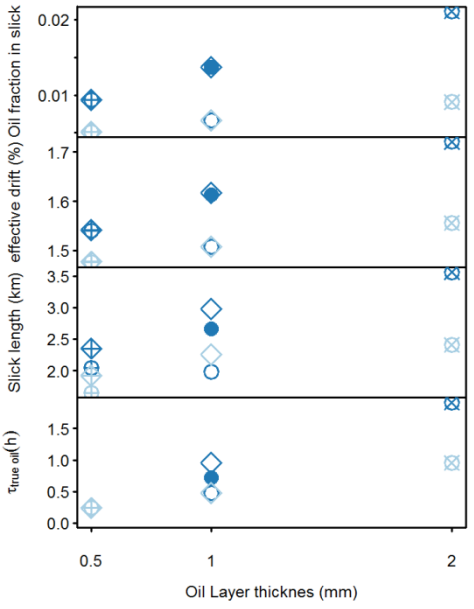

Figure 5-3. Simulation outputs as a function of starting layer thicknesses; (medium layer thickness at 5m/s wind). Outer symbols shape indicates initial slick length (O 250 m, ◇ 500 m), + and x indicate non-standard oil layer thicknesses (also in Fig. 5-2). The lighter blue shade indicates the oil is dispersant treated.

A curious observation is that initial slick thickness has a larger influence on slick length after 24 hours than the initial slick length does. With an equal initial mass of oil in the cross section, a longer thinner slick, will dissipate more easily than a thicker shorter slick. This is a result of the oil-layer-thickness-dependent droplet size distribution we employ, and matches with observations in the field.

This also means, that while oil properties as such did not affect the simulation result much (Fig. 5-2), they could seriously affect the slick development indirectly as they influence the initial slick spreading, and thus, thickness.

The fact that the droplet size distribution is influenced by oil layer thickness has a tremendous influence on the end result. The simulations of the most and least favorable dispersion conditions (Fig. 5-1) were duplicated with the droplet size distribution for the average thickness (S5.1.2). The transport of the slicks is very similar, yet the elongation process occurs at a much slower rate if the droplet size does not decrease with layer thickness. Ignoring the layer thickness dependence causes the total transition to sheen in the most favorable condition to take longer, and the least favorable condition to hardly develop a tail. The

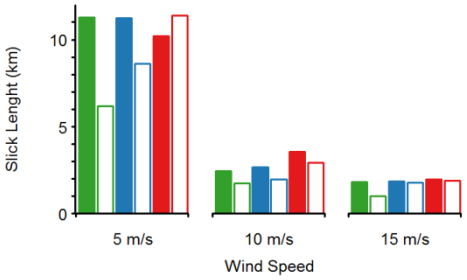

Figure 5-4. Slick travel distance after 24 hours, for the different oil types (colour) with (filled) and without (unfilled) application of dispersants.

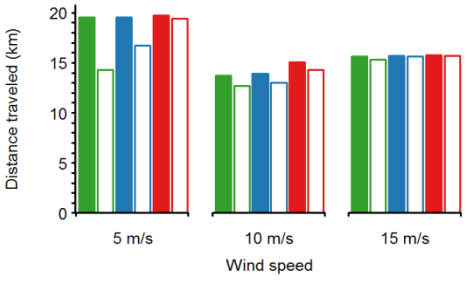

Figure 5-5. Total slick length after 24 hours, for the different oil types (colour) with (filled) and without (unfilled) application of dispersants.

dependence of droplet size on layer thickness explains why a thin initial tail disperses more efficient.

It is clear, that effective dispersion reduces the wind-driven transport of an oil slick. That is why chemical dispersion can be used to alter the transport of the slick (Lee et al., 2015). Our modelling outputs reveal that dispersant application only provides added benefit in 2 of the cases (Fig. 5-4, S5.1), namely the low wind speed and medium and light oil. In 24 hours, the light oil treated with dispersants and subjected to 5 m/s wind speed, moves 73% of the distance the untreated version did. For the medium oil this is 85%. In the 7 other cases dispersion is already very successful, and the additional reduction in transport by dispersants is less than 10%. Notice the relatively low transport distances at higher wind speeds, due to the lower effective drift factor caused by the dispersion.

Most well-known motive for dispersant use is to reduce the oil on the water surface. The benefit of dispersion is greatest in the 'critical region' of dispersion, where naturally occurring dispersion is only little (Fig. 5-2). Conversely, for the least favorable situation (heavy, 5 m/s), slick length after 24 hours was increased by dispersants (Fig. 5-5). The wind shear spreading of this slick was hampered by the oil viscosity, a mechanism that was overcome by the dispersants.

The impact of a surface slick is mostly due to the physical effects. Therefore impact is proportional with oil slick area yet largely independent of oil slick thickness. On the other hand, it is unlikely that presence of just a trace of oil could cause these impacts; A floating oil layer is considered to cause physical effects at layer thicknesses above 25 μm (Jongbloed et al., 2002a). In order to assess the total potential adverse impact of the surface slick, we calculated the slick length with a thickness exceeding this effects threshold, during its lifetime

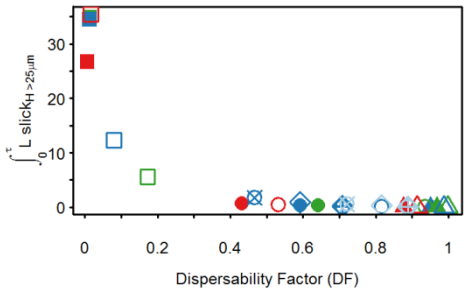

Figure 5-6. Time integrated length (km.h) of the slick part with a thickness > 25μm.

(Fig. 5-6).

This parameter, too, correlates nicely with DF, and shows a sharp decrease in the critical region ($0.17 < DF < 0.4$). In this region, a clear benefit of dispersant application is visible in reducing the thick slick area that can cause adverse effects over time.

These results illustrate how the expected benefit of dispersants in reducing slick surface expression greatly depends on environmental and initial spill conditions, and is predictable via the dispersability factor. Future research should aim at quantifying and validating full slick surface expression in 3D, also taking into account mass loss by other weathering processes that also depend on environmental conditions such as air and water temperature.

The proposed model is capable of simulating the oil slick elongation and transport over time. This phenomenon has been observed at sea, but cannot be perceived in bench scale or wave tank testing. Understanding and predicting oil slick elongation and transport over time is crucial in assessing the NET effect of dispersant application on the fate of oil spilled at sea.

S5. Annex to chapter 5 (supplementary information)

Data are publicly available through the Gulf of Mexico Research Initiative Information & Data Cooperative (GRIIDC) at https://data.gulfresearchinitiative.org (doi:http://dx.doi.org/10.7266/N7SQ8XFT).

S5.1 Model outcomes

Input Variables							Calculated variables							
	Uw [m/s]	L0 [m]	H0 [m]	rhoOil [kg/m3]	muOil [Pa.s]	ift_OW [N/m]	dX [m]	Tbw [s]	WCC [-/s]	zi [m]	Dlim [m]	Dmin [m]	Dmax99 [m]	Dmax [m]
1	5	250	0.001	886	0.1	0.03	10.1	572.2	0.002	0.79	1.49E-04	1.62E-07	7.94E-03	1.04E-03
2	10	250	0.001	886	0.1	0.03	11.0	119.5	0.008	3.14	6.53E-04	7.19E-08	3.64E-03	1.31E-03
3	15	250	0.001	886	0.1	0.03	11.0	47.8	0.021	7.07	1.55E-03	4.60E-08	2.33E-03	3.10E-03
4	5	250	0.001	936	1	0.03	10.1	572.2	0.002	0.79	1.87E-04	2.05E-07	1.01E-02	1.31E-03
5	10	250	0.001	936	1	0.03	11.0	119.5	0.008	3.14	8.17E-04	1.00E-07	5.09E-03	1.63E-03
6	15	250	0.001	936	1	0.03	11.0	47.8	0.021	7.07	1.94E-03	6.87E-08	3.48E-03	3.87E-03
7	5	250	0.001	986	10	0.03	10.1	572.2	0.002	0.79	2.82E-04	3.85E-07	1.89E-02	2.47E-03
8	10	250	0.001	986	10	0.03	11.0	119.5	0.008	3.14	1.23E-03	2.16E-07	1.10E-02	2.47E-03
9	15	250	0.001	986	10	0.03	11.0	47.8	0.021	7.07	2.93E-03	1.60E-07	8.10E-03	5.85E-03
10	5	250	0.001	886	0.1	0.003	10.1	572.2	0.002	0.79	1.49E-04	5.33E-08	2.61E-03	3.41E-04
11	10	250	0.001	886	0.1	0.003	11.0	119.5	0.008	3.14	6.53E-04	2.61E-08	1.32E-03	1.31E-03
12	15	250	0.001	886	0.1	0.003	11.0	47.8	0.021	7.07	1.55E-03	1.78E-08	9.04E-04	0.00E+00
13	5	250	0.001	936	1	0.003	10.1	572.2	0.002	0.79	1.87E-04	9.99E-08	4.90E-03	6.40E-04
14	10	250	0.001	936	1	0.003	11.0	119.5	0.008	3.14	8.17E-04	5.61E-08	2.84E-03	1.63E-03
15	15	250	0.001	936	1	0.003	11.0	47.8	0.021	7.07	1.94E-03	4.15E-08	2.10E-03	3.87E-03
16	5	250	0.001	986	10	0.003	10.1	572.2	0.002	0.79	2.82E-04	2.83E-07	1.39E-02	1.81E-03
17	10	250	0.001	986	10	0.003	11.0	119.5	0.008	3.14	1.23E-03	1.73E-07	8.79E-03	2.47E-03
18	15	250	0.001	986	10	0.003	11.0	47.8	0.021	7.07	2.93E-03	1.34E-07	6.76E-03	5.85E-03
19	10	500	0.001	936	1	0.03	11.0	119.5	0.008	3.14	8.17E-04	1.00E-07	5.09E-03	1.63E-03
20	10	500	5E-04	936	1	0.03	11.0	119.5	0.008	3.14	8.17E-04	1.00E-07	3.86E-03	1.63E-03
21	10	250	5E-04	936	1	0.03	11.0	119.5	0.008	3.14	8.17E-04	1.00E-07	3.86E-03	1.63E-03
22	10	250	0.002	936	1	0.03	11.0	119.5	0.008	3.14	8.17E-04	1.00E-07	6.71E-03	1.63E-03
23	10	500	0.001	936	1	0.003	11.0	119.5	0.008	3.14	8.17E-04	5.61E-08	2.84E-03	1.63E-03
24	10	500	5E-04	936	1	0.003	11.0	119.5	0.008	3.14	8.17E-04	5.61E-08	2.15E-03	1.63E-03
25	10	250	5E-04	936	1	0.003	11.0	119.5	0.008	3.14	8.17E-04	5.61E-08	2.15E-03	1.63E-03
26	10	250	0.002	936	1	0.003	11.0	119.5	0.008	3.14	8.17E-04	5.61E-08	3.75E-03	1.63E-03

(… continued)

	Input Variables						Outputs (after 24 hours)									
	Uw [m/s]	L0 [m]	H0 [m]	rhoOil [kg/m3]	muOil [Pa.s]	ift_OW [N/m]	F_floating [-]	F_susp [-]	F_loss [-]	F_visible Slick [-]	L_slick [m]	L_travel [m]	Drift F (%)	$\tau_{true\ oil}$ [h]	$\int$ L (h>25) [km.h]	DF
1	5	250	0.001	886	0.1	0.03	0.50	0.50	-9.49E-07	0.50	11278	19529	0.045	21.37	34.886	0.013
2	10	250	0.001	886	0.1	0.03	0.01	0.99	-8.09E-07	0.01	2473	13695	0.016	0.72	0.269	0.641
3	15	250	0.001	886	0.1	0.03	0.00	1.00	-8.94E-07	0.00	1835	15639	0.012	0.24	0.030	0.969
4	5	250	0.001	936	1	0.03	0.51	0.49	-8.88E-07	0.51	11248	19550	0.045	21.84	34.482	0.013
5	10	250	0.001	936	1	0.03	0.01	0.99	-8.04E-07	0.01	2660	13936	0.016	0.72	0.332	0.593
6	15	250	0.001	936	1	0.03	0.00	1.00	-8.99E-07	0.00	1868	15672	0.012	0.24	0.030	0.951
7	5	250	0.001	986	10	0.03	0.70	0.30	-1.04E-06	0.70	10215	19732	0.046	48.00	26.695	0.007
8	10	250	0.001	986	10	0.03	0.02	0.98	-8.07E-07	0.02	3572	15046	0.017	0.96	0.626	0.432
9	15	250	0.001	986	10	0.03	0.01	0.99	-8.97E-07	0.01	1978	15782	0.012	0.24	0.030	0.877
10	5	250	0.001	886	0.1	0.003	0.11	0.89	-7.78E-07	0.11	6196	14295	0.033	3.72	5.561	0.173
11	10	250	0.001	886	0.1	0.003	0.00	1.00	-8.01E-07	0.00	1737	12694	0.015	0.24	0.077	0.936
12	15	250	0.001	886	0.1	0.003	0.00	1.00	-8.93E-07	0.00	1022	15320	0.012	0.24	0.030	0.998
13	5	250	0.001	936	1	0.003	0.19	0.81	-7.61E-07	0.19	8616	16715	0.039	6.27	12.309	0.080
14	10	250	0.001	936	1	0.003	0.01	0.99	-8.06E-07	0.01	1978	13024	0.015	0.48	0.140	0.816
15	15	250	0.001	936	1	0.003	0.00	1.00	-8.95E-07	0.00	1791	15606	0.012	0.24	0.030	0.987
16	5	250	0.001	986	10	0.003	0.46	0.54	-8.81E-07	0.46	11390	19408	0.045	18.12	35.442	0.017
17	10	250	0.001	986	10	0.003	0.02	0.98	-8.07E-07	0.02	2946	14288	0.017	0.72	0.414	0.533
18	15	250	0.001	986	10	0.003	0.00	1.00	-9.00E-07	0.00	1912	15727	0.012	0.24	0.030	0.914
19	10	500	0.001	936	1	0.03	0.01	0.99	-4.02E-07	0.01	2979	13969	0.016	0.96	0.964	0.593
20	10	500	5E-04	936	1	0.03	0.01	0.99	-8.02E-07	0.01	2352	13321	0.015	0.24	0.228	0.710
21	10	250	5E-04	936	1	0.03	0.01	0.99	-1.61E-06	0.01	2044	13310	0.015	0.24	0.083	0.710
22	10	250	0.002	936	1	0.03	0.02	0.98	-4.03E-07	0.02	3561	14871	0.017	1.91	1.716	0.467
23	10	500	0.001	936	1	0.003	0.01	0.99	-4.03E-07	0.01	2253	13024	0.015	0.48	0.357	0.816
24	10	500	5E-04	936	1	0.003	0.01	0.99	-8.09E-07	0.01	1923	12760	0.015	0.24	0.060	0.888
25	10	250	5E-04	936	1	0.003	0.01	0.99	-1.62E-06	0.01	1649	12749	0.015	0.24	0.030	0.888
26	10	250	0.002	936	1	0.003	0.01	0.99	-3.99E-07	0.01	2407	13442	0.016	0.96	0.563	0.720

S5.1.1 – Slick graphs

Due to the large size, not all outcomes are shown here. The full list of images can be found at: doi:http://dx.doi.org/10.7266/N7SQ8XFT.

Shown here, are the light oil type (this page) and the heavy oil type (next page) for the two outer wind speeds, and with and without dispersants

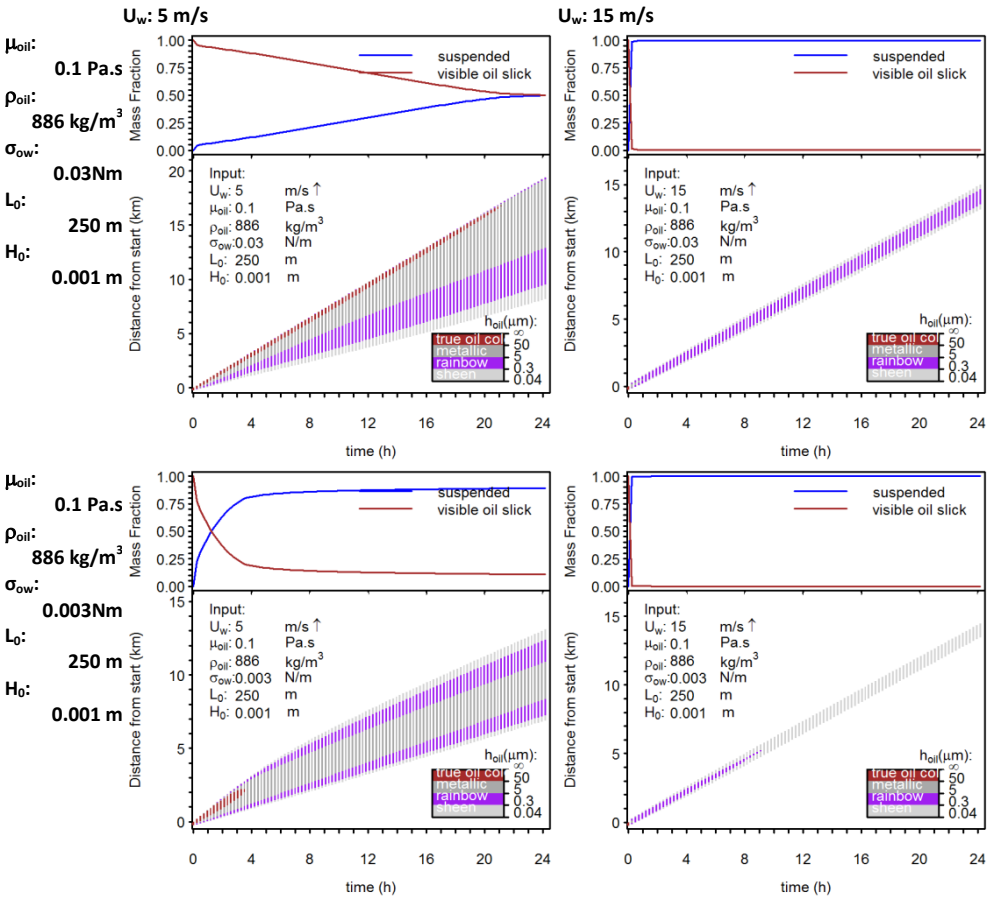

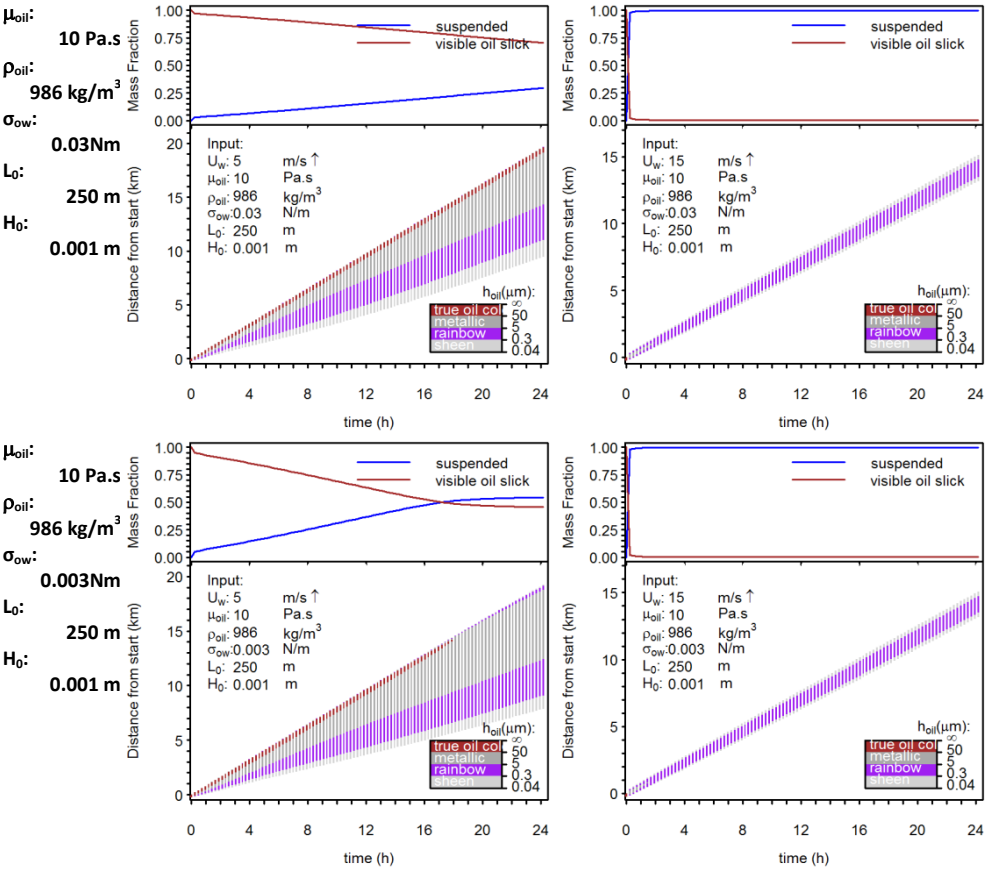
μoil:
10 Pa.s
ρoil:
986 kg/m3
σow:
0.03Nm
L0:
250 m
H0:
0.001 m
Mass Fraction
suspended
visible oil slick
Distance from start (km)
Input:
Uw: 5 m/s
μoil: 10 Pa.s
ρoil: 986 kg/m3
σow: 0.03 N/m
L0: 250 m
H0: 0.001 m
Input:
Uw: 15 m/s
μoil: 10 Pa.s
ρoil: 986 kg/m3
σow: 0.03 N/m
L0: 250 m
H0: 0.001 m
hoil(μm):
true oil col
metallic
rainbow
sheen
∞
50
5
0.3
0.04
time (h)
μoil:
10 Pa.s
ρoil:
986 kg/m3
σow:
0.003Nm
L0:
250 m
H0:
0.001 m
Input:
Uw: 5 m/s
μoil: 10 Pa.s
ρoil: 986 kg/m3
σow: 0.003 N/m
L0: 250 m
H0: 0.001 m
Input:
Uw: 15 m/s
μoil: 10 Pa.s
ρoil: 986 kg/m3
σow: 0.003 N/m
L0: 250 m
H0: 0.001 m

S5.1.2 - Slick graphs: Fixed Droplet size distribution vs oil layer dependent

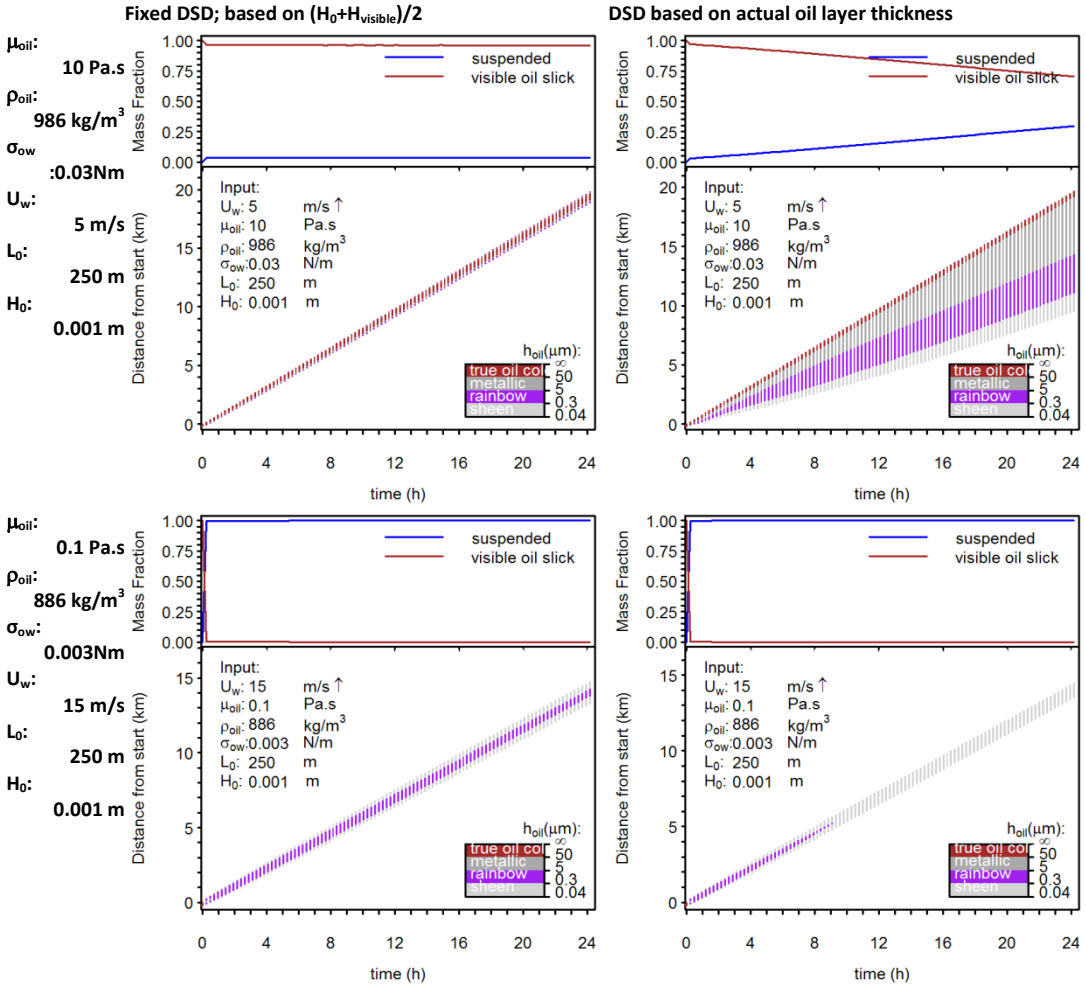

CHAPTER 6

General discussion

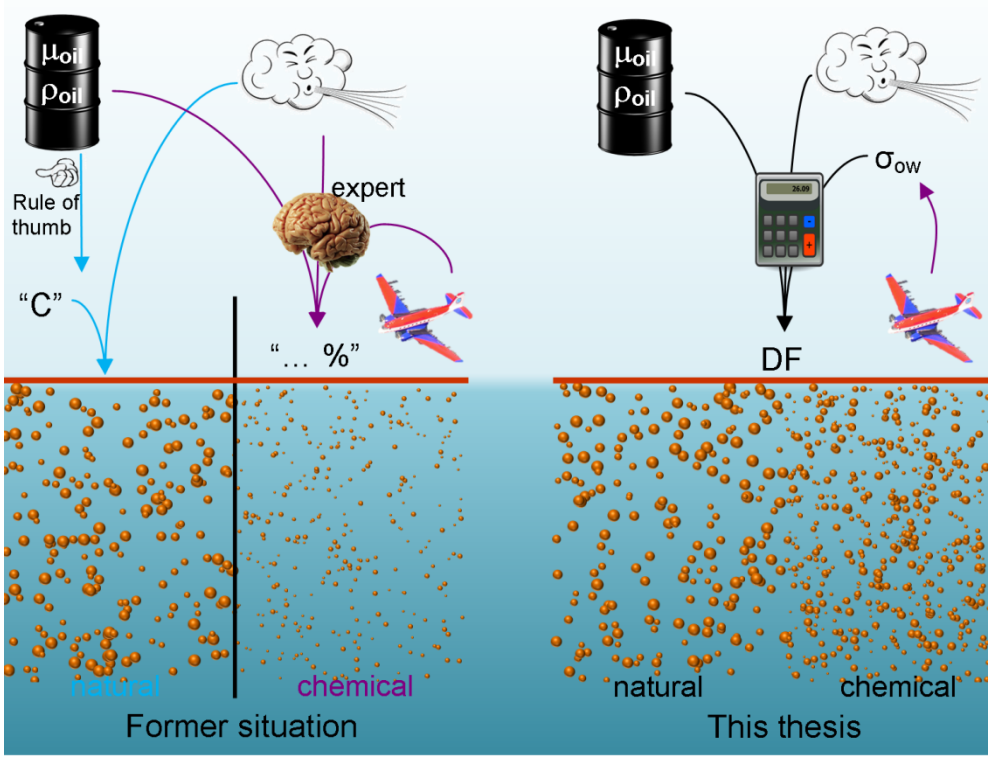

This thesis aims to create insight in the processes governing natural and chemical dispersion of spilled surface oil, and to provide a strategy to assess the added value of chemical dispersion for specific spill conditions and oil qualities.

Chapter 1 introduces the need to mitigate the adverse effects of oil spills and explains how dispersants can serve as a means to alter the fate and effects of oil.

Chapter 2 defines the key steps that make up the dispersion process: 1) Entrainment of floating oil into the water column. 2) Subsequent breakup of the entrained oil in droplets. 3) Vertical distribution of the oil droplets by the downward wave impact. 4) Subsequent buoyant oil droplet rise.
These steps determine the mass transferred to the water column per unit of time, and how long individual droplets can remain there or return to the surface. Due to the wind-driven transport of the floating slick, oil droplets that have been suspended sufficiently long resurface upwind of the original slick. Chemical dispersion follows these exact same steps, with changed oil properties that have become more susceptible to breakup.

Chapter 3 describes a plunging jet test method, developed for investigation of entrainment of oil and initial breakup into droplets by mimicking breaking wave impact. In this plunging jet test, an oil layer with a predefined height and known properties can be subjected to an impact of a falling body of water. Coupled camera equipment captures the events underwater and subsequent image analysis is used to quantify the entrainment and droplet sizes.

Chapter 4 investigates the influence of oil layer thickness, oil viscosity and presence of dispersants on the entrainment process and initial droplet breakup, using this plunging jet test. A relation between these parameters and entrainment is provided and an equation for mean droplet size is adopted.

In chapter 5, the presented impact of oil layer thickness, oil viscosity, wind speed, breaking wave impact and dispersant use on entrainment mass and droplet size are employed in a model for slick elongation and transport. This model is important in order to determine their implications on the natural and chemical dispersion process. In addition, the parameter Dispersability Factor (DF) is introduced that indicates the success in creating stably suspended droplets. This parameter is easily calculated from the conditions (wind speed, oil properties and slick thickness). Values of DF provided an indication of the elongation model outputs (oil slick length, wind driven transport, and mass suspended).

6.1 Main parameters that influence oil dispersion

It is clear that prediction capabilities of (natural and chemical) dispersion can and should be improved (CRRC et al., 2012). Natural dispersion calculations in the oil fate and transport models are based on the empirical results of Delvigne and Sweeney, of which it is generally agreed there is room for improvement (Delvigne and Sweeney, 1988; National Research Council of the National Academies, 2005; Reed et al., 1999). Furthermore, these calculations do not permit prediction of chemical dispersion. Calculation of chemical dispersion result in the current oil fate and transport models requires INPUT of the (estimated) effectiveness rather than that it provides output thereof (Chapter 2).

When considering the dispersion process as a number of separate steps, it becomes clear that the key parameters in dispersion affect these processes differently (Chapter 2). Therefore dispersion effectiveness, as a composite outcome, cannot directly be related to any of the individual parameters separately. The research presented in this thesis, focusses on quantifying the influence of a number of key parameters on the mixing processes (Fig. 2-1, [A]) of oil dispersion. The term dispersability (defined in chapter 5) summarizes the combined success of these processes in creating stably suspended droplets. Furthermore, a model was introduced to investigate how this dispersability, together with the separate transport processes of droplets and oil slick (Fig. 2-1, [B]), determines oil slick behaviour.

In the following sub-paragraphs the influence of different parameters on the dispersability and the oil slick elongation is discussed in more detail.

6.1.1 Oil type (viscosity & density)

As discussed in chapter 2, the viscosity of the oil is considered one of the most important parameters in the dispersion process. As viscosity is a counteracting force to droplet-breakup (Walstra, 2005), high viscosity oil results in larger oil droplets. The currently most used oil spill response models, apply the natural dispersion formula by Delvigne and Sweeney in which viscosity is incorporated in the standard dispersion algorithm in the form of one oil-type specific constant C (Delvigne and Sweeney, 1988). Following Stokes' law, the (viscosity-related) oil density is known to influence oil droplet rise speed (Robbins et al., 1995) and to bias certain dispersability tests (incorporating a settling step) as a consequence (SL Ross Environmental Research LTD and MAR Incorporated, 2011). However, in current oil spill modelling, often a fixed droplet size is assumed and

considered to be stably suspended, regardless of environmental conditions or oil density (Reed et al., 1999).
The influence of viscosity as a factor in oil droplet breakup, as commonly reported in small and large scale dispersion tests (Chapter 2), is also apparent from the plunging jet test results. As is shown in chapter 3 and 4, the mean droplet size increases with oil viscosity. This, however hardly affects the dispersability and the oil slick behaviour (Chapter 5). Partly because weather conditions are a much more dominant factor, and partly because of the correlation between oil viscosity and density: Most components in oil that cause a high oil viscosity also create a high oil density. The oil types tested in the model, were designed to reflect this viscosity ~ density relation (Chapter 5.2). This means that although high viscosity oil results in larger mean droplet size, these droplets rise to the water surface a bit slower. The mean droplet rise velocity of the full droplet size distribution for each of these oil types shows only little variation between them (Fig. 6-1, left panel). In the (unrealistic) scenario with equal densities for these three oil types (Fig. 6-1, right panel), mean rise velocity would be much more affected by oil type. Evidently, the density-viscosity correlation strongly reduces the influence of viscosity on the mean droplet rise velocity.
When modelling dispersion, both viscosity and density should be separate inputs, as a dis-proportion between these qualities can seriously affect the dispersability.

Apart from high viscosity oil resulting larger oil droplets in general, in the plunging jet test, dispersant treated high viscosity oil was found to create long thin oil filaments instead of spherical oil droplets. Such stable filaments were

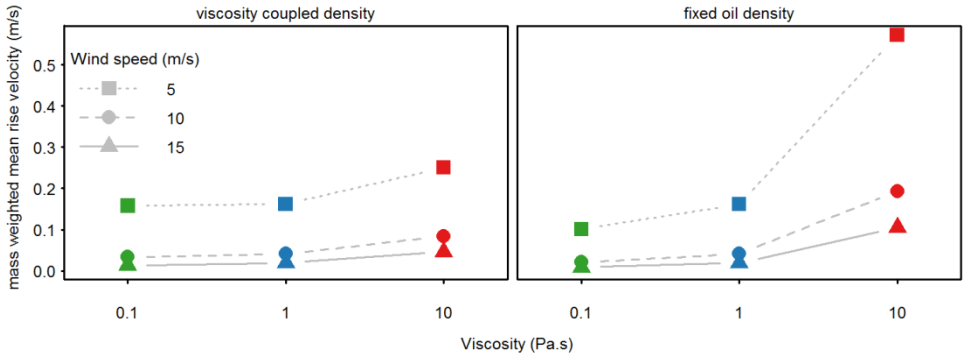

Fig. 6-1. Mean droplet rise velocity for droplet size distributions of different oil types (colours) and wind speeds (symbols/lines). In the model the oil density either matched viscosity (left) or was kept equal oil for the three oil types (right). Droplet size distributions are calculated assuming an oil layer thickness of H_{oil}=0.5 mm, and without dispersant.

observed in the test with chemically treated weathered oil type B_{evap} (Fig. 4-4). These filaments are an indication of viscosity being a much more dominant factor counteracting droplet breakup than interfacial tension. When interfacial tension (low capillary number) is dominant the oil would snap into multiple droplets after little deformation in order to attain the least relative surface area (Janssen, 1993). When viscosity is dominant adding more dispersants will not enhance droplet break-up as the interfacial tension is not the limiting factor.
The influence of this impaired breakup on the overall dispersion, however, is expected to be only slight: due to their shape, the formed filaments have a much lower rise velocity than an equal oil volume in a spherical droplet. The partially horizontal oriented fibres have a larger cross sectional area than a sphere would, and thereby experience larger drag force. Consequently, the filaments were still visible in the test tank 5 seconds after the plunge impact (chapter 4).
The entrainment images of one of the less viscous oil types without dispersants appear to show a similar effect (Fig. 4-4, oil type B); near the entrainment region long strands of oil are initially visible. These latter strands have much larger diameters and do subsequently contract to spherical droplets. Therefore they are part of the normal breakup process. These strands are not visible anymore after 5 seconds.

The plunging jet test revealed that the volume of oil entrained is largely unaffected by oil properties (Chapter 4). Except for oil viscosity exceeding 5 Pa.s, where the entrainment rate was 60 to 80% less than expected based on oil layer thickness (Fig. 4-3). The oil layer of this particular oil type (B_{evap}, 5 Pa.s) resists droplets being sheared off by the plunge to such extent it altered the flow profile of water around the jet impact (Fig. 4-4).
A similar entrainment limitation in a plunging jet test has been observed by other researchers (Reed et al., 2009). Both their plunge height and their maximum viscosity are twice that of our observation (Table 4-2, upper rows). An increased maximum viscosity with plunge (wave) height is logical as the impact from larger wave heightsis expected to be more successful in separating oil from the floating layer. Our plunging jet impact height of 30 cm represents a wind speed of 5.5 m/s, at which the viscosity threshold is 10 Pa.s. (eq. 5-5). More elaborate experiments could provide experimental data for the entrainment thresholds above these impacts.

The modelling study (chapter 5) did not incorporate the viscosity threshold for entrainment, yet this would be relevant for one of the cases as is shown in Fig. 6-2. The figure shows the model outcome without (left) and with (right) incorporation of the threshold. The slick was already considered quite persistent, and even more so with a realistic entrainment threshold. Nearly all of the oil remains on the water surface, and the little entrainment that does occur will cause a tail to form (8.1 km in 24 h).
As dispersants enhance the oil's susceptibility to breakup it would be expected that they would overcome this strong resistance to break-off. Although quantitative data could not be obtained for this specific oil type with dispersants, the images at least indicate the flow pattern around the impact to be similar to 'normal' entrainment (Fig. 4-4). It should be noted, that if adding dispersants would overcome the viscosity threshold, enhanced entrainment of such viscous (poorly dispersible) oil, could cause the slick length to increase. For the case in Fig. 6-2, a chemically treated oil without threshold resulted in an even longer slick length of 11.5 km in 24 h (S5.1.1, page 121).

Summarizing, viscosity above a (wave height dependent) threshold impedes oil entrainment and will limit the elongation of the slick. Below this viscosity threshold, oil droplet size is positively related with viscosity, yet the resulting effect on droplet suspension time is limited because of the inherent density difference with compensating influence on droplet rising velocity.
Besides the entrainment threshold, the viscosity also is relevant in the decision making for application of dispersants, as this will not enhance dispersability when the viscosity instead of interfacial tension is limiting.

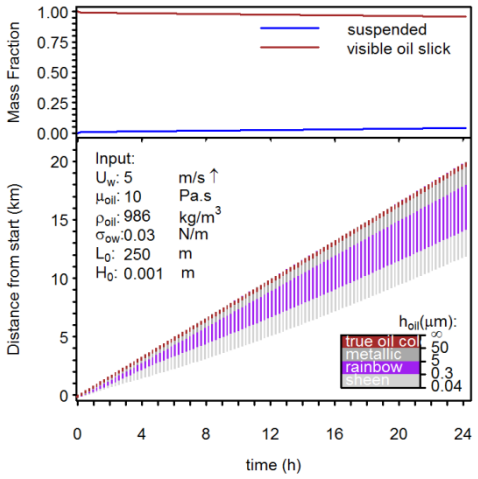

Fig. 6-2. Slick model output of the least susceptible as shown in chapter 4 (left) with 70% less entrainment (right), yet equal droplet size distributions.

6.1.2 Oil layer thickness

In operational guidelines for chemical dispersion of oil, oil layer thickness is not considered very relevant for oil fate modelling. It mainly is seen as a parameter relevant for dispersant dosages: spraying dispersants on a slick that's too thin, would cause the dispersant to fall through and be lost to the water column (Tamis et al., 2012). Spraying the thicker areas of the slick is advised, however, for too high thicknesses, multiple spray passes are required to reach the effective dosage (EMSA, 2009).
In the oil spill fate modelling work of Delvigne and Sweeney (1988), the increase in entrainment with layer thickness was thought only to involve a greater number of larger droplets, thereby having only little influence on the entrained volume of small droplets.

Using the plunging jet set-up (Chapters 3 & 4), the importance of the oil layer thickness in both entrainment and droplet breakup was revealed: the volume of oil entrained increases proportionally with layer thickness. The availability of oil per unit surface area (oil layer thickness) clearly determines the total volume entrained. With increasing oil layer thickness, not only the mean droplet size increases, but also the absolute amount of oil in small droplets (Table 3-3, Fig. 3-9, Fig. 4-5).
Further, thin layers have a higher dispersability than thick layers due to the larger relative portion of small droplets. This influence of layer thickness on dispersability also is crucial for the behaviour of the slick over time. With the same oil mass, a longer, thin slick is dispersed faster than a short thicker slick (Fig. 5-3) because the smaller droplets created move more mass to the water column. Such rapid removal of the thin slick areas while thicker parts remain, has been observed at sea too (Lewis et al., 1998).

These observations confirm that aiming the dispersion response at the thick slick portions (National Research Council of the National Academies, 2005) is most effective. For mechanical recovery, removal rates are much higher in thick oil, while in the meantime, the thinner tail can naturally attenuate. As the thin slick part will disperse more easily by itself, using dispersants on the thick part is expected to be most cost-effective. Mechanical dispersion on the thick slick part could enhance spreading and some initial dispersion that might enhance subsequent natural attenuation of the thinner slick layer.

6.1.3 Initial slick length

The model study presented in chapter 5 only briefly examined the influence of initial slick length on the dispersion process. We can however, make some prognoses based on the different elongation mechanisms.

For favourable conditions (Dispersability Factor > 0.4), the initial slick length will not be a large influence on the dispersion process. In these situations the mass is rapidly moved into the water phase, in a longer slick oil will simply move to the water phase over this larger area.
For less favourable conditions, initial slick length will be of larger influence on the outcome. A longer initial slick means that resurfacing oil from the downwind edge greatly 'feeds' the slick itself instead of the tail only. This means that the absolute elongation is hardly affected by initial slick length. The oil resurfacing back into a long slick slows down the decrease in thickness. As this decrease in thickness is necessary for more efficient dispersion, it takes longer for a longer slick to attenuate.

6.1.4 Wind Speed

Wind speed is considered an important variable in the dispersion process, as it indirectly provides the energy for the dispersion to occur. The currently used natural dispersion algorithm mostly assumes no dispersion at wind speeds below 5 m/s due to the lack of breaking waves (Delvigne and Sweeney, 1988). Furthermore, the dispersion flux increases with area fraction of breaking waves and with energy dissipation rate (both positively impacted by wind speed).

In the oil fate model studies presented in chapter 5, indeed, wind speed is a very dominant factor in the outcome. This wind speed, however, plays a role in several process parameters. The amount of entrainment and energy levels indeed depend on wind speed:

- The area fraction agitated increases; $A_{mix} \sim U_w^{2.26}$, resulting in a proportional increase of entrainment.
- The plunge height increases $H_{pl} \sim U_w^2$, causing smaller droplets to be formed (Eq. 4-2).

In addition, the mixing depth increases; $z_i \sim U_w^2$, and the time between breaking waves decreases; $T_{bw} \sim U_w^{-2.26}$, as a consequence much larger droplets can

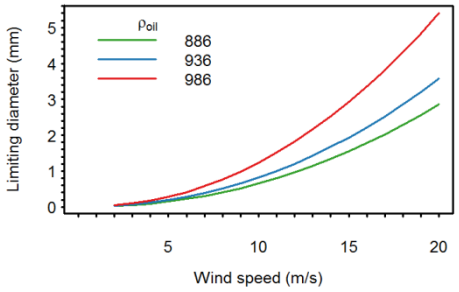

Fig. 6-3. Limiting diameter (largest droplet diameter that can remain suspended until the next breaking wave hits) as a function of wind speed (~zi, Tbw).

remain suspended until the next breaking wave hits (Fig. 6-3). Thus, in contrast to commonly assumed in the models (Reed et al., 1999), the droplet size that is stably suspended, is wind speed dependent: in more energetic conditions, larger droplets can be successful in remaining suspended. Also, when the slick moves faster, more rising droplets will end up in the tail than in the main slick area.

The mechanisms behind the wave spectrum and breaking wave formation depend on more parameters than wind speed alone: wind speed history current directions and bathymetry also play a part in the water surface dynamics. Our wind-speed parameterizations undoubtedly neglect some aspects of the wave spectrum that would be revealed in a full hydrodynamic model. However, our goal here is to demonstrate how changes in dispersion develop in at-sea conditions. For this purpose, we consider the chosen parameterization to provide a suitable prediction of conditions to be expected.

6.1.5 Dispersants

It is self-evident that addition of dispersants enhances the dispersion process. The main mode of dispersant action is to reduce the oil-water interfacial tension, thereby allowing smaller droplets to be formed. The Delvigne and Sweeney algorithm does not include chemical dispersion (Delvigne and Sweeney, 1988), although that would be very desirable when deciding on the added value of applying dispersants. Current oil spill models simulate chemical dispersion based on a treated oil volume and a user-predefined dispersant effectiveness (French-McCay, 2004; Reed et al., 2004). The product of these values (effectively treated oil volume) is then dispersed with an assumed fixed droplet size distribution observed for chemically dispersed oil in the field. However, as pointed out in Section 4.4.2., droplet size measurements at sea are highly skewed towards small stable droplets, as these 'accumulate' in the water column as dispersion continues.
The user predefined effectiveness value thus indicates the volume of treated oil broken up into stably suspended droplets. Therefore this estimated input value should already include the operational effectiveness of chemical dispersion (logistics, targeting, incorporation into the oil; Fig. 2-1 [D]), as well as the resulting dispersability of the treated oil at the current energy conditions (Fig.2-1 [A]). As a result, the current effectiveness assessment relies heavily on expert judgement (National Research Council, 2005a).

The effect of dispersants on droplet size is very strong. Our initial (high) dispersant dosages (1:50) caused the entrained oil to split up in large numbers of small droplets, making the test tank too crowded and murky for quantitative analysis (Fig. 3-8). The more viscous oils in the second test series (chapter 4)

with more conservative dispersant dosages did provide a quantifiable entrainment in most cases. A 1:200 dose of dispersants mixed into the oil caused the mass median oil droplet size to drop by 20 to 50%.

The (absolute) decrease of mass median droplet size with decreasing interfacial tension hardly depends on oil viscosity (Fig. 6-4), which is in accordance with the Weber and Reynolds number relation for droplet size (eq. 4-2). As the relative dispersant-induced decrease in droplet size is much smaller for high viscosity oils, the increase of dispersability is lower for these oil types.

Entrainment of oil by the plunging jet was not significantly influenced by the dispersant dosages applied (1:200), adding dispersants does not increase the amount of oil per surface area, thereby does not affect the entrainment rate.
On the other hand, highly dosed oil was found to entrain with unintentional (and less energetic) vertical input too in this thesis as in other work (chapter 3, (SL Ross Environmental Research LTD et al., 2006a)). This is because high dispersant dosages (1:20), can cause the oil-water interfacial tension can drop down to orders of 10^{-6} N/m (Fig. 2-6) at which hardly any energy is needed to commence droplet formation (Walstra, 1993).
It is, however, unlikely that the resulting extra entrainment will influence dispersion in at-sea conditions. For such highly dispersible oil, even at 5 m/s winds, the weak and infrequent breaking wave impact already causes such a stable dispersion (Fig. 6-5), that additional entrainment by other mechanisms couldn't affect the mass balance much. Although breaking waves decline even further at lower wind speeds, so does the presence of other sea surface features that could cause additional entrainment, for instance Langmuir circulation (Moum and Smyth, 1994).

In the presented model, dispersant application is simulated by a decrease of the oil-water interfacial tension. This still requires information about the success of dispersant application (logistics, targeting, incorporation into the slick,

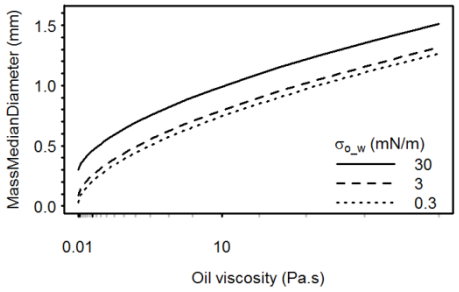

Fig. 6-4. Mass Median oil droplet Diameter as a function of oil viscosity, based on a wind speed of 10 m/s, oil layer thickness of 0.4 mm (eq 5-12).

dispersant effect on oil properties; chapter 2).
Such data on the effective dispersant dosage in the field and resulting oil-water-interfacial tension is not readily available, partly as it depends on so many factors (falling of the dispersant droplet, oil slick skin formation and the composition of the oil and the dispersant), and partly as interfacial tension measurements are highly influenced by the test settings and are not in agreement with each other (for more elaborate information see Chapter 2.4.3).
A strategy to obtain more information on the chemical effectiveness of dispersants could lie in the use of small scale laboratory tests. As such tests provide a measure of the susceptibility to breakup of the dispersant-oil combination; the test results provide an indication of the change in dispersability after addition of dispersants. To assess the effect of dispersants, results of treated and untreated oil should be compared. Furthermore the test design should allow for loss of surfactants, preventing incorrectly applied dispersants (lost to the water phase) to still (positively) influence the end result.

6.2 Oil slick elongation as a result of dispersion

The model presented in chapter 5, uses a number of relatively simple input parameters (Wind speed, Oil Viscosity, Oil Density, Oil-water Interfacial Tension, and initial slick length and thickness), to calculate the entrainment and subsequent resurfacing of oil over a predefined period of time, yielding the slick length, displacement and mass distribution (between slick & water column, and across slick length).

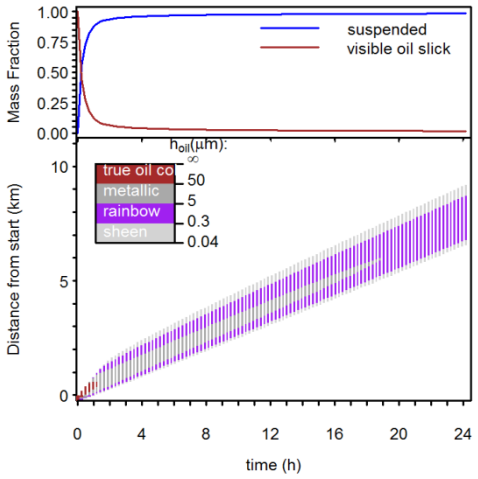

Fig. 6-5. Model output for oil slick fate at 5 m/s wind, low viscosity (0.1 Pa.s) oil, and an oil-water interfacial tension of 3 x 10^{-3} mN/m (very high dispersant dose).

Based on the modelling outcomes, we can make the following observations: When given enough time, an oil slick can disperse and elongate to yield an oil layer thickness that will hardly cause harm to surface organisms. For conditions favourable for dispersion, this is a vertical process: a substantial fraction of oil is quickly moved to the water column; the resulting thinner slick will disperse more efficiently and the mass balance increasingly shifts to the water column. For conditions were dispersion is less easy, the entrainment and resurfacing of oil causes the slick to spread lengthwise, forming a comet-like tail. This process proceeds until the thick slick part has lost sufficient mass to reach a thickness that is more susceptible for dispersion, after which before mentioned vertical process takes over. These findings are consistent with observations in sea trials, where long slicks with a thick portion downwind are found in conditions with low wind speeds and/or viscous oils, and more favourable conditions create smaller slicks with the thickest portion in the centre (Reed et al., 1994).

6.3 Decision making on chemical dispersion

As outlined in chapter 1, decision making towards chemical dispersion should consider three aspects: 1) the effectiveness, 2) the environmental benefit, 3) the logistical feasibility. The following sub chapters summarize how to assess the effectiveness of chemical dispersion as well as the potential environmental benefit. The logistical feasibility of chemical dispersion is mainly a practical consideration based on dispersant and equipment stocks and the travel time to reach the slick location. This aspect was not studied in this thesis and will not be discussed in this chapter.

6.3.1 Predicting chemical dispersion NET effectiveness

Estimating dispersant effectiveness in advance of commencing such oil spill response relies heavily on expert judgement (National Research Council, 2005a). A subsequent spray trial should then indicate the effectiveness based on whether visible dispersion is observed (National Research Council, 2005a; REMPEC, 2011).

The difficulty in prediction chemical dispersion is illustrated by the fact that, in a post-hoc assessment of the Deep Water Horizon oil spill, experts could not reach agreement on the amount of oil that was dispersed as a result of the use of dispersants (Federal Interagency Solutions Group, 2010).

A result-based measure for dispersant effectiveness would be how the 'time-integrated length of slick exceeding the effects threshold of 25 μm' is affected.

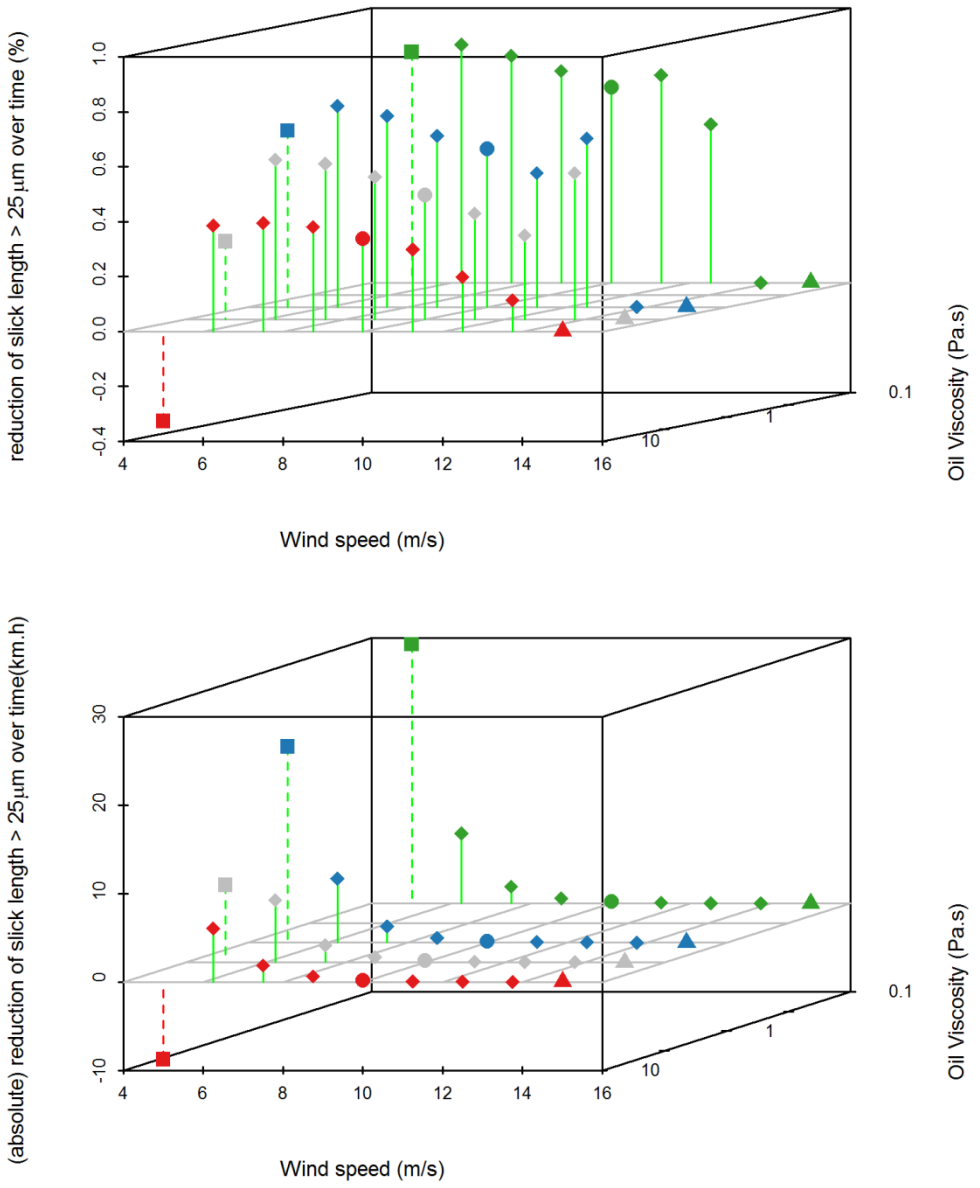

Fig. 6-6. Decrease in 'time-integrated slick length with H_{oil}>25μm' by a factor 10 reduction of oil-water-interfacial tension. Shown as a percentage of the untreated slick (top) or as absolute decrease (in km.h) (bottom). For cases with dashed lines (at 5 m/s wind), this thickness was still present at the end of the simulation, thus the value does not encompass the full lifetime. Model settings: L_0 = 250 m, H_0 = 0.001 m.

Fig. 6-6 shows to what extent this metric is reduced by decreasing the oil-water-interfacial tension from 30 to 3 mN/m in our simulations.
For wind speeds exceeding 10 m/s, the absolute decrease in slick area due to chemical dispersion is hardly discernible. These conditions create a small symmetrical surface slick, while most mass is in the water column. Dispersants will speed up the displacement of oil to the water column, yet the absolute effect is only slight as the surface area of such slicks is already relatively small.
In the transient regime of the range (U_w 6-10 m/s) dispersant addition creates the largest relative change (Fig. 6-6, top), with the highest absolute reduction of slick area around 6-7 m/s wind speeds (Fig. 6-6, bottom).
In most of these conditions the natural dispersion process will considerably increase the slick area through the elongation process. Adding dispersants will speed up the initial slick spreading process transitioning into the more efficient symmetrical spreading because of the more rapid layer thickness decline.

For the one least favourable condition, dispersants even cause an INCREASE in relevant (> 25 μm) slick length. It must be noted, that in these cases 24 h was not enough for the slick (> 25 μm) to be fully disappeared. Undoubtedly, the overall outcome of this case would be more positive if the full lifetime of the slick was considered. The quicker spreading of the slick may lead to a quicker final attenuation although it is questionable whether this serves a purpose for this persistent oil.

As expected, equal change in interfacial tension is more effective on the low viscosity oil, as the relative change in droplet size is higher (Fig. 6-4). Together with the observation that high viscosity hinders dispersant incorporation into the oil slick (Canevari, 1984), this means that chemical dispersion is relatively and absolutely less effective on higher viscosity than on low viscosity oils.

The optimal dispersion (vertical) regime already commences at Dispersability Factor (DF) of over 0.4. A DF calculation (Eq. 5-23) can indicate the (lowered) interfacial tension that would be necessary to reach this regime.
A smaller shift in dispersability might also be sufficient to alter the oil slick behaviour by helping the initial slick spreading and thereby quickening the transition into the vertical regime. Understanding this can help reduce the amount of dispersant applied for still successful dispersion.

Summarizing:
Sub-optimal natural dispersion causes the oil slick to elongate substantially in the wind direction, where the thick slick portion is followed by a long tail in the upwind direction. Dispersants can be beneficial in these situations, accelerating the spreading of the thick slick part the subsequent and transition into the phase

where size is slowly reduced as more and more mass moves to the water column. The chemical as well as operational effectiveness of dispersants does decrease with increasing viscosity.
For very low dispersability, elongation of the oil slick is hampered. In these cases, dispersant application will cause a larger slick on the short term.
The added benefit of dispersants is limited in optimal conditions for natural dispersion, which can be identified by only slight elongation of the slick where the slick thickness is symmetrical in wind direction, and its movement with the wind is reduced.

6.3.2 Environmental benefit

In the previous paragraph, the effectiveness of the response was already linked to success in reducing the > 25 μm oil slick area. Although effects of surface oil are often considered more serious (Chapter 1), success in removing the oil from the water surface does not necessarily indicate a NET environmental benefit. The enhanced volumes of suspended/dissolved oil can enhance adverse effects in the water column (O'Sullivan and Jacques, 2001).

Water column exposure can be only roughly indicated by the model presented in chapter 5. All the mass in the transect is conserved, thereby ignoring other processes that remove mass such as lateral spreading and weathering processes such as evaporation and dissolution. Loss of suspended oil droplets can occur via interaction with suspended particles and subsequent sinking. Suspended droplets, however, are more mobile and can also be transported out of the slick area by turbulent diffusion and other sub-surface processes (Boufadel et al., 2006). As such processes are not accounted for in our model, the water column concentrations will most likely be overestimated. The model outcomes, however, do show that the wind shear mechanism is more successful in spreading the oil mass in the least favourable case than it is in the favourable case. The suspended cloud in favourable dispersion, centres around the surface slick and is about 2 km wide (Fig. 6-7, right). In the less favourable case, less oil is transported to the water column, yet also smaller amounts of oil are spread across a larger area (Fig. 6-7, left).

Although the dispersants are designed to be low in toxicity (Chapter 1), the resulting enhanced acute exposure to hydrocarbons can cause extra toxic effects to water column biota. Where physical surface oil impacts are mass independent for thicknesses above the effects threshold (Jongbloed et al., 2002b), potential water column effects are more transient and depend on exposure time and maximum concentration (Lee et al., 2015).
The enhanced exposure to hydrocarbons by enhanced dispersion is only brief, as concentrations are expected to diminish quickly due to enhanced dilution (Lee et al., 2015). This dilution is, however, less evident in case of continuous dispersion of large spills such as the Deepwater Horizon incident, or in shallow or enclosed waters (Wissenschaft, 2016). Assessing potential toxic effects encompasses a lot of uncertainties such as species dependent sensitivity. Moreover, the precise exposure of the organisms over time depends on the specific spill conditions as well as the behaviour of the organisms (Tamis et al., 2012). Different laboratory tests are available simulating various exposure regimes (Redman and Parkerton, 2015), yet these may not necessarily match exposure regimes at sea.

In addition to chemical dispersion aiming to 'dilute' the pollutant quicker, it is also considered to enhance biodegradation of the suspended oil. The role of biodegradation in natural and chemically dispersed oil is unclear. Bacteria may also experience more acute toxic effects (Rahsepar et al., 2016) and conditions are heterogenic in space and time. As a result, conflicting information is available indicating whether biodegradation is enhanced, decreased or indifferent of chemical dispersion (Kleindienst et al., 2016; Lee et al., 2013; Rahsepar et al., 2016).

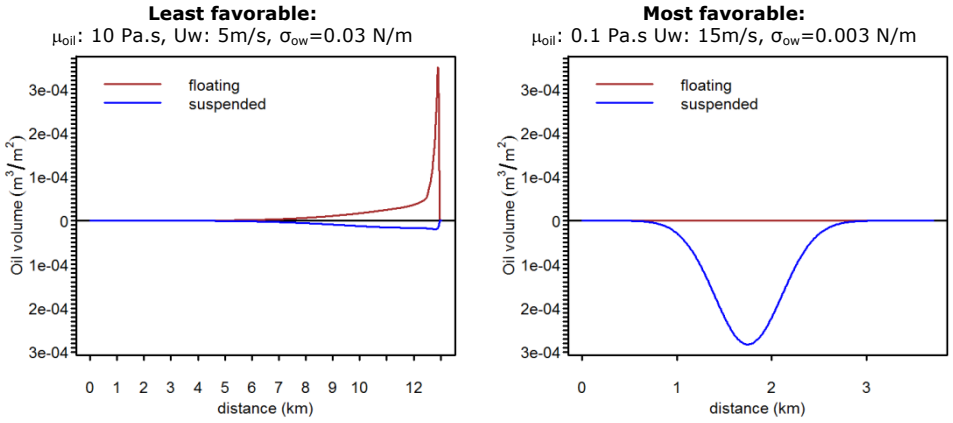

Fig. 6-7. Mass distribution of oil between water column and surface slick after 24 hours, across the slick length (downwind edge on the left). Please note the difference in x-axis.

Dispersed oil, can also re-concentrate on the sea-floor due to sedimentation (Khelifa et al., 2008) or the observed so-called MOSFFA mechanism (van Eenennaam et al., 2016; Vonk et al., 2015). This could cause long-lasting effects as the oil on/in the sediment is only slowly biodegraded under oxygen limited conditions and may cause prolonged local exposure to hydrocarbons (Lee et al., 2015).

Incorporating the presented evidence-based algorithms for entrainment and droplet breakup in the more elaborate oil spill fate and transport models, allows for better estimations of realistic water column concentrations based on environmental conditions, oil type, and the response scenario (natural dispersion vs chemical dispersion). Such more realistic exposure metrics are invaluable in correctly evaluating the effect of chemical dispersion on biodegradation and toxicity as well as in the potential 'interaction and sinking mechanisms'.

6.4 A view on the future

6.4.1 The future of dispersant use

Research efforts towards better understanding and improvement of oil spill dispersants continue (Chapman et al., 2007; CRRC, 2006), including; 1) Development of dispersants with enhanced effectiveness and/or natural origin (C-MEDS Consortium, n.d.); 2) Understanding the effectiveness and oil fate associated with sub-sea dispersant use (Brandvik et al., 2013; Paris et al., 2012; Socolofsky et al., 2015); 3) The implications of dispersant use in arctic conditions (Lewis and Daling, 2007). In addition, major efforts are still working on identifying and quantifying potential ecological effects and biodegradation of dispersants and dispersed oil.
The current extensive studies still carried out in the Gulf of Mexico, provide the scientific community with more information on unexpected oil fate pathways such as via the MOSSFA mechanism. Certain conditions may not be suitable for application of dispersants at sea, e.g. in situations of algal bloom or in situations with ice.

The debate on dispersant use will also continue, in part due to the existing uncertainties, and in part because it does not actually remove the pollutant from the environment. Nevertheless, chemical dispersion fills a niche where other response methods cannot compete. Given the potential adverse effects on fate and effects (acute oil toxicity), it is of utmost importance that the added value of dispersant application is evident before it is decided to apply them.

6.4.2 Future perspectives for predicting dispersion

In this thesis, the influence of oil properties and layer thickness on the entrainment process was experimentally investigated, yielding formulae for entrainment rate and droplet size. A model was constructed to demonstrate how these relations influence the dispersion process and oil surface slick behaviour. The NET benefit of dispersants in removing surface oil is much more convincing in situations where natural dispersion is sub-optimal.

Although oil viscosity is considered a key parameter on the dispersion process, its influence (via droplet size) on the elongation of the slick was found to be only limited.
The only exception was that viscosity above a certain threshold impedes entrainment. This threshold is dependent of (breaking wave) free fall height and the presence of dispersants, yet more research should reveal where this threshold is in at-sea conditions and the implications for the entrainment rate.
Combined, the latter two viscosity effects might provide an explanation for the observed limiting viscosity for chemical dispersion in field and wave tank tests. A better understanding of both mechanisms can provide a key to a strategy overcome them.

Further, the oil viscosity could also have a limiting effect on the operational effectiveness of the dispersants, a topic outside the scope of this thesis. The incorporation of dispersants into the oil layer, and their subsequent effect on oil properties, therefore deserve more attention in further research.

The droplet size relation was obtained from laboratory scale-tests. The other mechanisms in the dispersion process are based on theoretical considerations. Although the resulting elongation mechanisms observed in the model match observations in the field, validating the individual steps in the entrainment process (initial droplet size distribution, entrainment rate, intrusion depth) in the field would help identifying in which cases the prediction can and cannot be expected to match reality.

And finally, incorporation of the proposed oil-layer-thickness-dependent entrainment and droplet breakup in the existing, more comprehensive, oil spill fate models would enable assessment of the oil slick behaviour based on more elaborate hydrodynamic conditions and in conjunction with the other weathering processes that cause oil slick mass loss. Such an effort would facilitate calculation of realistic water column concentrations (with and without dispersants) as an indication for potential water column effects.

6.5 Overall conclusions

The aim of this thesis was to provide a method to predict the NET effectiveness of dispersant use at sea, by means of a better understanding of the processes involved. The entrainment and droplet-breakup processes were investigated by means of a plunging jet tests. The influence of the resulting quantified influences on dispersability, on oil slick elongation, was investigated by means of a model study. Based on these results, the following can be concluded.

The presented elongation model, allows for investigating the effects of altered dispersion on oil slick elongation. The proposed Dispersability Factor, includes all the relevant aspects of the dispersion process, and will therefore provide a better (quick) indication of dispersion success than current fixed droplet size cut-offs.

Formation of a comet-like tail in the upwind direction indicates sub-optimal (natural) dispersion. In most of such cases, adding dispersants will aid this slick to disappear more quickly.
A smaller oil slick, symmetrical in thickness in the wind-direction, indicates optimal natural dispersion. In this case more oil mass is underwater than above it. Dispersants are unlikely to benefit this process.

Above a (wave height dependent) viscosity threshold, oil entrainment is hampered because the oil-slicks resist shearing off. Although dispersants are thought to overcome this effect, application might cause the slick area to increase yielding a greater surface area problem on the short term.

The influence of oil type on the elongation process is only limited: the intrinsic higher density of these oil types allows larger droplets to be stably suspended. High viscosity oil, however, was found to benefit less from an (equal) decrease in interfacial tension, than a low viscosity oil.

Abbreviations and Symbols

Acronyms & abbreviations

ANOVA	ANalysis Of Variance
BFT	Baffled Flask Test
BIO	Bedford Institute of Oceanography
BLOB	Binary Linked OBject
DE	Dispersion Effectiveness
DOR	Dispersant to Oil Ratio
IFT	Interfacial Tension
SFT	Swirling Flask Test
VOC	Volatile Organic Compounds
VMD	Volume Mean Diameter
WAF	Water Accommodated Fraction

Symbols

A_{mix}	Area fraction agitated	s^{-1}
Ca	Capillary Number	-
d	Droplet diameter	m
D	Droplet size class	
D	Droplet size	m
D_a	fraction of sea surface dispersed per hour (Mackay)	-
D_b	fraction of oil permanently dispersed (Mackay)	-
D_{lim}	Limiting diameter	m
D_{50}	Number median droplet size	m
$F_v(D)$	Volume fraction of entrained oil in droplet size class D	-
g	Gravitational accelleration	m/s^2
H_{bw}	Breaking wave height	m
H_{oil}	Oil layer thickness	m
H_{plunge}	Plunge height/ free fall height	m
H_{sign}	Significant wave height	m
L_0	Initial oil slick length	m
MMD	Mass median diameter	m
Q_{entr}	Entrainment rate	m^3/m^2s
Re	Reynolds Number	-
T_{bw}	Breaking wave period (time between two ‘mixing incidents’ in one location)	s
U_h	Impact speed	m/s
u_{stokes}	Stokes induced velocity	$m\ s^{-1}$
u_{wind}	Wind induced velocity	$m\ s^{-1}$

$U_{d\|s}$	Relative velocity of a droplet at depth z compared to the surface slick	m s^{-1}
U_{slick}	Slick speed	m s^{-1}
U_w	Wind speed (at 10 m above water level)	m s^{-1}
v	Bouyant rise velocity	m s^{-1}
V_{res}	Volume of oil resurfacing in 1 timestep in 1 location	m^3 m^{-2}
WCC	Whitecap coverage	m^2 m^{-2}
We	Weber Number	-
z	Depth (from the water surface downwards)	m
z_i	Droplet injection depth	m
μ_c	Continuous phase viscosity	Pa.s (kg/ms)
μ_o	(oil) dynamic viscosity	Pa.s (kg/ms)
ρ_o	(oil) density	kg/m^3
σ	Oil-seawater interfacial tension	N/m
Υ	Shear rate	/s
τ	Lifetime of a breaking wave	s
Δt	Timestep length	s
Δx	Grid cell length	m
t, x	Time step & grid cell designation	

Units and conversions

Quantity Symbol SI units	**dynamic viscosity (μ) Pa.s**	**kinematic viscosity (ν) m^2/s**	**Interfacial tension (σ) N/m**
	= Ns/m^2 = kg/ms = 10^{-3} centiPoise (cP) = 0.1 * Poise(P)	($\nu = \mu / \rho$) = 10^{-4} Stokes (S) = 10^{-6} centistokes (cS)	= kg/s^2 = 10^{-3} dyne/cm

References

Aamo, O.M., Reed, M., Downing, K., 1997. OIL SPILL CONTINGENCY AND RESPONSE (OSCAR) MODEL SYSTEM: SENSITIVITY STUDIES. Int. Oil Spill Conf. Proc. 1997, 429–438. doi:10.7901/2169-3358-1997-1-429

Abdelrahim, M., 2012. Measurent of interfacial tension in hydrocarbon / water/ dispersant systems at deepwater conditions.

AMSA, n.d. Will a dispersant be effective in this case? [WWW Document]. URL https://www.amsa.gov.au/environment/marine-pollution-response/scientific-info/weathering-of-oil/index.asp (accessed 7.30.16).

Anguelova, M.D., Webster, F., 2006. Whitecap coverage from satellite measurements: A first step toward modeling the variability of oceanic whitecaps. J. Geophys. Res. 111, C03017. doi:10.1029/2005JC003158

Ardhuin, F., Marié, L., Rascle, N., Forget, P., Roland, A., 2009. Observation and Estimation of Lagrangian, Stokes, and Eulerian Currents Induced by Wind and Waves at the Sea Surface. J. Phys. Oceanogr. 39, 2820–2838. doi:10.1175/2009JPO4169.1

ARPEL Emergency Response Planning Working Group, 2007. Guideline for the Use of Dispersants on Oil Spills.

Australian Maritime safety Authority, 2013. National Plan for Maritime Environmental Emergencies. 1–78.

Belore, R., Trudel, K., Mullin, J., Guarino, A., 2009. Large-scale cold water dispersant effectiveness experiments with Alaskan crude oils and Corexit 9500 and 9527 dispersants. Mar. Pollut. Bull. 58, 118–128. doi:10.1016/j.marpolbul.2008.08.013

Berger, D., Mackay, D., 1994. The evaporation of viscous of waxy oils- when is a liquid-phase resistance significant?, in: Arctic and Marine Oilspill Program (AMOP). Vancouver, British Columbia, Canada, pp. 77–92.

Bonn Agreement, 2009. Aerial Operations Handbook.

Bonn Agreement, 2011. BAOAC Photo Atlas (Bonn Agreement Oil Appearance Code).

Boufadel, M.C., Bechtel, R.D., Weaver, J., 2006. The movement of oil under non-breaking waves. Mar. Pollut. Bull. 52, 1056–1065. doi:10.1016/j.marpolbul.2006.01.012

Brakstad, O.G., Daling, P.S., Faksness, L.G., Almås, I.K., Vang, S.H., Syslak, L., Leirvik, F., 2014. Depletion and biodegradation of hydrocarbons in dispersions and emulsions of the Macondo 252 oil generated in an oil-on-seawater mesocosm flume basin. Mar. Pollut. Bull. 84, 125–134. doi:10.1016/j.marpolbul.2014.05.027

Brandvik, P.J., Johansen, Ø., Leirvik, F., Farooq, U., Daling, P.S., 2013. Droplet breakup in subsurface oil releases - Part 1: Experimental study of droplet breakup and effectiveness of dispersant injection. Mar. Pollut. Bull. 73, 319–326. doi:10.1016/j.marpolbul.2013.05.020

Byford, D.C., Laskey, P.R., Lewis., A., 1984. Effect of low temperature and varying energy input on the droplet size distribution of oils treated with dispersants, in: Arctic and Marine Oilspill Program (AMOP). pp. 208–228.

Callaghan, A.H., 2013. An improved whitecap timescale for sea spray aerosol production flux modeling using the discrete whitecap method. J. Geophys. Res. Atmos. 118, 9997–10010. doi:10.1002/jgrd.50768

Callaghan, A.H., Deane, G.B., Stokes, M.D., Ward, B., 2012. Observed variation in the decay time of oceanic whitecap foam. J. Geophys. Res. Ocean. 117, n/a-n/a. doi:10.1029/2012JC008147

Canevari, G.P., 1984. A review of the relationship betweeen the characteristics ofspilled oil and dispersant effectiveness, in: Allen, T.E., American Society for Testing and Materials (Eds.), Oil Spill Chemical Dispersants: Research, Experience, and Reccomendation. Philadelphi, Pennsylvania, pp. 87–93.

Canevari, G.P., Calcavecchio, P., Becker, K.W., Lessard, R.R.R., Fiocco, R.J., 2001. Key

Parameters Affecting the Dispersion of Viscous Oil. Int. Oil Spill Conf. Proc. 2001, 479–483. doi:10.7901/2169-3358-2001-1-479

Cedre, 2005. Using dispersant oil slicks at sea, response manual.

Chanson, H., Cummings, P.D., 1994. Effects of plunging breakers on the gas contents in the ocean. Mar. Technol. Soc. J. 28, 22–32.

Chanson, H., Jaw-Fang, L., 1997. Plunging jet characteristics of plunging breakers. Coast. Eng. 31, 125–141. doi:10.1016/S0378-3839(96)00056-7

Chapman, H., Purnell, K., Law, R.J.R., Kirby, M.F.M., 2007. The use of chemical dispersants to combat oil spills at sea: A review of practice and research needs in Europe. Mar. Pollut. Bull. 54, 827–838. doi:10.1016/j.marpolbul.2007.03.012

Chiba, D., Baschek, B., 2010. Effect of Langmuir cells on bubble dissolution and air-sea gas exchange. J. Geophys. Res. 115, C10046. doi:10.1029/2010JC006203

Clark, J., Becker, K., Venosa, A., Lewis, A., 2005. ASSESSING DISPERSANT EFFECTIVENESS FOR HEAVY FUEL OILS USING SMALL-SCALE LABORATORY TESTS. Int. Oil Spill Conf. Proc. 2005, 59–63. doi:10.7901/2169-3358-2005-1-59

C-MEDS Consortium, n.d. Gomri C-MEDS Consortium [WWW Document]. URL http://dispersant.tulane.edu/publications.htm

Committee on Effectiveness of Oil Spill Dispersants, Marine Board, National Research Council, 1989. Using Oil Spill Dispersants on the Sea.

CRRC, 2006. Research & Development Needs For Addressing the Human Dimensions of Oil Spills.

CRRC, Response Planning Incorporated, NOAA, 2012. The Future of Dispersant Use in Oil Spill Response Initiative.

Curd, H., 2011. The Use of Dispersant for the Control of Volatile Organic Compounds. Int. Oil Spill Conf. Proc. 2011, abs359. doi:10.7901/2169-3358-2011-1-359

Dale, D., 2011. Response Options Calculator (ROC) - Users Guide.

Daling, P.S., Mackay, D., Mackay, N., Brandvik, P.J., 1990. Droplet Size Distributions in Chemical Dispersion of Oil Spills : Towards a Mathematical Model. Oil Chem. Pollut. 7, 173–198.

Daling, P.S., Moldestad, M.Ø., Johansen, Ø., Lewis, A., Rødal, J., 2003. Norwegian Testing of Emulsion Properties at Sea––The Importance of Oil Type and Release Conditions. Spill Sci. Technol. Bull. 8, 123–136. doi:10.1016/S1353-2561(03)00016-1

Daling, P.S., Singsaas, I., Reed, M., Hansen, O., 2002. Experiences in Dispersant Treatment of Experimental Oil Spills. Spill Sci. Technol. Bull. 7, 201–213. doi:10.1016/S1353-2561(02)00061-0

Davoust, L., Achard, J.L., El Hammoumi, M., 2002. Air entrainment by a plunging jet: the dynamical roughness concept and its estimation by a light absorption technique. Int. J. Multiph. Flow 28, 1541–1564.

Deane, G.B., Stokes, M.D., 2002. Scale dependence of bubble creation mechanisms in breaking waves. Nature 418, 839–44. doi:10.1038/nature00967

DeCola, E., Fingas, M., 2006. Observers' report. MMS Cold Water Dispersant Tests Ohmsett Testing Facility 28 February - 3 March 2006.

Delvigne, G.A.L., Hulsen, L.J.M., 1994. Simplified laboratory measurement of oil dispersion coefficient-- application in computations of natural oil dispersion, in: Arctic and Marine Oilspill Program (AMOP). Vancouver, Canada, pp. 173–187.

Delvigne, G.A.L., Sweeney, C.E., 1988. Natural dispersion of oil. Oil Chem. Pollut. doi:10.1016/S0269-8579(88)80003-0

Elliott, A.J., 1986. Shear diffusion and the spread of oil in the surface layers of the North Sea. Dtsch. Hydrogr. Zeitschrift 39, 113–137. doi:10.1007/BF02408134

Elliott, A.J., Hurford, N., Penn, C.J., 1986. Shear diffusion and the spreading of oil slicks. Mar. Pollut. Bull. 17, 308–313. doi:10.1016/0025-326X(86)90216-X

EMSA, 2009. Manual on the Applicability of Oil Spill Dispersants.

EMSA, 2010. Inventory of National Policies Regarding the Use of Oil Spill Dispersants in the EU Member States.

EMSA, 2014. Inventory of National Policies Regarding the Use of Oil Spill Dispersants in the EU Member States.

EMSA, 2016. Overview of national dispersant testing and approval policies in the EU.

Federal Interagency Solutions Group, 2010. Oil Budget Calculator.

Fingas, M., 2008. A Review of Literature Related to Oil Spill Dispersants 1997-2008.

Fingas, M., 2011a. Introduction to spill modelling, in: Fingas, M. (Ed.), Oil Spill Science and Technology. Elsevier, pp. 187–200. doi:10.1016/B978-1-85617-943-0.10008-5

Fingas, M., 2011b. Introduction to Oil Chemistry and Properties, in: Fingas, M. (Ed.), Oil Spill Science and Technology. Elsevier, pp. 51–59.

Fingas, M., Bier, I., Bobra, M., Callaghan, S., 1991. Studies on the Physical and Chemical Behavior of Oil and Dispersant Mixtures. Int. Oil Spill Conf. Proc. 1991, 419–426. doi:10.7901/2169-3358-1991-1-419

Fingas, M., DeCola, E., 2006. Oil Spill Dispersant Effectiveness Testing in OHMSETT february - march 2006.

Fingas, M., Fieldhouse, B., 2004. Formation of water-in-oil emulsions and application to oil spill modelling. J. Hazard. Mater. doi:10.1016/j.jhazmat.2003.11.008

Fingas, M.F., Kyle, D., Tennyson., E., 1995. Dispersant effectiveness: Studies into the causes of effectiveness variations, in: The Use of Chemicals in Oil Spill Response, ASTM STP 1252. American Society for Testing and Materials, Philadelphia, Pennsylvania, pp. 92–132.

Fiocco, R., Daling, P.S., DeMarco, G., Lessard, R.R., Canevari, G.P., 1999. Chemical dispersibility of heavy Bunker Fuel oilChemical dispersibility of heavy Bunker Fuel oil, in: Arctic and Marine Oilspill Program (AMOP). Calgary, Alberta, Canada, pp. 173–186.

Fisher, R.A., 1936. The use of Multiple Measurements in Taxonomic Problems. Ann. Eugen. 7, 179–188. doi:10.1111/j.1469-1809.1936.tb02137.x

French McCay, D.P., Mueller, C., Jayko, K., Longval, B., Schroeder, M., Terrill, E., Carter, M., Otero, M., Kim, S.Y., Payne, J.R., Nordhausen, W., Lampinen, M., Ohlmann, C., 2007. Evaluation of Field-Collected Data Measuring Fluorescien Dye Movements and Dispersion for Dispersed Oil Transport Modeling, in: Arctic and Marine Oilspill Program (AMOP). Emergencies Science Division, Environment Canada, Ottawa (ON), pp. 713–754.

French-McCay, D.P., 2004. Oil Spill Impact Modeling: Development and Validation. Environ. Toxicol. Chem. 23, 2441–2456. doi:10.1897/03-382

French-McCay, D.P., Payne, J.R., 2001. Model of oil fate and water concentrations with and without application of dispersants, in: Arctic and Marine Oilspill Program (AMOP). Environment Canada, Edmonton, Alberta, Canada, pp. 611–645.

Galt, J.A., 2014. Oil Weathering Technical Documentation and Recommended Use Strategies, Response Options Calculator (ROC).

Galt, J.A.A., Overstreet, R., 2009. Development of Spreading Algorithms for the ROC, Response Options Calculator (ROC).

Gemmrich, J., 2009. BREAKING WAVES AND NEAR-SURFACE TURBULENCE 431–438.

Genwest Systems, n.d. Response Options Calculator (ROC) - Technical documentation.

Gómez Ledesma, R., 2004. An experimental investigation on the air entrainment by

plunging jets.

Gopalan, B., Katz, J., 2010. Turbulent Shearing of Crude Oil Mixed with Dispersants Generates Long Microthreads and Microdroplets. Phys. Rev. Lett. 104, 54501. doi:10.1103/PhysRevLett.104.054501

Gros, J., Nabi, D., Würz, B., Wick, L.Y., Brussaard, C.P.D., Huisman, J., van der Meer, J.R., Reddy, C.M., Arey, J.S., 2014. First day of an oil spill on the open sea: early mass transfers of hydrocarbons to air and water. Environ. Sci. Technol. 48, 9400–11. doi:10.1021/es502437e

Guyomarch, J., Merlin, F.X., Colin, S., 1999. Study of the feasibility chemical dispersion of viscous oils and water-in-oil emulsions, in: Arctic and Marine Oilspill Program (AMOP). Calgary, Alberta, Canada, pp. 219–230.

Hénaff, M. Le, Kourafalou, V., Paris, C.B., Helgers, J., Aman, Z.M., Hogan, P.J., Srinivasan, A., 2012. Surface evolution of the Deepwater Horizon oil spill patch: combined effects of circulation and wind-induced drift. Environ. Sci. Technol. 46, 7267–7273.

Holder, E.L., Conmy, R.N., Venosa, A.D., 2015. Comparative Laboratory-Scale Testing of Dispersant Effectiveness of 23 Crude Oils Using Four Different Testing Protocols*. J. Environ. Prot. (Irvine,. Calif). 6, 628–639. doi:10.4236/jep.2015.66057

Hollebone, B., 2011. Measurement of Oil Physical Properties, in: Fingas, M. (Ed.), Oil Spill Science and Technology. Elsevier, pp. 63–85. doi:10.1016/B978-1-85617-943-0.10004-8

IPIECA, 2010. Choosing Spill Response Options To Minimize Damage - Net Environmental Benefit Analysis.

IPIECA, IOGP, 2015. Dispersants : surface application.

ITOPF, 2012. Use of dispersants to treat oil spills, in: Technical Information Papers.

Janssen, J.M.H., 1993. Droplet breakup mechanisms: Stepwise equilibrium versus transient dispersion. J. Rheol. (N. Y. N. Y). 37, 597. doi:10.1122/1.550385

Johansen, O., Brandvik, P.J., Farooq, U., 2013. Droplet breakup in subsea oil releases - Part 2: Predictions of droplet size distributions with and without injection of chemical dispersants. Mar. Pollut. Bull. 73, 327–35. doi:10.1016/j.marpolbul.2013.04.012

Johansen, Ø., Reed, M., Bodsberg, N.R., 2015. Natural dispersion revisited. Mar. Pollut. Bull. 93, 20–26. doi:10.1016/j.marpolbul.2015.02.026

Jongbloed, R.H., Tamis, J.E., Holthaus, K.I.E., Veen, D.P.C. van der, Velde, I. van der, Blankendaal, V.G., Goedhart, P.C., Jak, R.G., Koops, W., 2002a. TNO MEP 2002, Chemicals in combating oil spills. A literature review in perspective of the Dutch situation. Apeldoorn.

Jongbloed, R.H., Tamis, J.E., Holthaus, K.I.E., Veen, D.P.C. van der, Velde, I. van der, Blankendaal, V.G., Goedhart, P.C., Jak, R.G., Koops, W., 2002b. Chemicals In Combating Oil Spills a literature review in perspective of the Dutch Situation.

Katz, J., 2009. Measurements and Modeling of Size Distributions, Settling and Dispersions (turbulent diffusion) Rates.

Khelifa, A., Fingas, M., Brown, C., 2008. Effects of Dispersants on Oil-SPM Aggregation and Fate in US Coastal Waters.

Khelifa, A., Fingas, M., Hollebone, B.P., Brown, C.E., Pjontek, D., 2007. Effects of Chemical Dispersants on Oil Physical Properties and Dispersion, in: Arctic and Marine Oilspill Program (AMOP). Edmonton Alberta Canada, pp. 105–116.

Khelifa, A., So, L.L.C.L., 2009. Effects of Chemical Dispersants on Oil Brine Interfacial Tension and Droplet Formation, in: AMOP Technical Seminar on Environmental Contamination and Response. Ottawa (ON), pp. 383–396.

Kiger, K.T., Duncan, J.H., 2012. Air-Entrainment Mechanisms in Plunging Jets and Breaking Waves. Annu. Rev. Fluid Mech. doi:10.1146/annurev-fluid-122109-160724

Kingston, P., 1999. Recovery of the Marine Environment Following the Braer Spill, Shetland. Int. Oil Spill Conf. Proc. 1999, 103–109. doi:10.7901/2169-3358-1999-1-103

Kleindienst, S., Seidel, M., Ziervogel, K., Grim, S., Loftis, K., Harrison, S., Malkin, S.Y., Perkins, M.J., Field, J., Sogin, M.L., Dittmar, T., Passow, U., Medeiros, P., Joye, S.B., 2016. Reply to Prince et al.: Ability of chemical dispersants to reduce oil spill impacts remains unclear. Proc. Natl. Acad. Sci. 201600498. doi:10.1073/pnas.1600498113

Kleiss, J.M., Melville, W.K., 2011. The Analysis of Sea Surface Imagery for Whitecap Kinematics. J. Atmos. Ocean. Technol. 28, 219–243. doi:10.1175/2010JTECHO744.1

Law, R.J., 2011. The Torrey Canyon Oil Spill, 1967, in: Fingas, M. (Ed.), Oil Spill Science and Technology. Elsevier, pp. 1103–1106. doi:10.1016/B978-1-85617-943-0.10033-4

Lee, K., Boufadel, M., Chen, B., Foght, J., Hodson, P., Swanson, S., Venosa, A., 2015. Expert Panel Report on the Behaviour and Environmental Impacts of Crude Oil Released into Aqueous Environments.

Lee, K., Li, Z., Venosa, A.D., Boufadel, M.C., Miles, S.M., 2009. Wave Tank Studies on Dispersant Effectiveness as a Function of Energy Dissipation Rate and Particle Size Distribution.

Lee, K., Nedwed, T., Prince, R.C., Palandro, D., 2013. Lab tests on the biodegradation of chemically dispersed oil should consider the rapid dilution that occurs at sea. Mar. Pollut. Bull. 73, 314–318. doi:10.1016/j.marpolbul.2013.06.005

Lehr, W., Jones, R., Evans, M., Simecek-Beatty, D., Overstreet, R., 2002. Revisions of the ADIOS oil spill model. Environ. Model. Softw. 17, 189–197. doi:10.1016/S1364-8152(01)00064-0

Lehr, W.J., Cekirge, H.M., Fraga, R.J., Belen, M.S., 1984. Empirical studies of the spreading of oil spills. Oil Petrochemical Pollut. 2, 7–11. doi:10.1016/S0143-7127(84)90637-9

Lehr, W.J.W., Simecek-beatty, D., 2000. The relation of Langmuir circulation processes to the standard oil spill spreading, dispersion, and transport algorithms. Spill Sci. Technol. Bull. 6, 247–253. doi:10.1016/S1353-2561(01)00043-3

Leirvik, F., Almas, K., Per S. Daling, 2012. Laboratory Study of the dispersibility of DWH surface emulsions.

Lewis, A., 2007. The application of dispersants on oil in the North Sea. Rijswijk.

Lewis, A., Crosbie, A., Davies, L., Lunel, T., 1998. Dispersion of Emulsified Oil at Sea.

Lewis, A., Daling, P., 2001. Oil Spill Dispersants.

Lewis, A., Daling, P.S., 2007. Oil in Ice - JIP.

Lewis, A., Daling, P.S., Strøm-Kristiansen, T., Nordvik, A.B., Fiocco, R.J., 1995. WEATHERING AND CHEMICAL DISPERSION OF OIL AT SEA. Int. Oil Spill Conf. Proc. 1995, 157–164. doi:10.7901/2169-3358-1995-1-157

Lewis, A., Merlin, F.X., Daling, P., Reed, M., 2006. Applicability of Oil Spill Dispersants, Part I: Overview.

Lewis, A., Trudel, B.K., Belore, R., Mullin, J., 2010. Large-scale dispersant leaching and effectiveness experiments with oils on calm water. Mar. Pollut. Bull. 60, 244–254. doi:10.1016/j.marpolbul.2009.09.019

Li, M., Garrett, C., 1998. The relationship between oil droplet size and upper ocean turbulence. Mar. Pollut. Bull. 36, 961–970. doi:10.1016/S0025-326X(98)00096-4

Li, Z., Kepkay, P., Lee, K., King, T., Boufadel, M.C., Venosa, A.D., 2007. Effects of chemical dispersants and mineral fines on crude oil dispersion in a wave tank under breaking waves. Mar. Pollut. Bull. 54, 983–993. doi:10.1016/j.marpolbul.2007.02.012

Li, Z., Lee, K., Kepkey, P.E., Mikkelsen, O., Pottsmith, C., 2011a. Monitoring Dispersed Oil Droplet Size Distribution at the Gulf of Mexico Deepwater Horizon Spill Site. Int. Oil Spill Conf. Proc. 2011, abs377. doi:10.7901/2169-3358-2011-1-377

Li, Z., Lee, K., King, T., Boufadel, M.C., Venosa, A.D., 2008. Assessment of chemical dispersant effectiveness in a wave tank under regular non-breaking and breaking wave conditions. Mar. Pollut. Bull. 56, 903–912. doi:10.1016/j.marpolbul.2008.01.031

Li, Z., Lee, K., King, T., Boufadel, M.C., Venosa, A.D., 2009a. Evaluating crude oil chemical dispersion efficacy in a flow-through wave tank under regular non-breaking wave and breaking wave conditions. Mar. Pollut. Bull. 58, 735–44. doi:10.1016/j.marpolbul.2008.12.014

Li, Z., Lee, K., King, T., Boufadel, M.C., Venosa, A.D., 2009b. Evaluating Chemical Dispersant Efficacy in an Experimental Wave Tank: 2—Significant Factors Determining In Situ Oil Droplet Size Distribution. Environ. Eng. Sci. 26, 1407–1418. doi:10.1089/ees.2008.0408

Li, Z., Lee, K., King, T., Boufadel, M.C., Venosa, A.D., 2010. Effects of temperature and wave conditions on chemical dispersion efficacy of heavy fuel oil in an experimental flow-through wave tank. Mar. Pollut. Bull. 60, 1550–1559. doi:10.1016/j.marpolbul.2010.04.012

Li, Z., Lee, K., King, T., Kepkay, P., Boufadel, M.C., Venosa, A.D., 2009c. Evaluating Chemical Dispersant Efficacy in an Experimental Wave Tank: 1, Dispersant Effectiveness as a Function of Energy Dissipation Rate. Environ. Eng. Sci. 26, 1139–1148. doi:10.1089/ees.2008.0377

Li, Z., Lee, K., King, T., Niu, H., Boufadel, M.C., Venosa, A.D., 2011b. Application of entropy analysis of in situ droplet-size spectra in evaluation of oil chemical dispersion efficacy. Mar. Pollut. Bull. 62, 2129–2136.

Lunel, T., 1993. Dispersion: Oil droplet size measurements at sea. Int. Oil Spill Conf. Proc. 1993, 794–795. doi:10.7901/2169-3358-1993-1-794

Lunel, T., 1995. Understanding the mechanism of dispersion through oil droplet size measurements at sea, The Use of Chemicals in Oil Spill Response, ASTM STP 1252. Philadelphia, Pennsylvania.

McKeogh, E.J., Ervine, D.A., 1981. Air Entrainment Rate and Diffusion Pattern of Plunging Liquid Jets. Chem. Eng. Sci. 36, 1161–1172.

Merlin, F., Nanteuil, E. de, Guyomarch, J., 2006. Sea trials on chemical dispersion - depol 04, in: Interspill. Cedre, Brest, France, London.

Merlin, F.-X. (Cedre), Peigné, G. (Cedre), 2007. Use of Dispersants- State of Art.

Ming, L., Garrett, C., Li, M., Garrett, C., 1993. Cell merging and the jet/downwelling ratio in Langmuir circulation. J. Mar. Res. 51, 737–769. doi:10.1357/0022240933223945

Monahan, E.C., 1971. Oceanic Whitecaps. J. Phys. Oceanogr. 1, 139–144. doi:10.1175/1520-0485(1971)001<0139:OW>2.0.CO;2

Monahan, E.C., Callaghan, A.H., 2015. The Discrete Whitecap Method for Estimating Sea Salt Aerosol Generation: A Reassessment, in: 17th Conference on Atmospheric Chemistry.

Monahan, E.C., Woolf, D.K., 1989. Comments on "Variations of Whitecap Coverage with Wind stress and Water Temperature. J. Phys. Oceanogr. 19, 706–709. doi:10.1175/1520-0485(1989)019<0706:COOWCW>2.0.CO;2

Moum, J.N.N., Smyth, W.D.D., 1994. Upper Ocean Mixing Processes. Encycl. Ocean Sci. 3093–3100. doi:10.1006/rwos.2001.0156

Mukherjee, B., 2008. EFFECT OF MIXING ENERGY, MIXING TIME AND SETTLING TIME ON DISPERSION EFFECTIVENESS IN TWO BENCH-SCALE TESTING SYSTEMS. Int. Oil

Spill Conf. Proc. 2008, 651–656. doi:10.7901/2169-3358-2008-1-651

Mukherjee, B., Turner, J., Wrenn, B. a., 2011. Effect of Oil Composition on Chemical Dispersion of Crude Oil. Environ. Eng. Sci. 28, 497–506. doi:10.1089/ees.2010.0226

Mukherjee, B., Wrenn, B.A., 2009. Influence of Dynamic Mixing Energy on Dispersant Performance: Role of Mixing Systems. Environ. Eng. Sci. 26, 1725–1737. doi:10.1089/ees.2009.0159

Mukherjee, B., Wrenn, B.A., Ramachandran, P., 2012. Relationship between size of oil droplet generated during chemical dispersion of crude oil and energy dissipation rate: Dimensionless, scaling, and experimental analysis. Chem. Eng. Sci. 68, 432–442. doi:10.1016/j.ces.2011.10.001

Mukherjee, B., Wrenn, B. a., 2011. Effects of Physical Properties and Dispersion Conditions on the Chemical Dispersion of Crude Oil. Environ. Eng. Sci. 28, 263–273. doi:10.1089/ees.2010.0131

Nalco, 2011. COREXIT ingredients [WWW Document]. URL http://www.nalcoesllc.com/nes/1602.htm

National Research Council, 2005a. Making Decisions about Dispersant Use, in: Understanding Oil Spill Dispersants: Efficacy and Effects. pp. 21–50.

National Research Council, 2005b. Dispersant-Oil Interactions and Effectiveness Testing, in: Understanding Oil Spill Dispersants: Efficacy and Effects. pp. 51–133.

National Research Council of the National Academies, 2005. Understanding Oil Spill Dispersants : Efficacy and Effects. National Academies Press, Washington, D.C.

Nazir, M., Khan, F., Amyotte, P., Sadiq, R., 2008. Multimedia fate of oil spills in a marine environment—An integrated modelling approach. Process Saf. Environ. … 86, 141–148. doi:10.1016/j.psep.2007.10.002

Nedwed, T., Coolbaugh, T., 2008. DO BASINS AND BEAKERS NEGATIVELY BIAS DISPERSANT-EFFECTIVENESS TESTS? Int. Oil Spill Conf. Proc. 2008, 835–841. doi:10.7901/2169-3358-2008-1-835

Nedwed, T., Resby, J., Guyomarch, J., 2006. Dispersant Effectiveness after Extended Low-energy Soak Times, in: Interspill.

Nedwed, T.J., 2012. Dispersion of Oil Using Artificially Generated Waves. US20120285898 A1.

NHL University of Applied Sciences, n.d. VisionLab Course [WWW Document]. URL http://www.nhl.nl/werkenstudie/3333/computer-vision/studieopbouw/inhoud-studie

NHL University of Appliedd Sciences, 2013. VisionLab.

NOAA/HAZMAT, 2000. ADIOS version 2.0.1, help files.

O'Sullivan, A.J., Jacques, T.G., 2001. Impact reference system: Effects of Oil in the Marine Environment: Impact of Hydrocarbons on Fauna and Flora.

Owens, E.H., 2011. Shoreline Countermeasures, in: Fingas, M. (Ed.), Oil Spill Science and Technology. Elsevier, pp. 907–921. doi:10.1016/B978-1-85617-943-0.10024-3

Paris, C.B., Hénaff, M. Le, Aman, Z.M., Subramaniam, A., Helgers, J., Wang, D.-P., Kourafalou, V.H., Srinivasan, A., Le, M., 2012. Evolution of the Macondo Well Blowout: Simulating the Effects of the Circulation and Synthetic Dispersants on the Subsea Oil Transport. Environ. Sci. Technol. 46, 13293–302. doi:10.1021/es303197h

Payne, J.R., Deborah, I., Mueller, C., Jayko, K., Longval, B., Schroeder, M., Terrill, E., Carter, M., Otero, M., Kim, S.Y., Middleton, W., Chen, A., Lewis, R., Lampinen, M., Evans, T., 2009. Evaluation of Field-Collected Drifter and In Situ Fluorescence Data Measuring Subsurface Dye Plume Advection / Dispersion and Comparisons to High-Frequency Radar-Observation System Data for Dispersed Oil Transport Modelling.

Pelz, O., Brown, J., Huddleston, M., Rand, G., Gardinali, P., Stubblefield, W., BenKinney, M.T., Ahnell, A., 2011. Selection of a Surrogate MC252 Oil as a Reference Material for Future Aquatic Toxicity Tests and Other Studies, in: SETAC Meeting. Boston.

Phillips, O.M., 1985. Spectral and statistical properties of the equilibrium range in wind-generated gravity waves. J. Fluid Mech. 156, 505. doi:10.1017/S0022112085002221

Prince, R.C., 2015. Oil Spill Dispersants: Boon or Bane? Environ. Sci. Technol. 49, 6376–6384. doi:10.1021/acs.est.5b00961

Rahsepar, S., Smit, M.P.J., Murk, A.J., Rijnaarts, H.H.M., Langenhoff, A.A.M., 2016. Chemical dispersants: Oil biodegradation friend or foe? Mar. Pollut. Bull. 108, 113–119. doi:10.1016/j.marpolbul.2016.04.044

Ramachandran, S.D., Hodson, P. V, Khan, C.W., Lee, K., 2004. Oil dispersant increases PAH uptake by fish exposed to crude oil. Ecotoxicol. Environ. Saf. 59, 300–308. doi:10.1016/j.ecoenv.2003.08.018

Redman, A.D., Parkerton, T.F., 2015. Guidance for improving comparability and relevance of oil toxicity tests. Mar. Pollut. Bull. doi:10.1016/j.marpolbul.2015.06.053

Reed, M., Aamo, O.M., Brandvik, P.J., Daling, P.S., Nilsen, P.E., Furnes, G., 1997. DEVELOPMENT OF A DISPERSANT USE PLAN FOR A COASTAL OIL TERMINAL. Int. Oil Spill Conf. Proc. 1997, 643–653. doi:10.7901/2169-3358-1997-1-643

Reed, M., Aamo, O.M., Daling, P.S., 1995. Quantitative Analysis of Alternate Oil Spill Response Strategies using OSCAR. Spill Sci. Technol. Bull. 2, 67–74. doi:10.1016/1353-2561(95)00020-5

Reed, M., Daling, P., Lewis, A., Ditlevsen, M.K., Brørs, B., Clark, J., Aurand, D., 2004. Modelling of dispersant application to oil spills in shallow coastal waters. Environ. Model. Softw. 19, 681–690. doi:10.1016/j.envsoft.2003.08.014

Reed, M., Johansen, Ø., Brandvik, P.J., Daling, P., Lewis, A., Fiocco, R., Mackay, D., Prentki, R., 1999. Oil Spill Modeling towards the Close of the 20th Century: Overview of the State of the Art. Spill Sci. Technol. Bull. 5, 3–16. doi:10.1016/S1353-2561(98)00029-2

Reed, M., Leirvik, F., Johansen, Ø., Brørs, B., 2009. Numerical Algorithm to Compute the Effects of Breaking Waves on Surface Oil Spilled at Sea. Trondheim.

Reed, M., Rye, H., 1995. A THREE-DIMENSIONAL OIL AND CHEMICAL SPILL MODEL FOR ENVIRONMENTAL IMPACT ASSESSMENT. Int. Oil Spill Conf. Proc. 1995, 61–66. doi:10.7901/2169-3358-1995-1-61

Reed, M., Turner, C., Odulo, A., 1994. The role of wind and emulsification in modelling oil spill and surface drifter trajectories. Spill Sci. Technol. Bull. 1, 143–157. doi:10.1016/1353-2561(94)90022-1

REMPEC, 2011. part II: Basic information on dispersants and their application, in: Guidelines for the Use of Dispersants for Combating Oil Pollution at Sea in the Mediterranean Region.

Resby, J., Brandvik, P., Daling, P., 2007. Effects of Time on the Effectiveness of Dispersants.

Riehm, D. a., McCormick, A. V., 2014. The role of dispersants' dynamic interfacial tension in effective crude oil spill dispersion. Mar. Pollut. Bull. 84, 155–163. doi:10.1016/j.marpolbul.2014.05.018

Rijkswaterstaat, 2011. Beslisboom gebruik detergenten op olieverontreinigingen in het Nederlandse deel van de Noordzee.

Rijkswaterstaat Noordzee, 2014. Incidentbestrijdingsplan Noordzee.

Robbins, M.L., Varadaraj, R., Bock, J., Pace, S.J., 1995. EFFECT OF STOKES' LAW SETTLING ON MEASURING OIL DISPERSION EFFECTIVENESS. Int. Oil Spill Conf. Proc. 1995, 191–196. doi:10.7901/2169-3358-1995-1-191

Rogers, J., Beynet, P.A., 2013. Systems and methods for mechanical hydrocarbon dispersion. US20130161022 A1.

Roy, A.K., Maiti, B., Das, P.K., 2013. Visualisation of Air Entrainment by a Plunging Jet. Procedia Eng. 56, 468–473. doi:10.1016/j.proeng.2013.03.148

Salisbury, D.J., Anguelova, M.D., Brooks, I.M., 2013. On the variability of whitecap fraction using satellite-based observations. J. Geophys. Res. Ocean. 118, 6201–6222. doi:10.1002/2013JC008797

Salisbury, D.J., Anguelova, M.D., Brooks, I.M., 2014. Global distribution and seasonal dependence of satellite-based whitecap fraction. Geophys. Res. Lett. 41, 1616–1623. doi:10.1002/2014GL059246

Shigenaka, G., 2011. Effects of Oil in the Environment, in: Fingas, M. (Ed.), Oil Spill Science and Technology. Elsevier, pp. 985–1024. doi:10.1016/B978-1-85617-943-0.10027-9

Singsaas, I., Lewis, A., 2011. Behaviour of oil and other hazardous and noxious substances (HNS) spilled in Arctic waters (BoHaSA). Emergency Prevention Preparedness and Response (EPPR) working group.

SL Ross Environmental Research LTD, A. Lewis Oil Spill Consultancy, MAR Incorporated, 2005. Dispersant effectiveness testing: Relating results from ohmsett to at-sea tests.

SL Ross Environmental Research LTD, A. Lewis Oil Spill Consultancy, MAR Incorporated, 2006a. Chemical Dispersibility of U.S. Outer Continental Shelf Crude Oils in Non-Breaking Waves.

SL Ross Environmental Research LTD, A. Lewis Oil Spill Consultancy, MAR Incorporated, 2006b. Calm Sea Application of Dispersants.

SL Ross Environmental Research LTD, A. Lewis Oil Spill Consultancy, MAR Incorporated, 2007. Changes in Dispersant Effectiveness with Extended Exposure in Calm Seas.

SL Ross Environmental Research LTD, MAR Incorporated, 2011. Comparison of Large-Scale (Ohmsett) and Small-Scale Dispersant Effectiveness Test Results.

SL Ross Environmental Research, MAR Incorporated, 2009. Low-Dose Repeat-Application Dispersant Testing.

SL Ross Environmental Research, MAR Incorporated, 2010. Dispersant effectiveness testing on viscous, U.S. Outer continental shelf crude oils: Phase III.

Socolofsky, S. a., Adams, E.E., Boufadel, M.C., Aman, Z.M., Johansen, Ø., Konkel, W.J., Lindo, D., Madsen, M.N., North, E.W., Paris, C.B., Rasmussen, D., Reed, M., Rønningen, P., Sim, L.H., Uhrenholdt, T., Anderson, K.G., Cooper, C., Nedwed, T.J., 2015. Intercomparison of oil spill prediction models for accidental blowout scenarios with and without subsea chemical dispersant injection. Mar. Pollut. Bull. 96, 110–126. doi:10.1016/j.marpolbul.2015.05.039

Sorial, G.A., 2006. Laboratory Testing to Determine Dispersion Predictability of the Baffled Flask Test (BFT) and Swirling Flask Test (SFT).

Sørstrøm, S., Brandvik, P.J.P., Buist, I., Daling, P., Dickins, D., Faksness, L., Potter, S., Rasmussen, J.F., Singsaas, I., 2010. Joint Industry program on oil spill contingency for Arctic and ice-covered waters - Summary report.

Sterling, M., Bonner, J., Ernest, A., 2004. Chemical dispersant effectiveness testing: influence of droplet coalescence. Mar. Pollut. Bull. 48, 969–977. doi:10.1016/j.marpolbul.2003.12.003

Tamis, J.E., Jongbloed, R.H., Karman, C.C., Koops, W., Murk, A.J., 2012. Rational application of chemicals in response to oil spills may reduce environmental damage. Integr. Environ. Assess. Manag. 8, 231–241. doi:10.1002/ieam.273

Trudel, K., Belore, R., MAR Incorporated, 2005. Correlation of Ohmsett Dispersant Tests

With At-Sea Trials: Supplemental Tests.

Trudel, K., Belore, R.C., Mullin, J. V., Guarino, A., 2010. Oil viscosity limitation on dispersibility of crude oil under simulated at-sea conditions in a large wave tank. Mar. Pollut. Bull. 60, 1606–1614. doi:10.1016/j.marpolbul.2010.01.010

van Eenennaam, J.S., Wei, Y., Grolle, K.C.F., Foekema, E.M., Murk, A.J., 2016. Oil spill dispersants induce formation of marine snow by phytoplankton-associated bacteria. Mar. Pollut. Bull. 104, 294–302. doi:10.1016/j.marpolbul.2016.01.005

Venosa, A.D., King, D.W., Sorial, G. a, 2002. The Baffled Flask Test for Dispersant Effectiveness: A Round Robin Evaluation of Reproducibility and Repeatability. Spill Sci. Technol. Bull. 7, 299–308. doi:10.1016/S1353-2561(02)00072-5

Venosa, a. D., Lee, K., Boufadel, M., Li, Z., Wickley-Olsen, E., King, T., 2008. DISPERSANT EFFECTIVENESS AS A FUNCTION OF ENERGY DISSIPATION RATE IN AN EXPERIMENTAL WAVE TANK. Int. Oil Spill Conf. Proc. 2008, 777–783. doi:10.7901/2169-3358-2008-1-777

Vonk, S.M., Hollander, D.J., Murk, A.J., 2015. Was the extreme and wide-spread marine oil-snow sedimentation and flocculent accumulation (MOSSFA) event during the Deepwater Horizon blow-out unique? Mar. Pollut. Bull. doi:10.1016/j.marpolbul.2015.08.023

Walstra, P., 1993. Principles of Emulsion formation. Chem. Eng. Sci. 48, 333–349.

Walstra, P., 2005. 8 Emulsions, in: Lyklema, J. (Ed.), Fundamentals of Interface and Colloid Science. Elsevier, pp. 1–94.

Wang, W., Zheng, Y., Li, Z., Lee, K., 2011. PIV investigation of oil–mineral interaction for an oil spill application. Chem. Eng. J. 170, 241–249. doi:10.1016/j.cej.2011.03.062

Wang, Z., Hollebone, B.P., Fingas, M., Fieldhouse, B., Sigouin, L., Landriault, M., Smith, P., Noonan, J., Thouin, G., Weaver, J.W., 2003. Characteristics of spilled oils, fuels, and petroleum products: 1. Composition and properties of selected oils. USEPA Publ. EPA/600/R-, 1–286.

Wissenschaft, 2016. The use of dispersants to combat oil spills in Germany at sea. Federal Institute for Risk Assessment.

Wrenn, B.A., Virkus, A., Mukherjee, B., Venosa, A.D., 2009. Dispersibility of crude oil in fresh water. Environ. Pollut. 157, 1807–14. doi:10.1016/j.envpol.2009.01.025

Zeinstra-Helfrich, M., Koops, W., Dijkstra, K., Murk, A.J., 2015a. Quantification of the effect of oil layer thickness on entrainment of surface oil. Mar. Pollut. Bull. 96, 401–409. doi:10.1016/j.marpolbul.2015.04.015

Zeinstra-Helfrich, M., Koops, W., Dijkstra, K., Murk, A.J., 2015b. Supporting Information - Image Analysis Process performed on Plunging Jet Test Pictures.

Zeinstra-Helfrich, M., Koops, W., Murk, A.J., 2015c. The NET effect of dispersants — a critical review of testing and modelling of surface oil dispersion. Mar. Pollut. Bull. 100, 102–111. doi:10.1016/j.marpolbul.2015.09.022

Zeinstra-Helfrich, M., Koops, W., Murk, A.J., 2016. How oil properties and layer thickness determine the entrainment of spilled surface oil. Mar. Pollut. Bull. doi:10.1016/j.marpolbul.2016.06.063

Summary

Application of chemical dispersants on surface oil is a trade-off between surface effects (impact of floating oil) and sub-surface effects (impact of suspended oil). Making an informed decision regarding such response, requires insight in the induced changes in fate and adverse effects of the oil.
This thesis aims to provide a better understanding on the NET effectiveness of dispersant application on surface oil fate, based on a better mechanistic understanding of the dispersion process.

In **chapter 2**, a conceptual dispersion model is defined, and used as a basis to review the abundance of literature of dispersion testing. Steps distinguished in the general dispersion process as depicted in Fig. 2-1, are: 1) Entrainment of oil into the water column by (breaking) waves, 2) breakup of the oil into droplets, 3) vertical distribution of the droplets by the downward wave impact and 4) subsequent buoyant rise of the oil droplets. These processes determine the volume of oil suspended and the individual droplet's residence time (dispersability). The difference in horizontal velocity between the suspended droplets and the floating slick (subject to wind driven transport) causes part of those resurfacing droplets to resurface upwind of the original slick, forming a comet-like tail to the slick.
The commonly mentioned key variables in oil spill dispersion were found to have different effects on different sub-processes, which might explain why dispersion effectiveness can not be related to the variables directly. More energetic wave conditions (as a result of higher wind speed) cause more potential for entrainment by breaking waves, break up the oil into smaller droplets and propell these droplets deeper into the water column. High oil viscosity can counteract entrainment and resist breakup, as well as hinder dispersant incorporation.
Chemical dispersion follows these exact same steps, yet with oil properties altered to be more susceptible to dispersion because of reduced interfacial tension. For this to occur, the dispersants have to be successfully applied (and transferred to the oil-water-interface), as well as be able to influence the oil properties. The latter is not possible with very viscous (e.g. cold) oils.
For most of the distinguished processes information is available or can be deduced from existing test data. This was not the case for the entrainment of oil. As this has hardly been investigated separately, and apparently was insufficiently understood, this was studied further in this thesis with the focus on the role of oil layer height, oil core qualities and droplet size distribution.

A plunging jet test was developed (**chapter 3**), in order to investigate the entrainment process under simulated breaking waves. In this system (Fig. 3-1), an oil layer with predefined thickness and known properties can be subjected to impact by a falling body of water. The design of the test system allowed camera

and lighting arrangements to be installed around the test tank, recording the events under water. Subsequent image analysis was performed to yield the volume of oil droplets in the water column and the size of each droplet. Using this set-up the importance of oil layer thickness on the dispersion process was proven; the entrained volume was proportional to oil layer thickness. Although the mean droplet size slightly increased with layer thickness, the overall volume in small droplets also increased with layer thickness.

The influence of oil type and presence of dispersants on the entrainment process was investigated using this same plunging jet set-up (**chapter 4**). For these tests a range of 7 different oil qualities was created from 2 initial oil types, by making mixtures and evaporative weathering of the oils. Oil entrainment was largely unaffected by oil properties, even adding a 1:200 dose of dispersants did not significantly influence entrainment. However, entrainment of oil above a plunging-energy dependend viscosity threshold was very limited.
The droplet sizes formed in our experiments matched an existing function of Weber and Reynolds number for mean droplet diameter. The research revealed that mass median droplet size can be estimated using layer thickness, plunge height, oil viscosity and interfacial tension. Another observation was the formation of long thin filaments instead of spherical droplets with very viscous oils. These filaments are an indication that viscosity is much more dominant in the entrainment process than interfacial stress, so dispersants are not expected to have effects on dispersion of such oils.

The revealed importance of layer thickness and the droplet size equation were incorporated in a model (**chapter 5**) to be able to investigate how surface slick transport and elongation by wind are affected by the entrainment and resurfacing of oil. The mass in the slick and slick appearance over time were investigated for 18 different oil/weather combinations. Slick behaviour found to follow 2 distinct regimes: In conditions unfavourable for dispersion, the slick retains a downwind thick patch trailed by a long comet-like tail that is formed by the resurfacing of suspended droplets. In optimal conditions for dispersion, most of the oil mass is continuous moved to the water column. The resulting surface oil slick is only a temporary expression of the underwater oil mass, is much smaller than the unfavourable case and symmetrical in thickness in the wind direction.
Oil type had surprisingly little influence on the oil slick elongation because the effect of high viscosity causing larger droplets is partly counteracted by the larger density of the droplets, yielding small difference in refloat time with less viscous oils. In contrast, the influence of wind speed was very dominant. An overall dispersibility factor (DF) was defined from which the dispersion of oil under specific conditions can be determined. From the DF the following four

output parameters after 24 hours can be assessed: 1) mass of oil in the slick, 2) slick length, 3) effective wind drift factor and 4) lifetime of the oil coloured (thick) slick part. The DF can be quickly calculated from the following input conditions: Wind speed, oil layer thickness and oil properties (viscosity, density and interfacial tension).

Based on the model outcomes it can be determined under what conditions dispersant application is useful, the conditions where natural dispersion is not yet optimal. The NET effect of dispersants is larger on low viscosity oil than on high viscosity oil. Although the model can be further refined, application of this model can already prevent superfluous application of dispersants.

Nederlandse samenvatting
(speciaal voor niet-ingewijden)

Een olievlek die op het wateroppervlak ligt kan vanzelf verdwijnen door een proces dat natuurlijke dispersie wordt genoemd. Als oliebestrijdingstechniek kan er dispergeermiddel op de olievlek aangebracht worden (chemische dispersie). Het dispergeermiddel zou het dispersieproces moeten versnellen.
Dispersie zorgt er niet voor dat de olie uit het milieu verdwijnt, maar verplaatst deze alleen (tijdelijk) naar de waterkolom. Het toepassen van chemische dispersie is dus een afweging tussen (potentiële) effecten van de drijvende olievlek en (potentiële) effecten van de olie in de waterkolom. Bij een dergelijke afweging moet rekening worden gehouden met de hoeveelheid olie die op natuurlijke wijze zou dispergeren, en de hoeveelheid olie die door het dispergeermiddel extra 'verdwijnt' naar de waterkolom.
De inschatting of dispergeermiddelen zinvol zijn wordt in de huidige situatie gemaakt door een expert. Er bestaat een empirische berekening voor natuurlijke dispersie, maar voor chemische dispersie is er nog geen voorspelling. Het doel van dit proefschrift is om beter inzicht te bieden in het netto effect van dispergeermiddelen op de drijvende olievlek.

In **hoofdstuk 2** wordt beschreven in welke stappen het dispersieproces verloopt, en over welk van deze onderwerpen meer onderzoek nodig is. De stappen zijn (Fig 2-1):

- Door een verticale impact (een brekende golf die op de olielaag valt) wordt de olie op die plek onder water geduwd. We noemen dit in het Engels 'entrainment'.
- De energie die gepaard gaat met deze golf impact zorgt ervoor dat de ondergedompelde olie wordt opgebroken in druppels.
- Ook afhankelijk van de energie van de golf worden de gevormde druppels verdeeld over een bepaalde diepte onder het wateroppervlak.
- De gevormde oliedruppels zijn (bijna altijd) lichter dan water. Na de brekende golf zweven ze langzaam weer terug naar het wateroppervlak. Grotere druppels stijgen veel sneller op dan kleinere druppeltjes.

Deze 4 stappen samen bepalen hoeveel olie er naar de water kolom verplaatst wordt en hoe lang de individuele druppeltjes blijven zweven voordat ze weer boven zijn. Ondertussen verplaatst de drijvende vlek zich met de wind en de stroming, terwijl de druppeltjes in het water zich alleen met de stroming verplaatsen. Daardoor komen kleine olie druppels, die lang genoeg in de waterkolom blijven zweven, bovenwinds 'achter' de olievlek boven en vormen hier lange dunnere staart.
In dit proces zijn twee variabelen erg belangrijk: de windsnelheid en de olie-viscositeit. Een hogere windsnelheid zorgt ervoor dat er meer brekende golven zijn en er dus meer olie naar de waterkolom wordt verplaatst. Daarnaast neemt de golfhoogte toe met windsnelheid: door de hogere energie worden er kleinere oliedruppeltjes gevormd en worden ze over een grotere diepte verdeeld. Een

visceuze olie (hoge olie-viscositeit) betekend dat de olie erg dik (& stroperig) is. Bij gelijke energie vormt visceuze olie grotere druppels omdat de viscositeit het opbraakproces hindert.
Chemische dispersie volgt precies dezelfde stappen als natuurlijke dispersie, waarbij het dispergeermiddel ervoor zorgt dat de olie gemakkelijker in kleine druppels kan opbreken (omdat de grensvlakspanning is verlaagd). Dit gebeurt alleen als het dispergeermiddel goed op de olie vlek aangebracht is en niet daarnaast. Ook moet het middel in de olielaag worden opgenomen en hier een effect hebben op de olie-eigenschappen. Dit laatste is moeilijker bij olie met een hoge viscositeit.
Over de meeste van de genoemde processen kon voldoende informatie gevonden worden in de vakliteratuur. Over het onderdompelen van de olie (entrainment) was nog niet zoveel bekend, omdat het zelden afzonderlijk onderzocht wordt.

In **hoofdstuk 3** wordt een test methode omschreven, ontwikkeld om te onderzoeken hoe de olielaag (dikte en olie-eigenschappen) het entrainment-proces beïnvloedt. In deze plunging jet test (plonsopstelling, Fig. 3-1) wordt een specifieke hoeveelheid olie op zeewater gelegd, deze vormt een bepaalde laagdikte. De impact van een brekende golf wordt gesimuleerd door een hoeveelheid water bovenop het zee-water met de olielaag te laten vallen. De oliedruppels die hierdoor ontstaan onder water worden door gekoppelde camera-apparatuur vastgelegd. Met beeldanalyse kan vervolgens uit deze foto's worden vastgesteld hoeveel olie er onder water zit en hoe groot de verschillende individuele druppeltjes zijn.
Met deze testen kon het belang van de olielaagdikte in het dispersieproces vastgesteld worden: het volume olie dat ondergedompeld wordt is evenredig met de laagdikte. De gemiddelde druppelgrootte neemt iets toe met toenemende olielaagdikte (dikkere laag, grotere druppels). In totaal ontstaan er meer kleine druppels bij een dikke laag dan bij een dunne laag omdat er ook meer olie ondergedompeld wordt.

In dezelfde proefopstelling wordt in **hoofdstuk 4** de invloed van olietype en aanwezigheid van dispergeermiddelen onderzocht. Uit 2 types ruwe olie is een reeks van 7 verschillende olietypes gemaakt door ze te mengen in verschillende verhoudingen en ze te verwarmen tot de vluchtige componenten verdwenen zijn. Deze olietypen werden met en zonder dispergeermiddel getest.
De hoeveelheid olie die ondergedompeld wordt door de golf-impact blijft bijna altijd gelijk (zelfs als er dispergeermiddel is toegevoegd, in verhouding 1:200). Voor het meest visceuze olietype is het volume olie dat wordt ondergedompeld wel significant lager.

De gemiddelde druppelgroottes gemeten in de proefopstelling bleken overeen te komen met een eerder omschreven formule op basis van een soortgelijke test. Met deze formule kan de gemiddelde druppelgrootte voorspeld worden op basis van de olie-laagdikte, plons-hoogte, olieviscositeit en grensvlakspanning.

De gevonden relatie voor olie-druppel-grootte en het belang van laagdikte worden in **hoofdstuk 5** toegepast in een model dat de entrainment, het opstijgen van de verschillende olie-druppels en het transport van de olievlek berekend.
Voor 18 verschillende condities (olie & weersomstandigheden) is over een periode van 24 uur gekeken naar de dikte van de olievlek op het wateroppervlak. In het gedrag van de olievlek zijn twee verschillende situaties te onderscheiden:
Bij condities die zorgen voor weinig dispersie (weinig wind, visceuze olie) blijft de oorspronkelijke olievlek grotendeels in stand en vormt zich bovenwinds een lange staart die naar achteren toe steeds dunner wordt.
Bij condities heel geschikt voor dispersie (veel wind, laag visceuze olie) zien we dat de meeste olie in de waterkolom zit, omdat de druppels lang blijven zweven voordat ze bovenkomen. Boven deze gesuspendeerde olie is een kleinere olievlek zichtbaar, die symetrisch is in de windrichting. Deze vlek verplaatst zich nauwelijks met de wind.
Uit de modeluitkomsten blijkt dat het olietype maar een beperkte invloed heeft op het eindresultaat, maar dat de invloed van de windsnelheid erg dominant is. In dit hoofdstuk wordt ook de Dispersibility Factor gedefinieerd, die gemakkelijk kan worden berekend uit de relevante variabelen. De Dispersibility Factor geeft een goede indicatie van het te verwachten gedrag van de olievlek.

Op basis van de modeluitkomsten wordt duidelijk onder welke condities het toevoegen van dispergeermiddel het meest efficiënt is in het verkleinen van de olievlek op het oppervlak: dit is in geval van sub-optimale natuurlijke dispersie. Bij olie met een lage viscositeit is het effect van dispergeermiddel groter dan bij olie met een hoge viscositeit. Hoewel het model nog verder aangevuld moet worden met de overige processen (transport en verwering) die de olievlek beinvloeden, kan het model inzicht bieden in situaties waar chemische dispersie overbodig is (omdat het geen tot nauwlijks effect heeft op de grootte van de drijvende olievlek). In het voorkomen van negatieve (soms onverwachtte) effecten in de waterkolom is dit een belangrijke stap.

Dankwoord

Met het schrijven van dit hoofdstuk in mijn proefschrift, komt voor mij een einde aan een bijzondere periode. Zoals ongetwijfeld menig promovendus, ben ik deze uitdaging aangegaan zonder te bevatten wat dit allemaal voor mij ging betekenen. Ik heb de afgelopen jaren ervaren als een achtbaan van emoties en belevenissen waarin ik ontzettend veel heb geleerd: over gedrag van olie, over de wetenschap en over (de grenzen van) mezelf. En hoewel er maar één naam voor op dit proefschrift staat, zijn er een aantal personen die ik van harte wil bedanken voor de rol die zij in de afgelopen jaren vervuld hebben.

Wierd, van jou kwam het idee om te promoveren. Hoewel ik daar toch even over na heb moeten denken, zorgde jouw grenzeloze vertrouwen ervoor dat ik het durfde aan te gaan. Ik ben je erg dankbaar: zonder jou zou dit proefschrift er niet zijn geweest. Je kennis over ons vakgebied is enorm, en ondanks onze lange en intensieve samenwerking blijf je me verbazen met nieuwe voorbeelden en anekdotes.

Tinka, naast je rol als promotor was je voor mij een gids in de wereld van het wetenschappelijk onderzoek. Je was een zeer waardevolle leermeester op het gebied van schrijven van artikelen, en ondanks je volle agenda vond je altijd tijd om kritisch mijn teksten door te nemen om ze naar een hoger niveau te tillen. Naast de belangrijke rol die je inhoudelijk hebt vervuld, wil ik je bedanken voor je geduld en vertrouwen.

I would also like to thank our colleagues in the C-IMAGE consortium for providing an inspiring community of research. In particular Steven Murawski: thank you for believing in a joung woman and her one-page research proposal.

Ook mijn dank aan het C-IMAGE-NL team (Allette, Edwin, Justine, Martijn, Shokouh, Sophie), mijn collega's op afstand[c]: de verschillen in onze expertises (en vakgebieden) zorgen voor interessante en leerzame gesprekken.

Sjon, Martijn en Sandra wil ik bedanken voor het lezen van de laatste versie van het proefschrift en het aandragen van de laatste correcties. De opmaak van dit proefschrift is gebaseerd op dat van het proefschrift van Edwin, waarvoor ik graag zijn vrouw Gerda wil bedanken. Voor de opmaak van de omslag (en haar geduld) ben ik dank verschuldigd aan Trea.

[c] Hoewel de uren naast elkaar in vliegtuigstoelen of hotelkamers eigenlijk dubbel zouden moeten tellen!!

Daarnaast wil ik mijn collega's, vrienden en familie bedanken voor[d]:

- Het aanhoren van onsamenhangende verhalen over waar ik tegenaanloop (echt, het helpt).
- Het aanhoren van onsamenhangende verhalen over wat voor moois ik nu heb gemaakt.
- Het vooral even niet over promoveren praten.
- … en dan toch nog een keer dat zelfde verhaal aanhoren over iets dat mij erg hoog zat (in positieve of negatieve zin).
- Het voorzien in de brandstoffen voor totstandkoming van dit proefschrift, t.w.: koffie, suikers (…taart!), en broodjes.
- Het begrip voor mijn fysieke danwel mentale afwezigheid.

Hoewel ogenschijnlijk triviaal, zorgen deze gebaren ervoor dat ik met plezier gewerkt heb en me gesteund voelde in dit traject.

En tot slot, maar bovenal, ben ik dankbaarheid verschuldigd aan de mensen die het aller dichtst bij me staan en wellicht meer betrokken zijn geraakt dan we allemaal hadden voorzien:
Heit en mem, jullie hebben me meegegeven zelfstandig te zijn en dicht bij mezelf te blijven, maar wel mezelf te blijven ontwikkelen. Met mem haar nuchterheid is elk probleem te relativeren. Elize & Colin, jullie laten me elke dag weer beseffen wat écht belangrijk is in het leven. Douwe, zonder jouw onuitputtelijke steun had ik dit promotietraject niet tot een goed einde kunnen brengen. Sterker nog: zonder jouw steun had ik dat ook niet willen doen. Bedankt voor jullie begrip en geduld.

Marieke

[d] Ik weet dat ik mij er hiermee (erg!) gemakkelijk vanaf maak. Ter geruststelling: het oorspronkelijke plan was om aan elk van de genoemde aspecten weegfactoren toe te wijzen afhankelijk van het belang, aan (groepen) personen de relevante aspecten toe te wijzen, en vervolgens het aantal woorden per dankbetuiging af te stemmen aan de behaalde totaalscore.
Ik heb er uiteindelijk toch maar voor gekozen om de benodigde tijd en energie te steken in gedrag waarmee ik mijn fysieke en/of mentale afwezigheid de laatste tijd een beetje goed kan maken.

SENSE

Netherlands Research School for the
Socio-Economic and Natural Sciences of the Environment

D I P L O M A

For specialised PhD training

The Netherlands Research School for the
Socio-Economic and Natural Sciences of the Environment
(SENSE) declares that

Marieke Zeinstra-Helfrich

born on 12 July 1985 in Wûnseradiel, The Netherlands

has successfully fulfilled all requirements of the
Educational Programme of SENSE.

Wageningen, 21 November 2016

the Chairman of the SENSE board	the SENSE Director of Education
Prof. dr. Huub Rijnaarts	Dr. Ad van Dommelen

The SENSE Research School has been accredited by the Royal Netherlands Academy of Arts and Sciences (KNAW)

KONINKLIJKE NEDERLANDSE
AKADEMIE VAN WETENSCHAPPEN

The SENSE Research School declares that **Ms Marieke Zeinstra-Helfrich** has successfully fulfilled all requirements of the Educational PhD Programme of SENSE with a work load of 31.2 EC, including the following activities:

SENSE PhD Courses

- SENSE summer academy: Voice and presentation training (2013)
- Environmental research in context (2013)
- Research in context activity: 'Initiative and active membership of the PhD network for the NHL Hogeschool' (2013-2015)

External training at a foreign research institute

- Marine Pollution Expert Exchange Programme (EMPOLLEX), SINTEF, Trondheim, Norway (2011)
- Marine Pollution Expert Exchange Programme (EMPOLLEX), Cedre, Brest, France (2011)

Oral Presentations

- *Quantification of oil entrainment in water.* Gulf of Mexico Oil Spill & Ecosystem Science Conference, 26-29 January 2014, Mobile AL, US
- *Improved modelling of dispersion of oil.* Interspill Conference, 24-26 March 2015, Amsterdam, The Netherlands

SENSE Coordinator PhD Education

Dr. ing. Monique Gulickx

This research was made possible in part by a grant from the BP/Gulf of Mexico Research Initiative as an effort of the C-IMAGE consortium (grant contract #SA 12-10/GoMRI-007), and in part by the Wageningen UR TripleP@Sea innovation program (KB-14-007).

Laboratory facilities were made available by the Centre of Expertise Water Technology, Leeuwarden.

Cover photo: ITOPF, with permission
Cover design: Trea Keizer